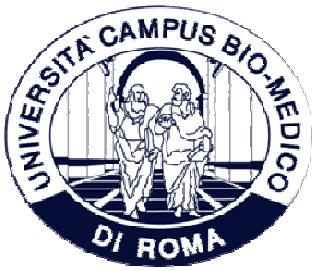

UNIVERSITÀ CAMPUS BIO-MEDICO DI ROMA

FACOLTÀ DI INGEGNERIA

DOTTORATO DI RICERCA IN INGEGNERIA BIOMEDICA

XXIV CICLO

Chitosan-based scaffold for osteochondral tissue engineering: comparison of fabrication and functionalization techniques and scaffolds characterization

Supervisor

Prof. Marcella Trombetta

Candidate
Liliana Liverani, M. Eng.

Academic year 2010-2011

Table of Contents

Abstract

This PhD thesis sets in tissue engineering (TE), a discipline which, starting from the principles of biology, medicine and engineering, it aims to restore, maintain, or enhance tissue and organ function. TE is performed following mainly three approaches: genetic engineering, cell therapy and scaffold/cells construct. The present work is focused on the latter approach for the regeneration of the osteochondral tissue and, in particular, to the fabrication of chitosan-based scaffolds by using electrospinning and phase separation techniques.

Among natural polymers, polysaccharides are a biomaterial class widely used for TE applications, mainly because of the critical role of saccharide moieties in numerous cell-signaling schemes and in the area of immune modulation; they affect also the process of extra cellular matrix (ECM) formation, by modulating the activities of molecules signaling and mediating certain intercellular signals. They are also biodegradable, hydrophilic, present a low toxicity, and could be synthesized by using several techniques. One of the most promising polysaccharide used for TE applications is chitosan, a deacetylated derivative of chitin, because of its high biocompatibility, biodegradability, and ability to promote cell adhesion. Given its polycationic behavior, it can also be conjugated with a bioceramic (i.e. hydroxyapatite) or bioactive glasses by spontaneous electrostatic bond. Moreover, it can be easily processed and tailored in various shapes, including beads, films, sponges, tubes, powders, and fibers.

To obtain a suitable construct, respecting all the requirements needed to successfully regenerate a complex interface tissue, like the osteochondral one, a great effort has been required in terms of integration of biomaterials (i.e. combined used of polymers and ceramics), fabrication techniques (to reproduce the native morphological structure of different tissue), and cell signaling.

1. Introduction

Index

1.1 General overview on tissue engineering in orthopedic field

NIH definition of tissue engineering (TE)/regenerative medicine is here reported: "*Tissue engineering/regenerative medicine is an emerging multidisciplinary field involving biology, medicine, and engineering that is likely to revolutionize the ways we improve the health and quality of life for millions of people worldwide by restoring, maintaining, or enhancing tissue and organ function. In addition to having a therapeutic application, where the tissue is either grown in a patient or outside the patient and transplanted, tissue engineering can have diagnostic applications where the tissue is made in vitro and used for testing drug metabolism and uptake, toxicity, and pathogenicity. The foundation of tissue engineering/regenerative medicine for either therapeutic or diagnostic applications is the ability to exploit living cells in a variety of ways. Tissue engineering research includes the following areas:*

1) Biomaterials: including novel biomaterials that are designed to direct the organization, growth, and differentiation of cells in the process of forming functional tissue by providing both physical and chemical cues.

2) Cells: including enabling methodologies for the proliferation and differentiation of cells, acquiring the appropriate source of cells such as autologous cells, allogeneic cells, xenogeneic cells, stem cells, genetically engineered cells, and immunological manipulation.

3) Biomolecules: including angiogenic factors, growth factors, differentiation factors and bone morphogenic proteins

4) Engineering Design Aspects: including 2-d cell expansion, 3-d tissue growth, bioreactors, vascularization, cell and tissue storage and shipping (biological packaging).

5) Biomechanical Aspects of Design: including properties of native tissues, identification of minimum properties required of engineered tissues, mechanical signals regulating engineered tissues, and efficacy and safety of engineered tissues

6) Informatics to support tissue engineering: gene and protein sequencing, gene expression analysis, protein expression and interaction analysis, quantitative cellular image analysis, quantitative tissue analysis, in silico tissue and cell modeling, digital tissue manufacturing, automated quality assurance systems, data mining tools, and clinical informatics interfaces.

Stem cell research - Includes research that involves stem cells, whether from embryonic, fetal, or adult sources, human and non-human. It should include research in which stem cells are isolated, derived or cultured for purposes such as developing cell or tissue therapies, studying cellular differentiation, research to understand the factors necessary to direct cell specialization to specific pathways, and other developmental studies. It should not include transgenic studies, gene knock-out studies nor the generation of chimeric animals."

A scheme of tissue engineering concept and its main steps could be summarized in the following figure.

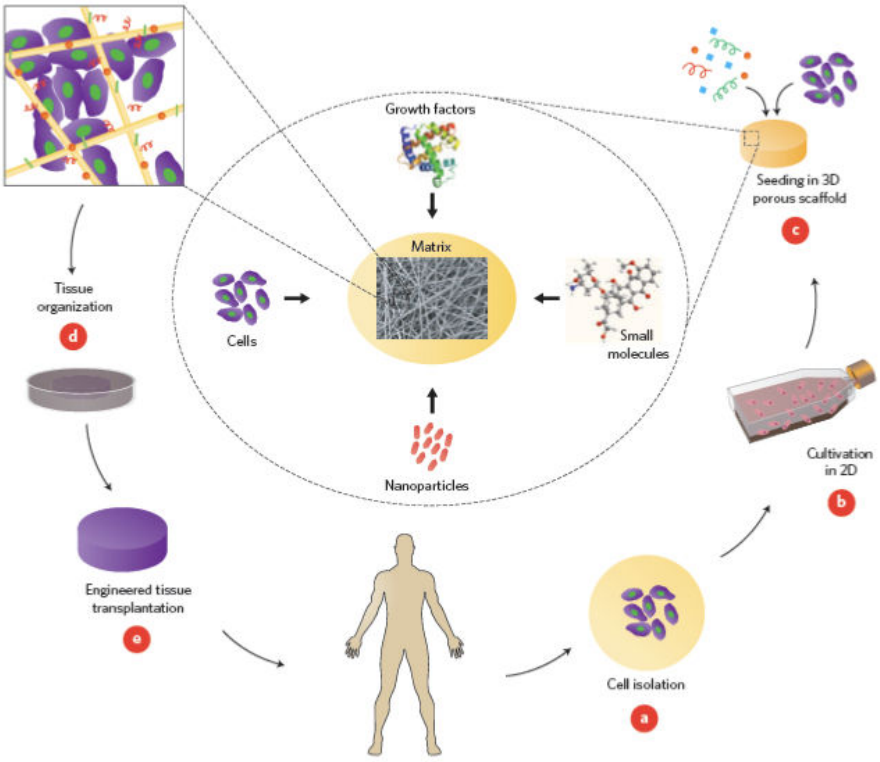

Figure 1.1 Scheme of tissue engineering concept and main steps: cell isolation (a), cultivation in 2D (b), seeding in 3D porous scaffold (c), tissue organization (d), and engineered tissue transplantation (e). [1]

For what concerns bone tissue engineering, it has become a rapidly expanding research field: the practices of this research area usually involve the use of biomaterials for scaffolds fabrication, in combination with biological cues and tissue cells [2, 3]. While, in the clinical practice, autograft represents the gold standard for bone repair after injuries or diseases. Despite surgical techniques may provide enough bone for grafting procedures, there are limitations in its use related to the availability of sufficient supply and patient morbidity. A major effort has been then produced to find alternatives to autologous bone grafts, such as allografts (either as fresh frozen, freeze-dried, or demineralized bone matrix), growth factors, degradable and non-degradable polymers, bioactive glass, and calcium phosphates [4].

An emerging field for orthopedic applications is represented by the interface tissue engineering (ITE), having the specific aim to regenerate functional tissues in order to repair or to promote neo-tissue formation in diseased or damaged area between different

tissue types, like ligament-to-bone, tendon-to-bone and cartilage-to-bone interfaces [5]. A representative scheme of the ITE is reported in the following figure.

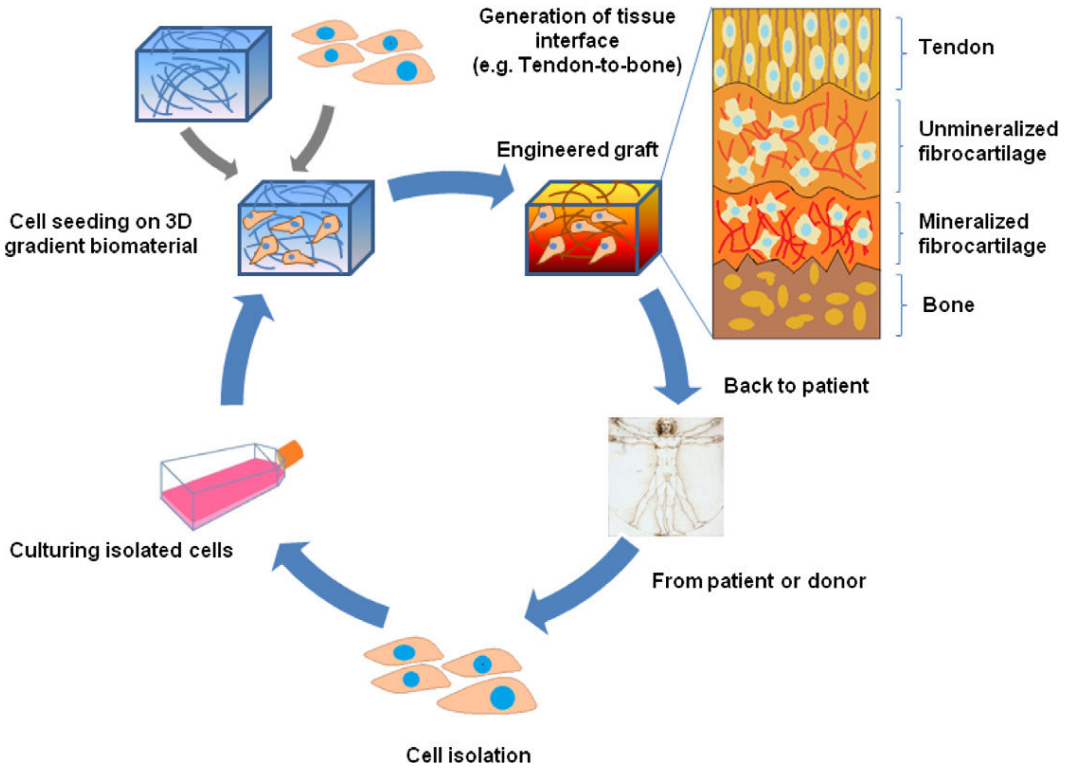

Figure 1.2 Scheme reporting the basic elements of ITE, as example is reported the tendon-to-bone interface application[5].

Considering the complexity of native interface tissues, scaffolds fabricated for ITE applications have the aim to completely replace (by tissue repair or regeneration) the normal functions of the healthy tissues, taking account also of interface tissue anisotropic structural properties, which gradually vary from one tissue to another. In fact, for that reason isotropic scaffolds, usually used for soft tissue regeneration, result not suitable for the integration with the hard tissue [6]. In particular, the graft function was affected by the lack of integrating interface, due to the use of homogeneous biomaterials (both, in composition and structure), unable to support the growth of heterogeneous cell populations that reside at the interface tissues, leading, often to the graft failure. In order to overcome this limit, biomimetic scaffolds with graded properties (i.e. in composition, structure and mechanical properties) are useful, especially for what concerns the improving of cell-cell communications, cell-matrix

integration, the supporting of cell growth and differentiation oriented towards the formation of a graded tissue, for the replacing of the disease interface [5].

1.2 Osteochondral defects: native tissue characteristics, traditional treatments and new challenges of tissue engineering

Articular cartilage is an avascular, aneural and alymphatic tissue absolving the role of providing a low-friction, wear-resistant surface. Moreover, it has the function of facilitating load support and load transfer while allowing for translation and rotation between bones. It is composed primarily of water, approximately 70-80 wt%, while the solid fraction is primarily composed of collagen (50-75%) and proteoglycans (15-30%), arranged in an integrated network. Matrix arrangement and composition are not constant within the tissue, but are organized in successive layers from the surface down to subchondral bone. Chondrocyte represents the main cell component of cartilage. Since articular cartilage is avascular, chondrocytes obtain nutrients by diffusion from the synovial fluid, facilitated during joint movement [7]. Cell scarcity and lack of vascularization imply that natural repair of cartilage damages is often poor, and is realized with the deposition of a biomechanically unsuitable fibrocartilagineous scar. Moreover, the complexity of articular cartilage is related to the coexistence of functionally different layers within the osteochondral segment which are deputed to different functions, i.e. lubrication and grafting to the underlying bone [8, 9].

For this reason, management of chondral and osteochondral defects is challenging and several surgical techniques have been used to repair such lesions. Surgical techniques can be roughly divided into reparative and regenerative. The rationale for reparative approaches, which include microfractures and subchondral bone drilling, is to stimulate the formation of new fibrocartilage to fill the lesion, although this repair tissue is biomechanically inferior to the original cartilage [10].

Regenerative techniques include autologous chondrocyte implantation (ACI), matrix-induced autologous chondrocyte implantation (MACI) and autologous or allogenic osteochondral grafting [11], schematically reported in figure 1.3. These methods provide a restoration of hyaline cartilage even though the clinical outcome is not always satisfactory because the regenerated cartilage is morphologically, biochemically, and biomechanically inferior to the original cartilage [12, 13].

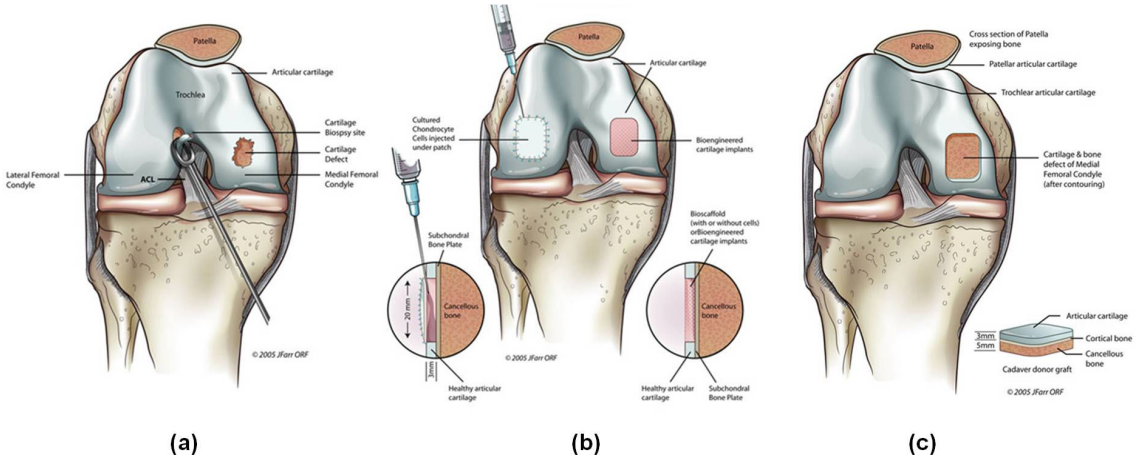

Figure 1.3 Regenerative techniques: chondrocyte harvest (a), ACI and MACI (b), and osteochondral allograft (c) (adapted from [14]).

Tissue engineering represents an innovative option to repair chondral and osteochondral defects and restore joint function. This approach requires a cell source, matrix or scaffold, and appropriate growth factors to promote formation of bone and cartilage. It is now possible to engineer biological replacements of cartilage and bone tissues using multi-potent human mesenchymal stem cells (hMSCs) [15].

Martin *et al.* have classified the different approaches for the fabrication of osteochondral composite constructs, by choosing the double criteria of the strategy for the selection of the scaffold and the cell source. They reported the following categories: (A) a scaffold for the bone component but a scaffold-free approach for the cartilage component; (B) different scaffolds for the bone and the cartilage components combined at the time of implantation; (C) a single but heterogeneous composite scaffold; or (D) a single homogenous scaffold for both components. These scaffolds have been (I) loaded with a single cell source having chondrogenic capacity, (II) loaded with two cell sources having either chondrogenic or osteogenic capacities, (III) loaded with a single cell source having both chondrogenic and osteogenic differentiation capacity, or (IV) used in a cell-free approach [16].

Recently, Panseri *et al.* investigated the osteochondral tissue engineering approaches for articular cartilage and subchondral bone regeneration. In particular among the different approaches of TE the best results will probably be achieved by the combination of

osteochondroconductive scaffolds, osteochondroinductive signals, osteochondrogenic precursor cells, and suitable fixation to the defect site [17]. Osteochondroconductive scaffolds are tissue-conductive system, that in order to recreate a biomimetic scaffold, reproduce the architectures of native tissues and combining it with the use of synthetic materials with cell-recognition sites of naturally derived materials [18, 19].

Osteochondroinductive signals refers to the use of adequate protein molecules (i.e. growth factors and cytokines) for the induction of osteochondral tissue formation, by stimulating stem cells to differentiate into desired specific phenotype. Widely used protein molecules are Bone Morphogenetic Proteins (BMPs), Epidermal Growth Factor (EGF), Platelet-Derived Growth Factor (PDGF), Fibroblast Growth Factors (FGFs), Parathyroid Hormone-Related Peptide (PTHrp), Insulin-like Growth Factors (IGFs), Transforming Growth Factor-Beta (TGF-b), and Vascular Endothelial Growth Factors (VEGFs) [20].

Osteochondrogenic precursor cells refers to the problem of the lack of a sufficient amount of tissue-forming cells around the graft site, that could induce graft failure. The combination of TE approach with cell therapy could represent a possible solution to that problem [21, 22].

The problem of the suitable fixation to the defect site represent a critical step in tissue regeneration, in fact it is important to achieve a biological fixation, functional integration, avoiding micromotion at the interfaces of the implanted graft. A multidisciplinary approach is mandatory to solve this problem, that became, recently focus of several investigations [23].

1.3 Biomaterials for osteochondral tissue engineering: natural polymers and bioglasses

In ITE field, for scaffold fabrication, polymers (both natural and synthetic) and ceramics are usually employed, also in combination, in order to modulate final scaffold properties, having the final aim to replicate natural tissue complexity, in particular for osteochondral segment regeneration.

Among natural polymers, polysaccharides are a biomaterial class widely used for TE applications, mainly because of the critical role of saccharide moieties in numerous cell-signaling schemes and in the area of immune modulation; they affect also the process of

extra cellular matrix (ECM) formation, by modulating the activities of molecules signaling and mediating certain intercellular signals. They are also biodegradable, hydrophilic, present a low toxicity, and could be synthesized by using several techniques. One of the most promising polysaccharide used for ITE applications is chitosan, a deacetylated derivative of chitin, because of its high biocompatibility, biodegradability, and ability to promote cell adhesion. Given its polycationic behavior, it can also be conjugated with growth factors by spontaneous electrostatic bond [24]. Moreover, it can be easily processed and tailored in various shapes, including beads, films, sponges, tubes, powders, and fibers [25].

On the other hand, ceramics, such as hydroxyapatite (HA) or other calcium phosphate ceramics or bioactive glasses (BG) are known to promote, when implanted, the formation of a bone-like apatite layer on their surfaces [26-28]. They have been investigated extensively during the last decades and are widely used for bone replacement, due to their osteoconductivity and high biocompatibility, also associated with stem cells therapy [29].

The design of multilayered scaffolds for ITE applications, and in particular for osteochondral regeneration could represent the simplest solution to mimic tissue interface. The main problem that immediately arose was represented by the need to ensure continuity between the scaffold layer, in fact, several techniques were adopted to overcome this limit [30].

Representative examples of the combined use of polymer with ceramics for the fabrication of multilayered composite scaffolds for osteochondral tissue engineering, by using different fabrication techniques are briefly reported.

Harley *et al.* reported the design and the fabrication of multilayered scaffolds constituted by a mineralized, type I collagen-glycosaminoglycan (CGCaP) suspension, that mimics the composition of subchondral bone, and unmineralized type II collagen-glycosaminoglycan (CG) suspension, mimicking the structure of articular cartilage, as reported in figure 1.4. After the "liquid-phase cosynthesis", which allows the formation of the continuous, gradual interface between the two layer, samples were lyophilized. Beyond the continuous structure, these scaffolds did not require the use of sutures, glue or other fixation systems to be allocated, and showed compressive deformation behavior that mimics the behavior observed in natural articular joints [30-32].

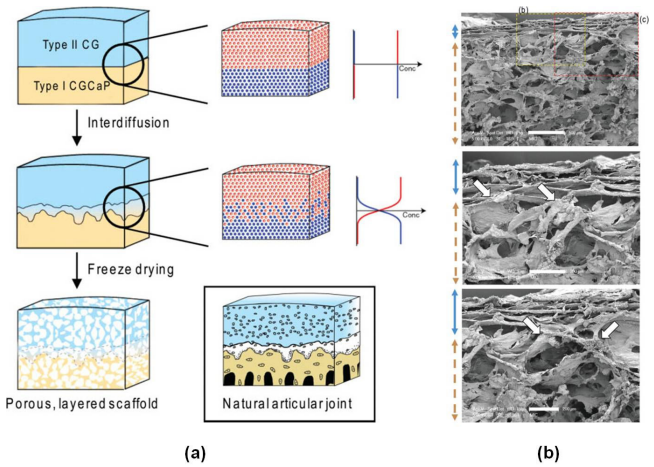

Figure 1.4 Schematic representation of multilayered scaffold fabrication process (a), SEM micrographs showing scaffold cross section at different magnifications (adapted from [30]).

Oliveira *et al.* presented the combined use of chitosan with HA for the fabrication of a bilayered scaffold. Briefly, they fabricated at first HA-based scaffolds by foam replica method, then, the obtained samples were immersed in chitosan solution, frozen at –80 °C and then lyophilized. Positive results were obtained from samples characterization, as resistance to layer delamination and from *in vitro* cell culture studies performed by using goat bone marrow stromal cells (GBMCs) to investigate the cell differentiation induced by bilayered scaffolds, evaluating the different stimuli of each layer [26].

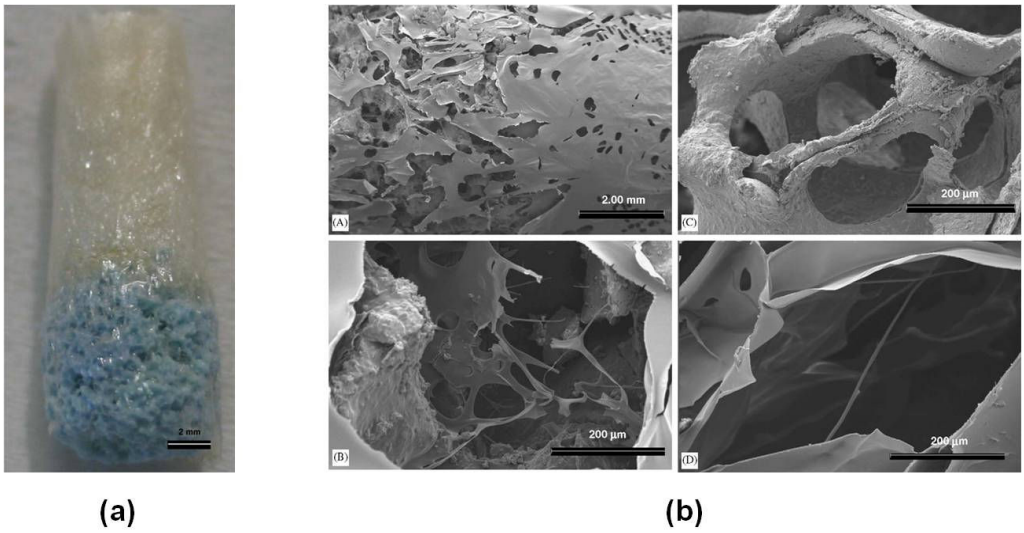

Figure 1.5 Digital camera image of the obtained bilayered scaffold (a); SEM micrographs of the HA scaffold seeded with GBMCs and cultured for 14 days in osteogenic media: surface of the cell-HA constructs (A, B), GBMCs infiltration into a HA macropore (C), and GBMCs on the core of the HA scaffolds (D) (adapted from [26]).

Yunos *et al.* proposed an integration of the foam replica method and the electrospinning techniques for the fabrication of a composite scaffold for osteochondral tissue engineering. Briefly, a 45S5 Bioglass®-based porous scaffold, obtained by foam replica method, was at first immersed in a poly-DL-lactide (PDLLA) solution, then was used as target collector for the electrospinning of a PDLLA solution. Positive results were obtained in terms of scaffold characterization and after preliminary *in vitro* studies performed by using chondrocyte cells (ADTC5), that showed in particular positive outcomes in terms of cell migration into the scaffold [33].

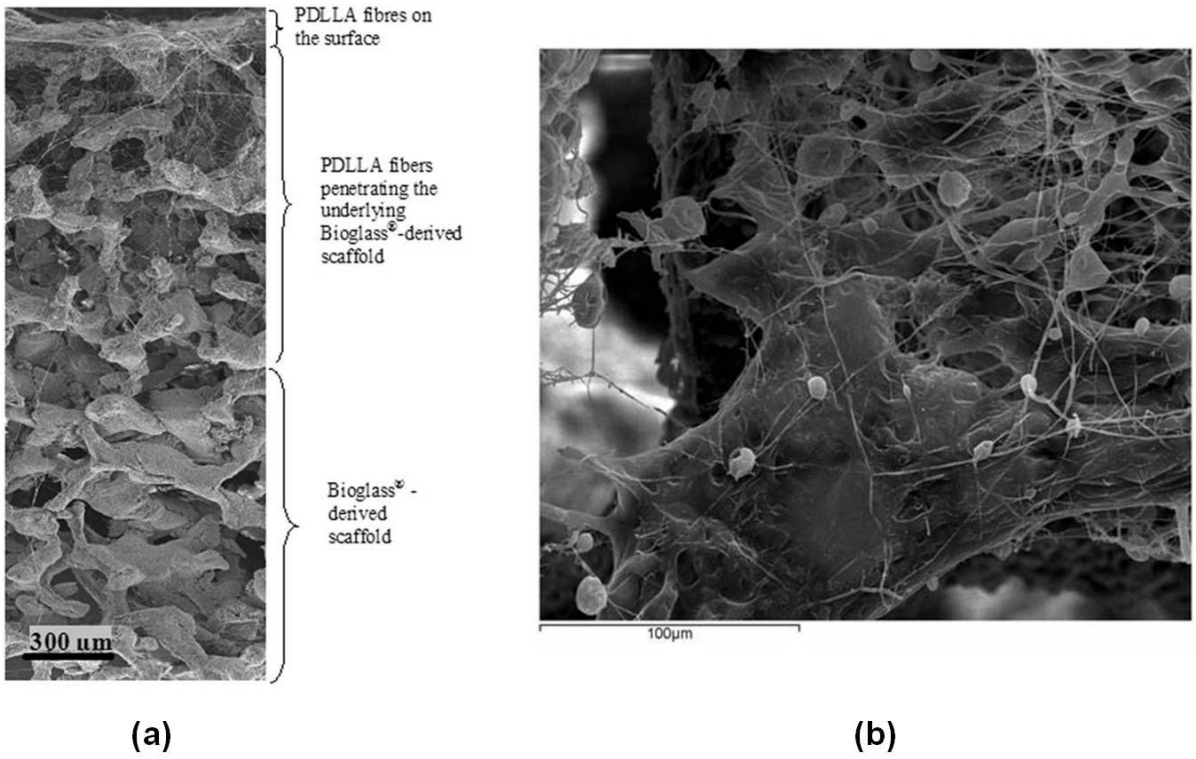

Figure 1.6 SEM composite image showing the cross-section of a typical PDLLA/Bioglass® obtained stratified scaffold (a), and SEM micrograph showing ADTC5-cells migrating through the pores and growing within layers of the PDLLA fibrous network after 14 days (b) (adapted from [33]).

In conclusion, it is possible to summarize that in order to obtain a suitable construct, respecting all the requirements needed to successfully regenerate a complex interface tissue, like the osteochondral one, a great effort is required in terms of integration of

biomaterials (i.e. combined used of polymers and ceramics), fabrication techniques (to reproduce the native morphological structure of different tissue), and cell signaling.

1.4 Outline

The present PhD thesis is focused on tissue engineering, in particular to the fabrication of chitosan-based scaffolds potentially useful for the regeneration of osteochondral tissue.

The chitosan versatility allows the fabrication of scaffold for tissue engineering by using several fabrication techniques, as the electrospinning and the phase separation ones.

The experimental activities are introduced by a chapter (n. 2) devoted to the explanation in details of the materials synthesis, scaffold fabrication protocols and characterization techniques used during the next chapters, where there are cross references to the chapter 2.

The experimental investigations report starts with the description of the optimization of pure chitosan electrospinning process, without the addition of copolymer, and the crosslinking processes, needed to enhance chitosan electrospun samples resistance to physiological environment, in particular two different processes are analyzed and the use of two chitosan crosslinkers has been evaluated (chapter 3).

Keeping in mind the final scaffolds function and the tissue target of regeneration, a biomimetic approach aiming to the fabrication of scaffolds with structure and composition similar to natural bone, has been investigated by the introduction of inorganic phase (hydroxyapatite (HA) nanopowder or bioactive glass (BG) particles) within the polymeric fibers.

The addition of HA or BG, directly in the chitosan solution before the electrospinning process, has been evaluated separately, because it required accurate investigations and analysis of obtained samples (chapter 4 and 5, respectively).

A possible application of the obtained chitosan-based electrospun membranes is presented in this thesis work, as the external coating in a stratified multilayer composite scaffold for osteochondral tissue engineering. This stratified composite constructs were obtained by the integration of three different techniques widely used for scaffold

fabrication: the foam replica method, the freeze drying and freeze gelation, and the electrospinning (chapter 6).

The other kind of scaffold produced in the present thesis work have been obtained by using phase separation technique for the fabrication of chitosan foam scaffolds. Also in this case, a biomimetic approach has been pursed and HA and BG particles were dispersed inside chitosan porous structure (chapter 7).

Finally, a chapter containing the conclusive considerations and comments on the obtained results showed in the previous chapters, is reported (chapter 8).

References

[1] Dvir T, Timko BP, Kohane DS, Langer R. Nanotechnological strategies for engineering complex tissues. Nat Nano. 2011;6:13-22.

[2] Ehrbar M, Lütolf MP, Rizzi SC, Hubbell JA, Weber FE. Artificial extracellular matrices for bone tissue engineering. Bone. 2008;42:S72-S.

[3] Di Martino A, Liverani L, Rainer A, Salvatore G, Trombetta M, Denaro V. Electrospun scaffolds for bone tissue engineering. Musculoskeletal Surgery. 2011;95:69-80.

[4] Di Martino A, Silber JS, Vaccaro AR. Bone graft alternatives in spinal surgery. In: Wilkins LWa, editor. Spondylolysis, Spondylolysthesis, and Degenerative Spondylolysthesis. Philadelphia: Gunzburg, R.; Szpalski, M. ; 2006. p. 237-55.

[5] Seidi A, Ramalingam M, Elloumi-Hannachi I, Ostrovidov S, Khademhosseini A. Gradient biomaterials for soft-to-hard interface tissue engineering. Acta Biomaterialia. 2011;7:1441-51.

[6] Lohmander LS, Östenberg A, Englund M, Roos H. High prevalence of knee osteoarthritis, pain, and functional limitations in female soccer players twelve years after anterior cruciate ligament injury. Arthritis & Rheumatism. 2004;50:3145-52.

[7] Athanasiou KA, Darling EM, Hu JC. Articular Cartilage Tissue Engineering: Morgan & Claypool Publishers; 2009.

[8] Giannini S, Buda R, Vannini F, Di Caprio F, Grigolo B. Arthroscopic Autologous Chondrocyte Implantation in Osteochondral Lesions of the Talus. The American Journal of Sports Medicine. 2008;36:873-80.

[9] Giannini S, Buda R, Vannini F, Cavallo M, Grigolo B. One-step Bone Marrow-derived Cell Transplantation in Talar Osteochondral Lesions. Clinical Orthopaedics and Related Research®. 2009;467:3307-20.

[10] Browne JE, Branch TP. Surgical Alternatives for Treatment of Articular Cartilage Lesions. Journal of the American Academy of Orthopaedic Surgeons. 2000;8:180-9.

[11] Bartlett W, Skinner JA, Gooding CR, Carrington RWJ, Flanagan AM, Briggs TWR, et al. Autologous chondrocyte implantation versus matrix-induced autologous chondrocyte implantation for osteochondral defects of the knee: A PROSPECTIVE, RANDOMISED STUDY. J Bone Joint Surg Br. 2005;87-B:640-5.

[12] Willers C, Chen J, Wood D, Xu J, Zheng MH. Autologous chondrocyte implantation with collagen bioscaffold for the treatment of osteochondral defects in rabbits. Tissue Engineering. 2005;11:1065-76.

[13] Micheli LJ, Browne JE, Erggelet C, Fu F, Mandelbaum B, Moseley JB, et al. Autologous Chondrocyte Implantation of the Knee: Multicenter Experience and Minimum 3-Year Follow-Up. Clinical Journal of Sport Medicine. 2001;11:223-8.

[14] Indiana CRCo. Regeneration, Repair, or Replacement of Damaged Articular Cartilage. 2012.

[15] Sundelacruz S, Kaplan DL. Stem cell- and scaffold-based tissue engineering approaches to osteochondral regenerative medicine. Seminars in Cell & Developmental Biology. 2009;20:646-55.

[16] Martin I, Miot S, Barbero A, Jakob M, Wendt D. Osteochondral tissue engineering. Journal of biomechanics. 2007;40:750-65.

[17] Panseri S, Russo A, Cunha C, Bondi A, Di Martino A, Patella S, et al. Osteochondral tissue engineering approaches for articular cartilage and subchondral bone regeneration. Knee Surgery, Sports Traumatology, Arthroscopy. 2011:1-10.

[18] Tampieri A, Sprio S, Sandri M, Valentini F. Mimicking natural bio-mineralization processes: A new tool for osteochondral scaffold development. Trends in Biotechnology. 2011;29:526-35.

[19] Tampieri A, Sandri M, Landi E, Pressato D, Francioli S, Quarto R, et al. Design of graded biomimetic osteochondral composite scaffolds. Biomaterials. 2008;29:3539-46.

[20] Getgood A, Brooks R, Fortier L, Rushton N. Articular cartilage tissue engineering: TODAY'S RESEARCH, TOMORROW'S PRACTICE? J Bone Joint Surg Br. 2009;91-B:565-76.

[21] Caplan AI. Why are MSCs therapeutic? New data: new insight. The Journal of Pathology. 2009;217:318-24.

[22] Liu Y, Shu XZ, Prestwich GD. Osteochondral Defect Repair with Autologous Bone Marrow–Derived Mesenchymal Stem Cells in an Injectable, In Situ, Cross-Linked Synthetic Extracellular Matrix. Tissue Engineering. 2006;12:3405-16.

[23] Bekkers JEJ, Tsuchida AI, Malda J, Creemers LB, Castelein RJM, Saris DBF, et al. Quality of scaffold fixation in a human cadaver knee model. Osteoarthritis and cartilage / OARS, Osteoarthritis Research Society. 2010;18:266-72.

[24] Heng BC, Cowan CM, Davalian D, Stankus J, Duong-Hong D, Ehrenreich K, et al. Electrostatic binding of nanoparticles to mesenchymal stem cells via high molecular weight polyelectrolyte chains. Journal of Tissue Engineering and Regenerative Medicine. 2009;3:243-54.

[25] Muzzarelli RAA. Chitins and chitosans for the repair of wounded skin, nerve, cartilage and bone. Carbohydrate Polymers. 2009;76:167-82.

[26] Oliveira JM, Rodrigues MT, Silva SS, Malafaya PB, Gomes ME, Viegas CA, et al. Novel hydroxyapatite/chitosan bilayered scaffold for osteochondral tissue-engineering applications: Scaffold design and its performance when seeded with goat bone marrow stromal cells. Biomaterials. 2006;27:6123-37.

[27] Depan D, Venkata Surya PKC, Girase B, Misra RDK. Organic/inorganic hybrid network structure nanocomposite scaffolds based on grafted chitosan for tissue engineering. Acta Biomaterialia. 2011;7:2163-75.

[28] Rainer A, Giannitelli SM, Abbruzzese F, Traversa E, Licoccia S, Trombetta M. Fabrication of bioactive glass–ceramic foams mimicking human bone portions for regenerative medicine. Acta Biomaterialia. 2008;4:362-9.

[29] Marcacci M, Kon E, Moukhachev V, Lavroukov A, Kutepov S, Quarto R, et al. Stem Cells Associated with Macroporous Bioceramics for Long Bone Repair: 6- to 7-Year Outcome of a Pilot Clinical Study. Tissue Engineering. 2007;13:947-55.

[30] Harley BA, Lynn AK, Wissner-Gross Z, Bonfield W, Yannas IV, Gibson LJ. Design of a multiphase osteochondral scaffold III: Fabrication of layered scaffolds with continuous interfaces. Journal of Biomedical Materials Research Part A. 2010;92A:1078-93.

[31] Harley BA, Lynn AK, Wissner-Gross Z, Bonfield W, Yannas IV, Gibson LJ. Design of a multiphase osteochondral scaffold. II. Fabrication of a mineralized collagen–glycosaminoglycan scaffold. Journal of Biomedical Materials Research Part A. 2010;92A:1066-77.

[32] Lynn AK, Best SM, Cameron RE, Harley BA, Yannas IV, Gibson LJ, et al. Design of a multiphase osteochondral scaffold. I. Control of chemical composition. Journal of Biomedical Materials Research Part A. 2010;92A:1057-65.

[33] Yunos DM, Ahmad Z, Salih V, Boccaccini AR. Stratified scaffolds for osteochondral tissue engineering applications: Electrospun PDLLA nanofibre coated Bioglass®-derived foams. Journal of Biomaterials Applications. 2011.

2. Scaffolds synthesis and characterization

Index

Overview

In this chapter all the methodologies, starting from the biomaterials and synthesis, processes and characterization techniques used for scaffold fabrication, were described in detail. This chapter is divided in sections, where the materials used for electrospun, composite and foam scaffolds fabrication, the processes used and their parameters (electrospinning technique, composite fabrication and phase separation-based technique) followed by the scaffold characterization techniques, were reported.

2.1 Electrospun scaffolds fabrication

In this section all the chitosan solutions used for obtaining homogeneous electrospun pure chitosan membrane defect-free, were reported. The obtained electrospun chitosan-based membranes needed to be crosslinked in order to avoid their dissolution in aqueous solution, for that reason several techniques and crosslinker agents were employed and listed in this section. The further step was the functionalization of the obtained electrospun meshes by adding nanopowder of hydroxyapatite and bioactive glass particles. Beyond the functionalization, the use of other addictives, like salts, were evaluated to improve the yield of the electrospinning process.

2.1.1 Solutions for obtaining electrospun pure chitosan meshes

The basic material used in this experimental section is the chitosan Medium Molecular Weight (MMW) (MW 190-300 kDa, degree of deacetylation 75-85%) purchased from Sigma Aldrich (Milwaukee, MI). Relevant attention was devoted to the chitosan solvents used during the optimization of solution properties in order to perform the electrospinning, in particular all the solvents used are listed below:

- Acetic Acid (AA) (≥ 99.7%, Sigma Aldrich),
- Lactic Acid (LA) (≥ 85%, Sigma Aldrich),
- Trifluoroacetic Acid (TFA) (99%, Sigma Aldrich),
- Dichloromethane (DCM) (≥ 99.9%, Sigma Aldrich) even if DCM is a non-solvent for chitosan, it was used to improve solutions spinnability.

In order to use not only pure solvents solutions, but also solvents and non-solvent mixtures, preliminary miscibility tests were successfully performed (i.e. miscibility tests on AA/DCM and TFA/DCM mixture).

The following solutions were used to set-up the process of pure chitosan electrospinning:

1. 4 % w/v chitosan in AA (aqueous solution 30% v/v)
2. 2.5 % w/v chitosan in AA (aqueous solution 90% v/v)
3. 4 % w/v chitosan in AA (aqueous solution 90% v/v)
4. 2 % w/v chitosan in AA (aqueous solution 90% v/v)/DCM (80:20)
5. 2.6 % w/v chitosan in AA/DCM (80:20)
6. 4 % w/v chitosan in AA/DCM (70:30)
7. 3 % w/v chitosan in aqueous LA solution (2% v/v in deionized water (DI water))
8. 2.7 % w/v chitosan in TFA
9. 5 % w/v chitosan in TFA
10. 6 % w/v chitosan in TFA
11. 8 % w/v chitosan in TFA
12. 4 % w/v chitosan in TFA/DCM (80:20)
13. 8 % w/v chitosan in TFA/DCM (80:20)
14. 12.5% w/v of chitosan in TFA. Complete dissolution of CS occurred in 36 hours. Then, DCM was added to the solution at 1:4 volume ratio with respect to TFA. (final concentration: 10% w/v chitosan in TFA/DCM (80:20))

2.1.2 Crosslinker agents and crosslinking processes for electrospun chitosan scaffolds

After the optimization of electrospinning process, corresponding to the solution n. 14 described above, the focus was shifted on the crosslinking processes. The selected chitosan crosslinkers are listed below:

- glutaraldehyde (GA) (aqueous solution 50%v/v, Sigma Aldrich),
- genipin (GEN) (($\geq$ 98%, Sigma Aldrich).

Crosslinker solutions could be grouped separately for each type of process, as follows:

- **Two steps process**: the obtained electrospun membranes were crosslinked by exposure to glutaraldehyde vapors. A schematic diagram of that process is reported in figure 2.1. Samples were placed in a sealed glass container and exposed to the GA vapors for 3 hours. Additionally, longer crosslinking time (18 and 24 hours), were evaluated. The crosslinker solution used for this process was: GA aqueous solution 25 % v/v (GA 25%v/v). The amount of GA solution put into sealed container is 0.2 mL/cm^2, considering the sample effective exposed area.

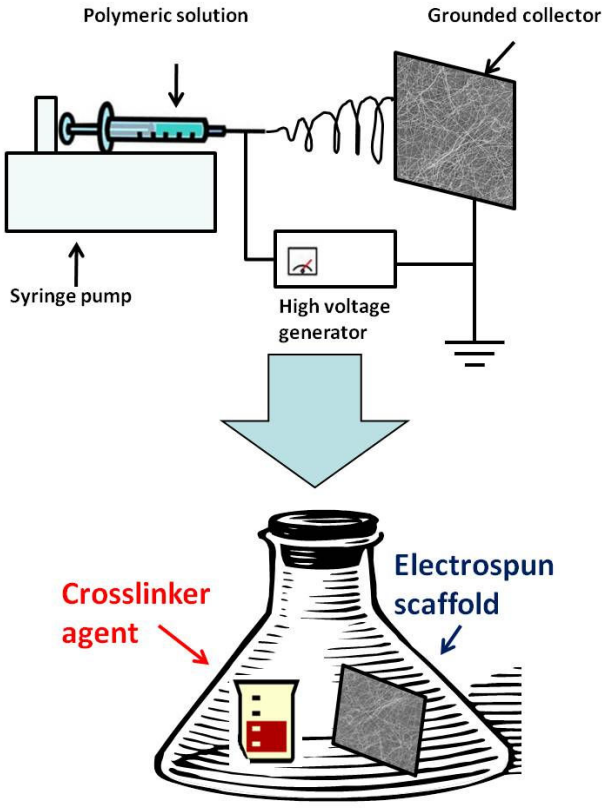

Figure 2.1 Schematic diagram of the electrospinning process and the following two-steps crosslinking process.

- **One step process:** the crosslinker solution was added directly to the polymeric solution before the electrospinning process, briefly reported in figure 2.2. The obtained electrospun membrane was already crosslinked. The following crosslinker solutions were tested:

- GA aqueous solution 4 % v/v: GA (4% v/v)
- GA aqueous solution 10 % v/v: GA (10% v/v)
- GA aqueous solution 50 % v/v: GA (50% v/v)
- GEN 1,25 % v/v in DI water/EtOH (50:50) solution: GEN 1.25

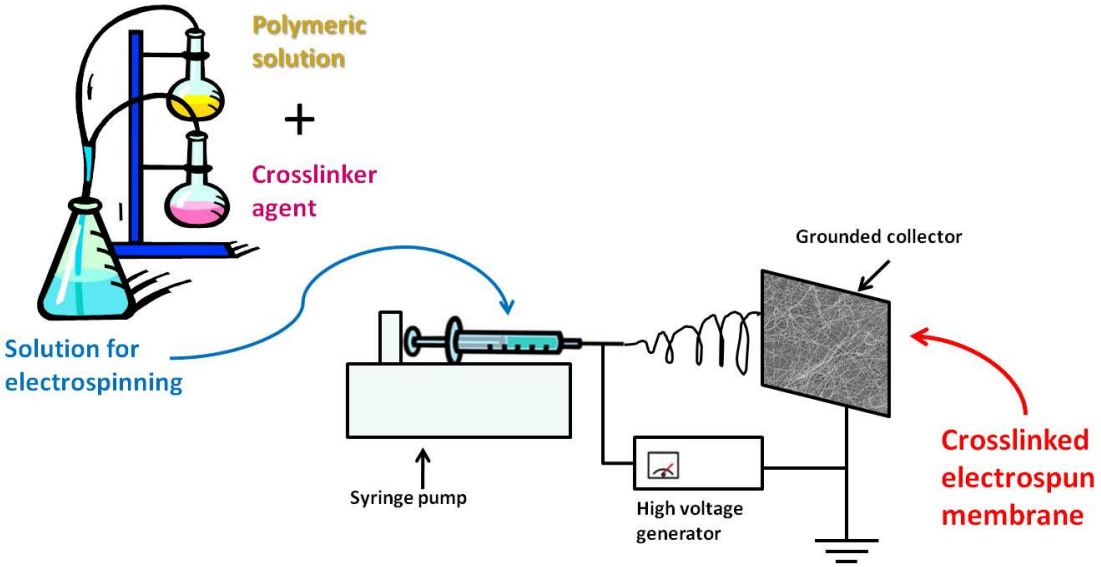

Figure 2.2 Schematic diagram of the electrospinning process and one-step crosslinking process.

Samples names and type, classified on the basis on the applied crosslinking process (labeled XL), are reported in the table below and used as reference also in the following chapters. The starting sample was obtained from solution n. 14, i.e. ElectroSpun ChitoSan, nd it was labeled ESCS:

Crosslinking process	Crosslinker	Sample name
None	None	ESCS
Two-steps (3 hours)	GA (25% v/v)	ESCSXL3
Two-steps (18 hours)	GA (25% v/v)	ESCSXL18
Two-steps (24 hours)	GA (25% v/v)	ESCSXL24
One-step	GA (4 % v/v)	ESCSXLGA4
One-step	GA (10 % v/v)	ESCSXLGA10
One-step	GA (50 % v/v)	ESCSXLGA50

One-step	GEN 1.25 (8 % v/v)	ESCSXLGEN8
One-step	GEN 1.25 (20 % v/v	ESCSXLGEN20

Table 2.1 Summary of crosslinking process, crosslinkers used and name of obtained samples.

For what concerns GEN crosslinked samples, the number at the end of the sample name indicates the amount (expressed in % v/v) of crosslinker solution in chitosan solution.

2.1.3 Functionalization of chitosan electrospun scaffolds

A biomimetic approach aiming to the fabrication of scaffolds with structure and composition similar to natural bone, was pursued by the introduction of inorganic phases (hydroxyapatite (HA) nanopowder or bioactive glass particles) within the polymeric fibers. The process of functionalization is showed in figure 2.3.

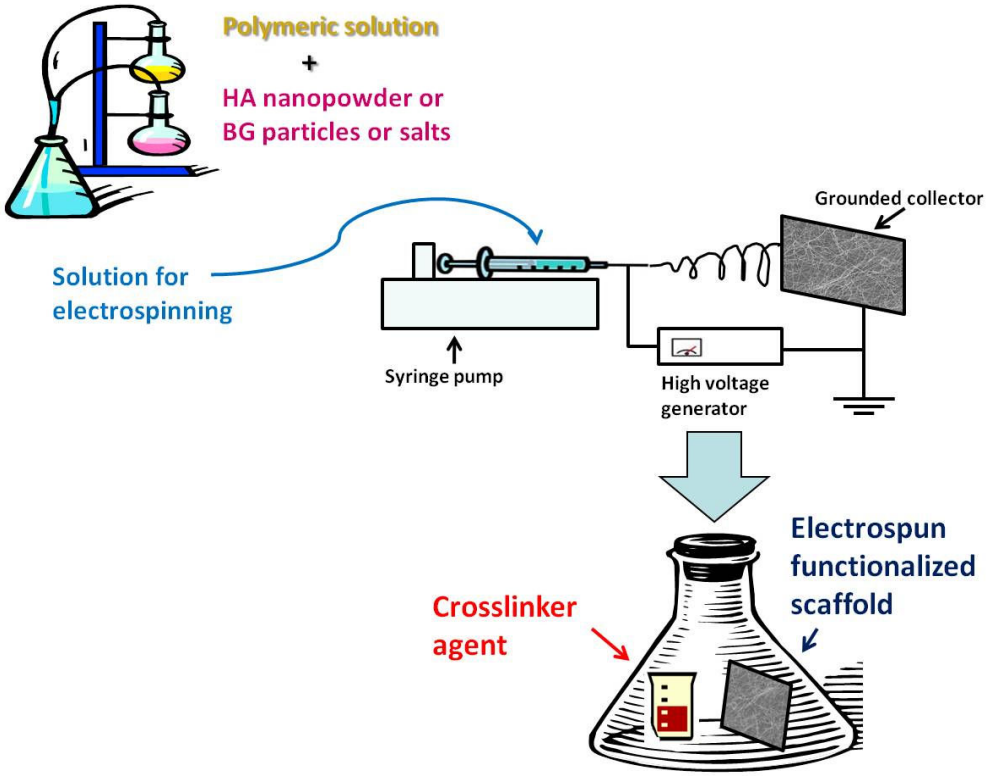

Figure 2.3 Schematic diagram of functionalization of electrospun membrane, by the addition of HA nanopowder or bioactive glass particles, directly to the solution before the electrospinning process. The obtained membranes were crosslinked by two-steps crosslinking process.

Addition of hydroxypapatite

Hydroxyapatite nanopowder (HA, average size: less than 200 nm) was purchased by Sigma Aldrich. As showed in Figure 2.3, the HA was added directly to chitosan solution (solution n.14, list § 2.1.1) before the electrospinning process. After the addition of HA nanopowder, the homogeneous chitosan/HA suspension was immediately electrospun. The presence of HA modified solution spinnability and also the yield of the process. Different amount of HA was tested, until reaching a limit of HA concentration in that chitosan solution. The obtained composite chitosan/HA membranes were crosslinked by two-steps process for 3 hours, by using GA 25% v/v aq. solution. In the following table, the amount of HA, crosslinking process and sample names are reported.

Amount of hydroxyapatite	Crosslinking process	Crosslinker	Sample name
5 % w/w respect to chitosan	None	None	ESCSHA5
5 % w/w respect to chitosan	Two-steps (3 hours)	GA (25% v/v)	ESCSHA5XL
10 % w/w respect to chitosan	None	None	ESCSHA10
10 % w/w respect to chitosan	Two-steps (3 hours)	GA (25% v/v)	ESCSHA10XL
30 % w/w respect to chitosan	None	None	ESCSHA30
30 % w/w respect to chitosan	Two-steps (3 hours)	GA (25% v/v)	ESCSHA30XL

Table 2.2 Summary of HA amount, crosslinking process and related sample name.

Addition of bioactive glass

Bioactive glass (BG) powder was obtained by sol-gel process, accordingly to Rainer *et al.* [1]. Briefly, for the preparation of the bioglass, a sol–gel technique was used, according to Vallet-Regì *et al.* [2]. Tetraethylorthosilicate (TEOS, Sigma Aldrich, 99%), triethylphosphate (Sigma Aldrich, 99%) and calcium nitrate hexahydrate (Sigma Aldrich, 99%) were mixed in a Teflon beaker, in the stoichiometric ratio

SiO_2:CaO:P_2O_5 = 70:26:4. For a batch containing 25 mL of TEOS, 19 mL of 1 M nitric acid was added as a catalyst. Gelation was performed at 70 °C for 3 days. After desiccation, performed at 150 °C for 24 h, the product obtained was crushed to obtain a powder.

BG particles were homogeneously dispersed in the chitosan solution (solution n.14, list § 2.1.1) before the electrospinning process. The obtained homogeneous suspension was immediately electrospun. It was performed the electrospinning of two different solution concentrations, the first one contained 2 wt% of BG powder respect to chitosan, was used to investigate the suspension stability before, during and after the process of electrospinning. After checking solution stability, conductivity and effects on the yield of the electrospinning process respect to electrospun pure chitosan, the other solution tested contained 15 wt% of BG powder respect to chitosan. The obtained composite chitosan/BG membranes were crosslinked by two-steps process for 3 hours, by using GA 25% v/v aq. solution. In the following table, the amount of BG, crosslinking process and sample names are reported.

Amount of BG	Crosslinking process	Crosslinker	Sample name
2 % w/w respect to chitosan	None	None	ESCSBG2
2 % w/w respect to chitosan	Two-steps (3 hours)	GA (25% v/v)	ESCSBG2XL
15 % w/w respect to chitosan	None	None	ESCSBG15
15 % w/w respect to chitosan	Two-steps (3 hours)	GA (25% v/v)	ESCSBG15XL

Table 2.3 Summary of BG amount, crosslinking process and related sample name.

Salts addition

The effects of the addition of several salts to chitosan solution were investigated in terms of improvement of solution spinnability and solution preservation before the electrospinning process (as previously reported in literature [3]). The selected salts were sodium chloride, calcium chloride and magnesium chloride, all of them purchased from Sigma Aldrich. Salts amount was added to chitosan solution (solution n.14, list § 2.1.1), just before the electrospinning process. The amount of salt concentration was fixed at

1.67 % w/w respect to chitosan. For what concerns sodium chloride, also a double concentration was tested. The obtained membranes were crosslinked by two-steps process for 3 hours, by using GA 25% v/v aq. solution. In the following table, the salt type, salt amount, crosslinking process and sample names are reported.

Salt type	Amount of salt	Crosslinking process	Crosslinker	Sample name
NaCl	1.67 % w/w respect to chitosan	None	None	ESCSNa1
	1.67 % w/w respect to chitosan	Two-steps (3 hours)	GA (25% v/v)	ESCSNa1XL
	3.33 % w/w respect to chitosan	None	None	ESCSNa3
	3.33 % w/w respect to chitosan	Two-steps (3 hours)	GA (25% v/v)	ESCSNa3XL
$CaCl_2$	1.67 % w/w respect to chitosan	None	None	ESCSCa
	1.67 % w/w respect to chitosan	Two-steps (3 hours)	GA (25% v/v)	ESCSCaXL
$MgCl_2$	1.67 % w/w respect to chitosan	None	None	ESCSMg
	1.67 % w/w respect to chitosan	Two-steps (3 hours)	GA (25% v/v)	ESCSMgXL

Table 2.4 Summary of salt type, salt amount, crosslinking process and sample name.

2.2 Composite scaffolds fabrication

A simple method for the fabrication of stratified composite scaffolds by the deposition of a thin chitosan nanofibrous layer on a rigid porous bioactive glass foam-like substrate was developed. These two layers are assembled through a polymeric solution which should act as a functional "glue" to effectively join the nanofibrous membrane to the porous glass substrate, absolving also the function of coating for the Bioglass®-based scaffold, thereby improving its mechanical properties without modifying its intrinsic porous structure.

2.2.1 Bioglass® scaffolds fabrication by foam replica method

Bioglass® rigid substrate for composite scaffolds were fabricated by using the foam replica method, according to [4] and briefly reported in § 2.4.3. Materials used in that process are polyurethane (PU) foam with 45 ppi (pores per inch) (Eurofoam GmbH, Wiesbaden, Germany) as sacrificial materials, and for the slurry polyvinylalcohol (PVA, Merck KGaA, Darmstadt, Germany) dissolved in DI water at the concentration of 1,5 10^{-3} M containing 40 wt% of bioactive glass powder. Bioglass® powder was provided by collaborators at University of Erlangen-Nuremberg, Germany (45S5 Bioglass® (Vitryxx® SCHOTT, Mainz, Germany); mean size < 5.0 μm).

2.2.2 Intermediate layer solutions

All the reagents (chitosan, sodium alginate, gelatin, sucrose, calcium chloride, acetic acid) were purchased by Sigma Aldrich, except from sodium hydroxide that was purchased from Merck. The detailed protocols related to bioglass® porous substrate coating and the stratified composite scaffold fabrication are reported in § 2.4.2.2.

Considering the behavior of chitosan electrospun membrane in aqueous solutions, and with the aim of using a solution that could be a chitosan solvent, promoting, in this way, the attachment of the electrospun meshes, the first tests have been performed with the following solutions:

1. DI water
2. Acetic Acid: 2 % v/v Acetic Acid (AA) aq. solution

Then also polymeric solutions were used for bioglass scaffold coating and electrospun membranes attachment:

1. Chitosan Solution: 4 % w/v chitosan (MMW) in 2 % v/v Acetic Acid aq. solution
2. Chitosan Solution: 2 % w/v chitosan (MMW) in 2 % v/v Acetic Acid aq. solution
3. Chitosan Solution: 2 % w/v chitosan (MMW) in 5 % v/v Acetic Acid aq. solution
4. Gelatin solution: 2 % w/v gelatin (from porcine skin, G1890, Sigma) in DI water

5. Gelatin solution: 1 % w/v gelatin in DI water
6. Sucrose: 10 % w/v sucrose in DI water
7. Sodium alginate solution: 2 % w/v sodium alginate in DI water
8. Chitosan/sodium alginate solution: 4,8 % w/v chitosan/sodium alginate (1:1)

2.2.3 Electrospun chitosan membranes

All the chitosan crosslinked electrospun membranes were fabricated accordingly to §2.4.1. and their composition was previously reported in §2.1. Pure chitosan, chitosan/HA and chitosan/BG electrospun crosslinked samples were used.

2.3 Chitosan-based foam scaffolds fabrication

In order to obtain foam scaffolds able to induce cell signaling and induction towards chondrogenesis and/or osteogenesis pathway, foam scaffolds composed by pure chitosan and chitosan doped with the addition of nanopowder of hydroxyapatite (HA) and bioactive glass (BG) particles were fabricated. Chitosan-based foam scaffolds were fabricated by using phase separation-based techniques.

The chitosan solutions employed for these experimental activities were the following:

- 2% w/v chitosan (MMW, Sigma Aldrich) in 2% v/v aq. solution of acetic acid (AA, Panreac) [SOL. A];
- 2% w/v chitosan (MMW, Sigma Aldrich) in 2% v/v aq. solution of lactic acid (LA, Sigma Aldrich) [SOL. B];

The selected crosslinker agent for these scaffolds was the glutaraldehyde (GA, Sigma Aldrich). Several crosslinking tests (e.g. several concentrations of GA, expressed in terms of molar ratio, respect to chitosan) were performed in order to evaluate and optimize chitosan crosslinking. In the following table, all the values related to added GA amount respect to chitosan (molar ratio) are reported.

For what concerns doped samples, the addition of HA and BG (10% w/w respect to chitosan, for both HA and BG) introduced some modification (i.e. the amount of GA, as listed in the following table) and other steps in the protocol used for pure chitosan (reported in details in § 2.4.2).

Chitosan-based solution	GA aq. solution [% v/v]	GA amount respect to chitosan [% mol/mol]	Note	Protocols used for foam scaffold fabrication (see § 2.4.2)
SOL. A	4 %	1%	Effective crosslinking in time not useful for the application (slow crosslinking)	1
SOL. A	4 %	1,5%	Effective crosslinking in time not useful for the application (slow crosslinking)	1
SOL. A	4 %	2%	Optimization between effective crosslinking and time of crosslinking	1
SOL. A	4 %	3%	Effective crosslinking in time not useful for the application (fast crosslinking)	1
SOL. A	4 %	10%	Effective crosslinking in time not useful for the application (fast crosslinking)	1
SOL. B	4 %	1%	Effective crosslinking in time not useful for the application (slow crosslinking)	1
SOL. B	4 %	1,5%	Effective crosslinking in time not useful for the application (slow crosslinking)	1
SOL. B	4 %	2%	Optimization between effective crosslinking and time of crosslinking	1, 2, 3
SOL. B	4 %	3%	Effective crosslinking in time not useful for the application (fast crosslinking)	1
SOL. B	4 %	10%	Effective crosslinking in time not useful for the application (fast crosslinking)	1
SOL. A + addition of HA	4 %	2%	Effective crosslinking in time not useful for the application (fast crosslinking)	1
SOL. A + addition of HA	4 %	1%	Optimization between effective crosslinking and time of crosslinking	1
SOL. B + addition of HA	4 %	2%	Effective crosslinking in time not useful for the application (fast crosslinking)	1, 2, 3
SOL. B + addition of	4 %	1%	Optimization between effective crosslinking and	1

HA			time of crosslinking	
SOL. B + addition of BG	4 %	2%	Effective crosslinking in time not useful for the application (fast crosslinking)	2
SOL. B + addition of BG	4 %	1%	Optimization between effective crosslinking and time of crosslinking	2

Table 2.5 Summary of crosslinker (GA) solution concentration in chitosan solution, crosslinking tests and protocol type for foam fabrication.

2.4 Scaffolds fabrication techniques

2.4.1 Electrospinning

A typical electrospinning standard setup was showed in the following figure. The electrospinning setup used for these experimental activities was constituted by an high voltage generator (ES30, Series ES, Gamma High Voltage Research, Ormond Beach, FL), a syringe pump (KD100, KD Scientific, Holliston, MA) for the regulation of the flow rate of the polymeric solution, contained in a glass syringe, and a metallic grounded fiber collector. All the experiments were performed at room temperature and in non-conditioned atmosphere.

The main electrospinning parameters, as distance tip-collector, voltage value, solution flow rate, needle diameter used for chitosan electrospun membranes fabrication were reported in the following tables and they are grouped accordingly to the same classification presented above in §2.1.

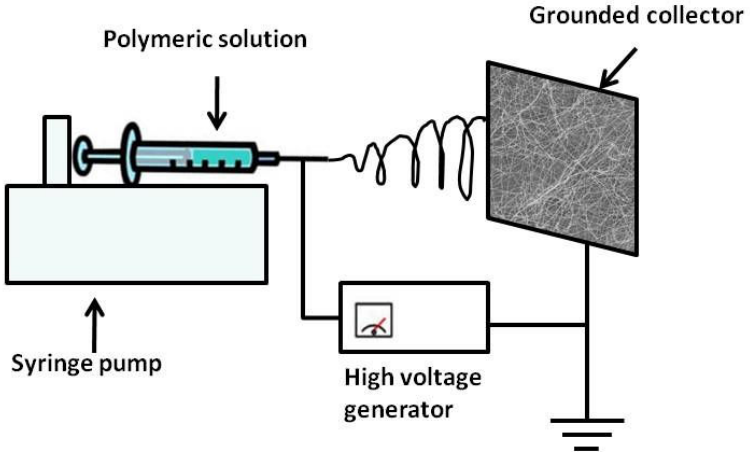

Figure 2.4 Schematic diagram of standard electrospinning setup, similar to the setup used for the experimental activities presented in this thesis work.

Electrospun pure chitosan meshes

In the following table are listed all the electrospinning parameters tested, and a brief comment about each solution, in order to justify all performed tests aimed to optimize the combination of chitosan solutions and the electrospinning parameters.

	Solutions	**Electrospinning parameters**
1	**4 % w/v chitosan in AA (aq. solution 30%v/v)**	Distance tip-target: range between 5 to 15 cm. Solution feed rate: range between 1.5 to 5 mL/h. Voltage: range between 10 to 25 kV. Note: Only drops on the target (electrospraying). Electrospraying phenomena reduced by increasing polymeric solution feed rate (i.e. 5 mL/h). No samples preserved for further investigations.
2	**2.5 % w/v chitosan in AA (aq. solution 90% v/v)**	Fibers and drops on the target. Distance tip-target: tested range from 5 to 15 cm, good results (target covered by white layer) with 5-7 cm. Solution feed rate: too high value (i.e. 5 mL/h) or too low value (i.e. 1 mL/h) lead to drops deposition on the target. Good range between 3 and 4 mL/h, evaluated in terms of deposition of white layer on the target (it was not possible separate the white layer from the Al substrate). Voltage: tested the range between 15 and 30 kV (increasing 1 kV, for each test). The others parameters were fixed at the following values: distance tip-target: 7 cm; solution feed-rate: 4 mL/h. Good results (target covered by white layer) for the range 20-25 kV.
3	**4 % w/v chitosan in AA (aq. solution 90% v/v)**	It was not possible to electrospin that solution.
4	**2 % w/v chitosan in AA (aq. solution 90% v/v)/DCM (80:20)**	Drops on the target. Distance tip-target: range: 7 -10 cm. Solution feed rate: range: 1.0 – 3.0 mL/h. Voltage: range: 10-25 kV. No samples preserved for further investigations.
5	**2.6% w/v chitosan in AA/DCM (80:20)**	It was not possible to electrospin that solution.
6	**4 % w/v chitosan in AA/DCM (70:30)**	It was not possible to electrospin that solution.
7	**3% w/v chitosan in aq. lactic acid solution (2% v/v in DI water)**	Only drops on the target (electrospraying)

8	**2.7% w/v chitosan in TFA**	Distance tip-collector	voltage	solution feed rate	needle diameter	
		15 cm	15 kV	2 mL/h	23G	
		7 cm	26 kV	1.2 mL/h	23G	
		Not fibers collected on the target. (it was not possible separate the white layer from the Al substrate)				
9	**5% w/v chitosan in TFA**	Distance tip-collector	voltage	solution feed rate	needle diameter	
		5 cm	20 kV	0.05 mL/h	21G	No fibers
		5 cm	20 kV	0.1 mL/h	21G	No fibers
		4 cm	18 kV	0.15 mL/h	21G	No fibers
		4 cm	18 kV	0.15 mL/h	21G	
		10 cm	18 kV	0.2 mL/h	21G	
10	**6% w/v chitosan in TFA**	Distance tip-collector	voltage	solution feed rate	needle diameter	
		8 cm	17 kV	0.5 mL/h	21G	
		10 cm	17 kV	0.5 mL/h	21G	No fibers
		8 cm	17 kV	0.2 mL/h	21G	
		10 cm	17 kV	0.3 mlLh	21G	
11	**8% w/v chitosan in TFA**	Distance tip-collector	voltage	solution feed rate	needle diameter	
		10 cm	17 kV	0.8 mL/h	21G	
		10 cm	20 kV	0.8 mL/h	21G	No fibers
		10 cm	20 kV	0.5 mL/h	21G	
		10 cm	23 kV	0.5 mL/h	21G	
12	**4% w/v chitosan in TFA/DCM (80:20)**	Distance tip-collector	voltage	solution feed rate	needle diameter	
		15 cm	15 kV	0.03 mL/h	21G	No fibers
		10 cm	15 kV	0.03 mL/h	21G	No fibers
		15 cm	15 kV	0.10 mL/h	21G	No fibers
		10 cm	15 kV	0.10 mL/h	21G	
		10 cm	15 kV	0.05 mL/h	21G	
		10 cm	15 kV	0.20 mL/h	21G	
		15 cm	15 kV	0.15 mL/h	21G	
		10 cm	20 kV	0.10 mL/h	21G	
		10 cm	20 kV	0.05 mL/h	21G	
		10 cm	20 kV	0.15 mL/h	21G	
13	**8% w/v chitosan in TFA/DCM (80:20)**	Distance tip-collector	voltage	solution feed rate	needle diameter	
		15 cm	15 kV	0.10 mL/h	21G	
		15 cm	15 kV	0.15 mL/h	21G	
		15 cm	20 kV	0.10 mL/h	21G	
14	**10% w/v chitosan in TFA/DCM (80:20)**	Distance tip-collector	voltage	solution feed rate	needle diameter	
		15 cm	15 kV	0.10 mL/h	21G	
		15 cm	15 kV	0.10 mL/h	23G	

Table 2.6 Electrospinning parameters for the optimization of pure chitosan electrospun meshes fabrication.

One-step crosslinking process on chitosan electrospun meshes

Electrospinning parameters related to one-step crosslinking process (crosslinking is embedded in the electrospinning process) are reported in the following table.

Polymeric solution	Crosslinker	Distance tip-collector [cm]	Voltage [kV]	Solution Flow Rate [ml·h^{-1}]	Needle diameter [Gauge]
ESCSXLGA4	GA	15	14	0.1	23
ESCSXLGA10	GA	15	15	0.1	23
ESCSXLGA50	GA	15	15	0.1	23
ESCSXLGEN8	GEN	12	18	0.2	21
ESCSXLGEN20	GEN	12	18	0.25	21

Table 2.7 Electrospinning parameters for the optimization of one-step crosslinking process of chitosan electrospun meshes, by using different crosslinker agents.

Functionalization of chitosan-based electrospun membranes

In this section the electrospinning parameters for functionalized electrospun chitosan-based meshes are summarized in two devoted subsection. Another subsection contains electrospinning parameters related to salts addition.

Addition of hydroxypapatite

All the electrospinning parameters related to chitosan/HA suspensions (§ 2.1.3) are reported in table 2.8. The section note containing comments about solution spinnability, reveals that a great amount of HA (as 30 wt% respect to chitosan) does not allow the fabrication of electrospun meshes.

Polymeric solution	Distance tip-collector [cm]	Voltage [kV]	Solution Flow Rate [ml·h^{-1}]	Needle diameter [Gauge]	Note
ESCSHA5	15	15	0.15	23	
ESCSHA10	15	15	0.15	23	
ESCSHA30	--	--	--	--	It is not possible to electrospin that solution

Table 2.8 Electrospinning parameters for chitosan/HA solutions.

Addition of bioactive glass

The addition of bioactive glass particles affected chitosan solution spinnability, in fact it was necessary the variation of several parameters values respect to pure chitosan solution, as reported in the following table.

Polymeric solution	Distance tip-collector [cm]	Voltage [kV]	Solution Flow Rate [ml·h^{-1}]	Needle diameter [Gauge]
ESCSBG2	15	18	0.2	21
ESCSBG15	15	18	0.5	21

Table 2.9 Electrospinning parameters for chitosan/BG solutions.

Salts addition

All the electrospinning parameters related to the addition of salts to chitosan solutions (§ 2.1.3) are reported in table 2.10.

Polymeric solution	Distance tip-collector [cm]	Voltage [kV]	Solution Flow Rate [ml·h^{-1}]	Needle diameter [Gauge]
ESCSNa1	15	15	0.3	21
ESCSNa3	15	15	0.3	21
ESCSCa	15	15	0.3	21
ESCSMg	15	15	0.3	21

Table 2.10 Electrospinning parameters for chitosan-based solutions with the addition of salts.

2.4.2 Fabrication of composite scaffolds

For stratified composite scaffolds fabrication, the manufacturing techniques involved a combination of methods, including: the sponge replica method for bioactive glass scaffold fabrication, acting as substrate, drying at room temperature, freeze drying and freeze gelation methods for the synthesis of the intermediate layer and the electrospinning for the fabrication of the upper nanofibrous layer.

The foam replica method, according to [4], used for 45S5 Bioglass® porous scaffolds fabrication, was reported in detail in the following paragraph (§ 2.4.2.1).

Considering that the intermediate layer has to absolve the function of coating for bioglass® substrate, without closing its porosity, and "gluing" the upper electrospun layer, for the synthesis of this intermediate layer has been applied the fabrication techniques usually employed for foam scaffolds fabrication as freeze drying and freeze gelation [5, 6].

For the upper layer chitosan-based crosslinked electrospun membranes (as reported in § 2.2.3) were used.

The schematic representation of the entire process of stratified composite scaffolds fabrication is briefly illustrated in the following figure.

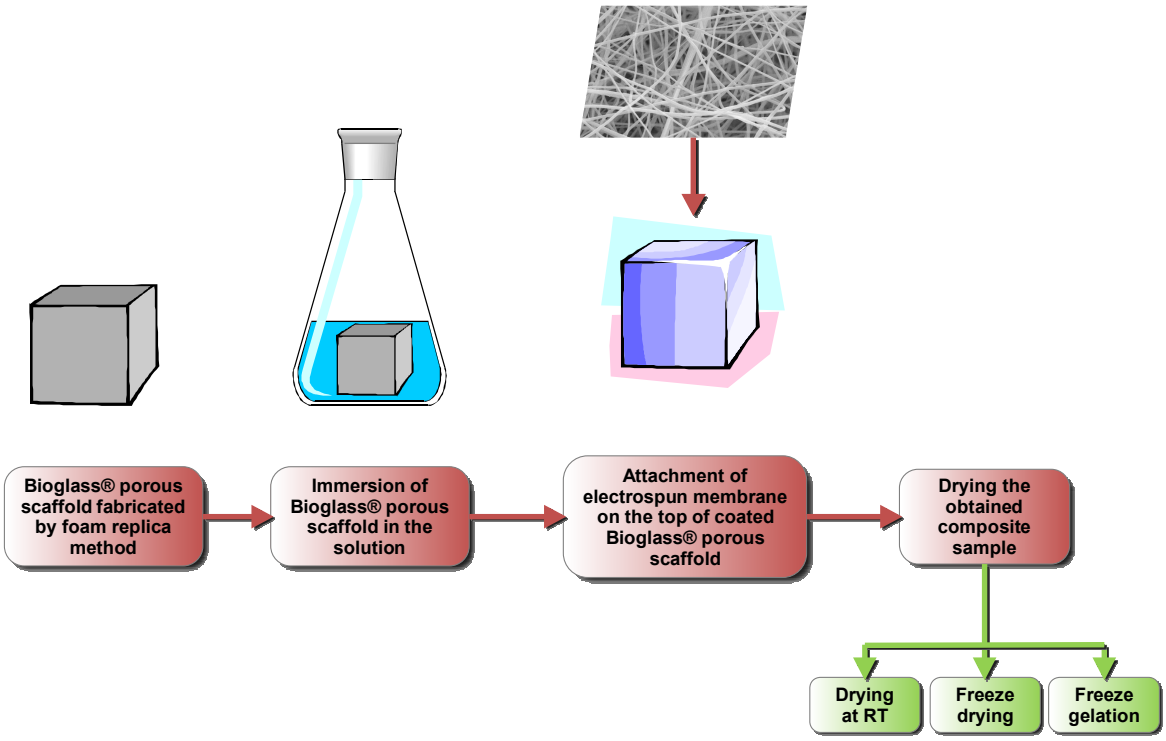

Figure 2.5 Schematic representation of the protocol for composite scaffold fabrication, by integrating several well-known scaffold fabrication techniques.

Briefly, bioglass® scaffolds fabricated by foam replica-method were immersed in an intermediate layer solution (all tested solutions are listed in § 2.2.2), after removing the excess of solution, when the sample was still wet, the electrospun membrane was put on the top of the sample. The obtained sample was then dried, according to the protocol reported for each type of intermediate layer solution in § 2.4.2.2.

2.4.2.1 Foam replica method for Bioglass® scaffold fabrication

The foam replica method for the fabrication of 45S5 Bioglass® macroporous scaffolds is schematically reported in the following diagram.

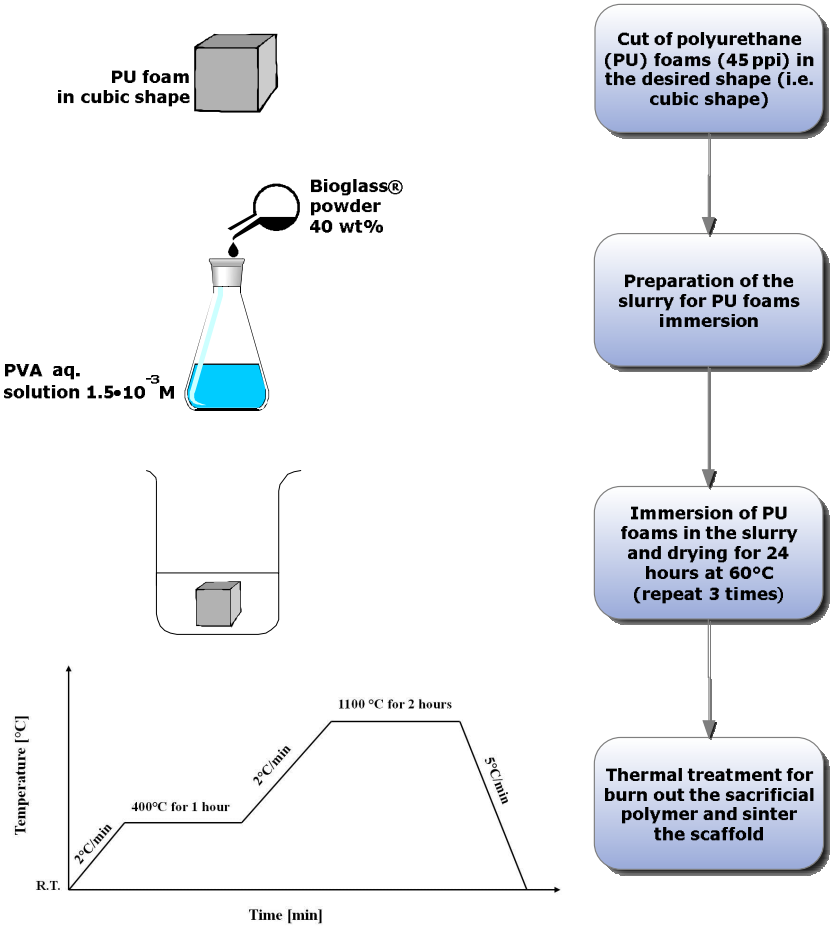

Figure 2.6 Schematic diagram reporting the main steps of the protocol for 45S5 Bioglass® scaffolds fabrication.

As showed in figure 2.6, the sacrificial template for the replica method was a polyurethane (PU) foam with 45 ppi (pores per inch) (Eurofoam GmbH, Wiesbaden, Germany). The foam, cut in a cubic shape (10x10x10 mm^3), was immersed in a slurry prepared from polyvinylalcohol (PVA) (Merck KGaA, Darmstadt, Germany) dissolved in water at the concentration of $1{,}5 \cdot 10^{-3}$ M containing 40 wt% of bioactive glass powder (mean size < 5.0 μm). The rinsed foam was tweezed manually in order to remove the excess of slurry and dried at 60 °C for 24 hours. The rinsing and the following drying steps were repeated three times. Finally, a heat treatment was necessary in order to burnout the sacrificial PU foam and to sinter the Bioglass® powder. This process was carried out at 1100 °C for 2 hours, with a previous hold at 400 °C for 1 hour.

2.4.2.2 Solutions and protocols for gluing electrospun nanofibrous membrane to Bioglass® macroporous scaffold

As previously grouped in § 2.2.2, in tables 2.11 and 2.12 are reported the solutions, the protocols for the intermediate layer of stratified scaffold fabrication, the drying techniques, and the kind of electrospun (ES) membrane put on the top of the coated substrate.

The first tests have been performed with the following solutions:

1. DI water
2. Acetic Acid: 2 % v/v Acetic Acid (AA) aq. solution

Solution	Sample	Protocol	Drying Technique	ES membrane
DI water	DIW_1	- Cut the BG sample to smooth the surface - Drop dH_20 on BG sample - When BG sample is completely wet, put ES membrane on it - Dry at RT (on tissue paper)	Dry at RT	ESCSXLGA50
"	DIW_2	- Cut the BG sample to smooth the surface - Drop dH_20 on BG sample - When BG sample is completely wet, put ES membrane on it - Dry at RT (on tissue paper)	Dry at RT	ESCSHA10XL
Acetic Acid (2% v/v aq sol)	AA_1	- Cut the BG sample to smooth the surface - Drop Acetic Acid solution on BG sample - When BG sample is completely wet, put ES membrane on it - Dry at RT (on tissue paper)	Dry at RT	ESCSXLGA50
"	AA_2	- Cut the BG sample to smooth the surface - Drop Acetic Acid solution on BG sample - When BG sample is completely wet, put ES membrane on it - Dry at RT (on tissue paper)	Dry at RT	ESCSHA10XL

Table 2.11 Interface solutions, electrospun membranes and protocols for bioactive glass coating.

The polymeric solutions used for bioglass scaffold coating are:

1. Chitosan Solution: 4 % w/v chitosan (MMW) in 2 % v/v Acetic Acid aqueous solution
2. Chitosan Solution: 2 % w/v chitosan (MMW) in 2 % v/v Acetic Acid aqueous solution
3. Chitosan Solution: 2 % w/v chitosan (MMW) in 5 % v/v Acetic Acid aqueous solution
4. Gelatin solution: 2 % w/v gelatin (from porcine skin, G1890, Sigma) in DI water
5. Gelatin solution: 1 % w/v gelatin in DI water
6. Sucrose: 10 % w/v sucrose in DI water
7. Sodium alginate solution: 2 % w/v sodium alginate in DI water
8. Chitosan/sodium alginate solution: 4,8 % w/v chitosan/sodium alginate (1:1)

In the following table the solutions, protocols, ES membranes, drying techniques and sample name are reported. In particular sample name is assigned following this order rules:

- Drying technique (D = drying at RT; F.D. = Freeze drying, followed by the time of F.D.; F.G. = Freeze gelation),
- Polymer (C = chitosan; G = gelatin; S = sucrose; A = alginate)
- Solution concentration (in the case of solutions 2 and 3, listed above, the solvent concentration is also reported)
- Progressive number for different kind of attached ES membranes

Solution	Sample	Protocol	Drying Technique	ES membrane
Chitosan (4 % w/v chitosan in 2%v/v AA aq. sol)	D._C4_1	- Cut the BG sample to smooth the surface - Rinse the BG in 4 % w/v chitosan solution for 30 sec - Do not remove the excess of solution - Put ES membrane on the surface - Dry at RT (on tissue paper)	Dry at RT	ESCSXLGA50
	D._C4_2	- Cut the BG sample to smooth the surface	Dry at RT	ESCSXLGA50

		- Rinse the BG in 4 % w/v chitosan solution for 5 min - Remove the excess of solution from BG - Put ES membrane on the surface - Dry at RT (on tissue paper)		
	D._C4_3	- Cut the BG sample to smooth the surface - Drop DI water on BG - Rinse the BG in 4 % w/v chitosan solution for 10 min - Remove the excess of solution from BG - Put ES membrane on the surface - Dry at RT (on tissue paper)	Dry at RT	ESCSXLGA50
	D._C4_4	- Cut the BG sample to smooth the surface - Rinse the BG in 4 % w/v chitosan solution for 10 min - Remove the excess of solution from BG - Put ES membrane on the surface - Dry at RT (on tissue paper)	Dry at RT	ESCSHA10XL
	D._C4_5	- Cut the BG sample to smooth the surface - Rinse the BG in 4 % w/v chitosan solution for 10 min - Remove the excess of solution from BG - Put ES membrane on the surface - Dry at RT (on tissue paper)	Dry at RT	ESCSHA10XL
	F.D._C4_6	- Cut the BG sample to smooth the surface - Rinse the BG in 4 % w/v chitosan solution for 10 min	Freeze drying	ESCSHA10XL

		- Remove the excess of solution from BG - Put ES membrane on the surface - After drying at RT, put the sample at -20°C overnight - Put sample in freeze dryer for 5h		
	F.D.5_C4_7	- Cut the BG sample to smooth the surface - Rinse the BG in 4 % w/v chitosan solution for 10 min - Remove the excess of solution from BG - Put ES membrane on the surface - After drying at RT, put the sample at -20°C overnight - Put sample in freeze dryer for 5h	Freeze drying	ESCSXLGA50
	F.D.24_C4_8	- Cut the BG sample to smooth the surface - Rinse the BG in 4 % w/v chitosan solution for 10 min - Remove the excess of solution from BG - Put ES membrane on the surface - After drying at RT, put the sample at -20°C overnight - Put sample in freeze dryer for 24h	Freeze drying	ESCSHA10XL
Chitosan (2%w/v chitosan in 2%v/v AA aq. sol)	F.D.24_C2_2_1	- Cut the BG sample to smooth the surface - Rinse the BG in 2 % w/v chitosan solution for 10 min - Remove the excess of solution from BG - Put ES membrane on the surface - After drying at RT, put	Freeze drying	ESCSHA10XL

		the sample at -20°C overnight - Put sample in freeze dryer for 24h		
	F.D.24_C2_2_2	- Cut the BG sample to smooth the surface - Rinse the BG in 2 % w/v chitosan solution for 10 min - Remove the excess of solution from BG - Put ES membrane on the surface - After drying at RT, put the sample at -20°C overnight -Put sample in freeze dryer for 24h	Freeze drying	ESCSHA10XL
	F.D.24_C2_2_3	- Cut the BG sample to smooth the surface - Rinse the BG in 2 % w/v chitosan solution for 10 min - Remove the excess of solution from BG - Put ES membrane on the surface - After drying at RT, put the sample at -20°C overnight - Put sample in freeze dryer for 24h	Freeze drying	ESCSXL3
Chitosan (2%w/v chitosan in 5%v/v AA aq. sol)	F.D.90_C2_5_1	- Cut the BG sample to smooth the surface - Rinse the BG in 2 % w/v chitosan solution for 10 min - Remove the excess of solution from BG - Put ES membrane on the surface - After drying at RT, put the sample at -20°C overnight - Immerse samples in precooled (-20°C) solution 0,75%w/v NaOH	Freeze drying	ESCSBGXL

		in EtOH/DI water for 15 min at -20°C - Freeze drying for 90h		
	F.D.90_C2_5_2	- Cut the BG sample to smooth the surface - Rinse the BG in 2 % w/v chitosan solution for 10 min - Remove the excess of solution from BG - Put ES membrane on the surface - After drying at RT, put the sample at -20°C overnight - Immerse samples in precooled (-20°C) solution 0,75%w/v NaOH in EtOH/DI water for 15 min at -20°C - Freeze drying for 90h	Freeze drying	ESCSXL3
	F.G._C2_5_3	- Cut the BG sample to smooth the surface - Rinse the BG in 2 % w/v chitosan solution for 10 min - Remove the excess of solution from BG - Put ES membrane on the surface - After drying at RT, put the sample at -20°C overnight - Immerse samples in precooled (-20°C) solution 0,75%w/v NaOH in EtOH/DI water for 15 min at -20°C - Dry at RT	Freeze gelation	ESCSBGXL
	F.G._C2_5_4	- Cut the BG sample to smooth the surface - Rinse the BG in 2 % w/v chitosan solution for 10 min - Remove the excess of solution from BG - Put ES membrane on the surface	Freeze gelation	ESCSXL3

		- After drying at RT, put the sample at -20°C overnight - Immerse samples in precooled (-20°C) solution 0,75%w/v NaOH in EtOH/DI water for 15 min at -20°C - Dry at RT		
Gelatin (2 % w/v gelatin in DI water)	D._G2_1	- Cut the BG sample to smooth the surface - Rinse the BG in 2 % w/v gelatin solution for 2 min - Remove the excess of solution from BG - Put ES membrane on the surface - Dry at RT for 1h - Rinse sample in DI water for 2 min to remove gelatin - Dry at RT	Dry at RT	ESCSHA10XL
	D._G2_2	- Cut the BG sample to smooth the surface - Rinse the BG in 2 % w/v gelatin solution for 2 min - Remove the excess of solution from BG - Put ES membrane on the surface - Dry at RT for 1h - Rinse sample in DI water for 2 min to remove gelatin - Dry at RT	Dry at RT	ESCSXLGA50
	D._G2_3	- Cut the BG sample to smooth the surface - Rinse the BG in 2 % w/v gelatin solution for 2 min - Remove the excess of solution from BG - Put ES membrane on the surface - Dry at RT	Dry at RT	ESCSHA10XL
	D._G2_4	- Cut the BG sample to smooth the surface - Rinse the BG in 2 % w/v	Dry at RT	ESCSXLGA50

		gelatin solution for 2 min - Remove the excess of solution from BG - Put ES membrane on the surface - Dry at RT		
Gelatin (1 % w/v gelatin in DI water)	D._G1_1	- Cut the BG sample to smooth the surface - Rinse the BG in 2 % w/v gelatin solution for 2 min - Remove the excess of solution from BG - Put ES membrane on the surface - Dry at RT for 1h - Rinse sample in DI water for 2 min to remove gelatin - Dry at RT	Dry at RT	ESCSBGXL
Sucrose (10 % w/v sucrose in DI water)	D._S10_1	- Cut the BG sample to smooth the surface - Drop dH_20 on BG sample - Rinse BG sample in sucrose solution for 10 min. - Put the ES membrane on wet BG sample - Dry at RT (on tissue paper)	Dry at RT	ESCSHA10XL
	D._S10_2	- Cut the BG sample to smooth the surface - Drop dH_20 on BG sample - Rinse BG sample in sucrose solution for 10 min. - Put the ES membrane on wet BG sample - Dry at RT (on tissue paper)	Dry at RT	ESCSXLGA50
	D._S10_3	- Cut the BG sample to smooth the surface - Drop dH_20 on BG sample - Rinse BG sample in sucrose solution for 10 min. - Put the ES membrane on	Dry at RT	ESCSBG15XL

		wet BG sample - Dry at RT (on tissue paper)		
Sodium alginate (2 % w/v Sodium alginate in DI water)	F.D.24_A2_1	- Cut the BG sample to smooth the surface - Rinse the BG in 2 % w/v alginate solution for 10 min - Remove the excess of solution from BG - Put ES membrane on the surface - Immerse sample in $CaCl_2$ solution (0,5M in dH_20) - After drying at RT, put the sample at -20°C overnight -Put sample in freeze dryer for 24h	Freeze drying	ESCSHA10XL
	F.D.90_A2_2	- Cut the BG sample to smooth the surface - Rinse the BG in 2 % w/v alginate solution for 10 min - Remove the excess of solution from BG - Put ES membrane on the surface - Frozen at -20°C for 24 h - Immerse sample in a precooled (-20°C) $CaCl_2$ solution (4% w/v in EtOH/dH_20) for 15 min at -20°C -Put sample in freeze dryer for 90h	Freeze drying	ESCSBGXL
	F.D.90_A2_3	- Cut the BG sample to smooth the surface - Rinse the BG in 2 % w/v alginate solution for 10 min - Remove the excess of solution from BG - Put ES membrane on the surface - Frozen at -20°C for 24 h - Immerse sample in a	Freeze drying	ESCSXL3

		precooled (-20°C) $CaCl_2$ solution (4% w/v in EtOH/dH_20) for 15 min at -20°C -Put sample in freeze dryer for 90h		
	F.G._A2_4	- Cut the BG sample to smooth the surface - Rinse the BG in 2 % w/v alginate solution for 10 min - Remove the excess of solution from BG - Put ES membrane on the surface - Frozen at -20°C for 24 h - Immerse sample in a precooled (-20°C) $CaCl_2$ solution (4% w/v in EtOH/dH_20) for 15 min at -20°C -Dry at RT	Freeze gelation	ESCSBGXL
Chitosan/Alginate (4,8 % w/v chitosan:alginate (1:1))	F.D.90_CA_1	- Cut the BG sample to smooth the surface - Rinse the BG in 4,8 % w/v chitosan/alginate solution for 10 min - Remove the excess of solution from BG - Put ES membrane on the surface - Frozen at -20°C for 6 h - Freeze drying for 24 h - Immerse sample in $CaCl_2$ solution (1% w/v in dH_20) for 15 min - Rinse with dH_20 - -Freeze drying for 90h	Freeze drying	ESCSBGXL

Table 2.12 Interface polymeric solutions, electrospun membranes and protocols for bioactive glass coating. (Abbreviations: min= minutes, h= hours).

2.4.3 Techniques for chitosan-based foams fabrication

In order to obtain foam scaffolds, three different protocols were used.

The first protocol (n. 1, as previously cited in table 2.5) is reported below:

1. Filter the chitosan solutions, SOL. A and B, in order to remove all the impurities (by using a filter having 70 μm cut off).
2. Insert GA to both chitosan solutions (GA amount respect to chitosan: 2% mol/mol).
3. Stir the obtained solution manually, insert the solution in the container of desired shape.
4. Put the obtained solutions at – 80 °C, overnight.
5. Immerse the samples in precooled acetone at – 20 °C and leave in immersion at – 20 °C for 15 minutes.
6. Rinse the samples in 1M NaOH aq. solution and wash them in DI water.
7. Put the sample in the Critical Point Drier (CPD) (K850 CPD, EMITECH, Ashford, UK) overnight.

For what concerns samples doped by the addition of hydroxyapatite (HA) nanopowder, some differences were introduced in the previous protocol. In fact, the addition of HA (10% w/w respect to chitosan) was performed just after the chitosan solution filtration. The suspension was then stirred until that the it became homogeneous. After that, GA was added (the amount of GA was reduced to 1% mol/mol respect to chitosan).

The initial thermal treatments were performed in order to regulate foam pore size, according to previous investigations [7]. By using this protocol, the acetone substitutes ice crystals, preserving foam porosity. The obtained samples microstructure was investigated by SEM analysis. Not satisfied results were obtained, and other protocols were tested.

The second protocol (n. 2, as previously cited in table 2.5):

1. Filter the chitosan solution (SOL. B), in order to remove all the impurities (by using a filter having 70 μm cut off).
2. For doped samples, add HA or BG (70:26:4 bioactive glass composition) to chitosan solution (in both cases the amount of HA or BG was 10% w/w respect to chitosan).
3. Insert GA to chitosan solution (GA amount respect to chitosan: 2% mol/mol for pure chitosan samples, while is 1% mol/mol for samples with HA or BG).
4. Stir the obtained solution manually, insert the solution in the container of desired shape (usually 5 mL beaker).

5. After solution gelification, dialyze samples in NaOH 10^{-2} M for 8 hours, changing the solution 4 times. Then dialyze samples in DI water for 4 hours refreshing water 4 times.
6. Put the obtained samples at – 20 °C, overnight.
7. Put the obtained samples at – 80 °C, at least for 5 hours.
8. Lyophilize samples for 72 hours. Then put samples under vacuum until their final use.

As revealed by pH measurements, these samples are not suitable for direct use in biological applications, because their needed to be neutralized in extended NaOH bath before the uses for cellular experiments. For this reason the protocol 2 was modified as follows and is called protocol 3.

The third protocol (n. 3, as previously cited in table 2.5):

1. Filter the chitosan solution (SOL. B), in order to remove all the impurities (by using a filter having 70 μm cut off).
2. For doped samples, add HA or BG (70:26:4 bioactive glass composition) to chitosan solution (in both cases the amount of HA or BG was 10% w/w respect to chitosan).
3. Insert GA to chitosan solution (GA amount respect to chitosan: 2% mol/mol for pure chitosan samples, while is 1% mol/mol for samples with HA or BG).
4. Stir the obtained solution manually, insert the solution in the a dialysis membrane (14 kDa cut off).
5. After solution gelification, dialyze samples in DI water for 1 week, changing the solution 2 times each day.
6. Put the obtained samples at – 80 °C, at least for 5 hours.
7. Lyophilize samples for 72 hours. Then put samples under vacuum until their final use.

2.5 Scaffolds characterization techniques

2.5.1 Morphological analysis

The morphology of all electrospun chitosan-based fibers before and after crosslinking (both type of crosslinking processes) and chitosan-based foams was observed by means of Field Emission Scanning Electron Microscopy (FE-SEM, Supra 1535, Leo Electron Microscopy, Cambridge, UK). The average fiber diameter, regarding to the electrospun samples and pore size of chitosan foams were determined by image analysis (Image J, NIH, USA).

All the investigations of the composite scaffolds microstructure were performed by using a Light Microscope (Light Microscope Axioplan Lab.A1 Carl Zeiss Micro Imaging GmbH, Germany) and a Scanning Electron Microscope (SEM, Leo 435 VP, Cambridge, UK) at Friedrich Alexander University of Erlangen-Nuremberg (Department of Material Science and Engineering).

2.5.2 ATR/FT-IR analysis

The structural characterization of the electrospun chitosan-based nanofibers, before and after crosslinking, and chitosan-based foams was performed by Attenuated Total Reflectance Fourier Transform Infra-Red spectroscopy (ATR/FT-IR). ATR/FT-IR spectra were collected in the range 4000–500 cm^{-1}, on a Nicolet Nexus 8700 spectophotometer (Thermo Scientific, Waltham, MA), equipped with a Golden Gate MK2 Diamond cell (Specac, Orpington, UK). Spectra were recorded positioning the samples on cell platform operating at room temperature (32 scans, 2 cm^{-1} resolution).

Nicolet 6700 FT-IR spectrometer (Thermo Scientific, Waltham, MA), equipped with diamond ATR cell, was used for the structural characterization of composite scaffolds, at Friedrich Alexander University of Erlangen-Nuremberg (Department of Material Science and Engineering). ATR/FT-IR spectra were collected in the range 4000–525 cm^{-1} and positioning the samples on cell platform operating at room temperature (64 scans, 4 cm^{-1} resolution).

2.5.3 XRD analysis

XRD patterns of chitosan electrospun scaffolds (CSHA and CSBG) were obtained at room temperature using a Panalytical X'PERT PRO diffractometer (Cu Kα radiation) operating at a voltage of 40 kV. XRD was taken at 2ϑ angle range of 10–40° and the process parameters were: scan step size 0.002 (7 hours) and time per step 4 s.

2.5.4 Mechanical properties

Tensile tests for electrospun samples

In order to reduce the operator-dependant bias introduced during electrospun samples preparation for the tensile tests, a devoted fiber collector was developed. This target, showed in the following figure (in particular figure 2.7.a and 2.7.b), was fabricated on a copper substrate, and allowed the production of regular slices (five to perform quintuplicate samples for each test) having a size of 0.5 cm x 4 cm, ready for tensile test, minimizing the sample handling before the test. Tensile tests on electrospun membranes were performed with an Instron instrument (model 3365) with cell load of 10 N, in deformation-control mode, at a strain rate of 2 mm/min.

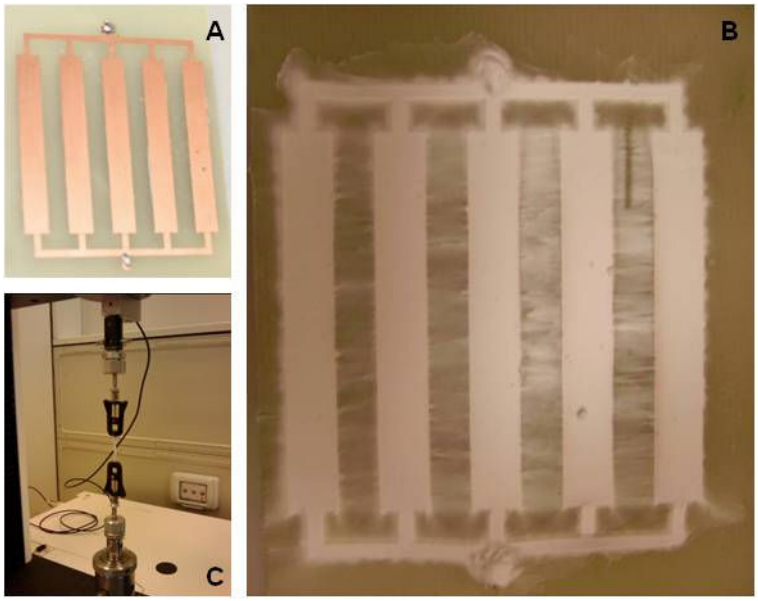

Figure 2.7 Devoted fiber collector for tensile test of electrospun samples. Copper target collector (A) and the same collector covered with electrospun membrane, after the electrospinning (B). Representative tensile test of a single electrospun slice obtained by using this collector (C).

Compressive strength tests

Compressive strength tests on coated 45S5 Bioglass® scaffolds were performed in order to evaluate the structural integrity of the coated scaffolds, by using Zwick/Roell Z050 mechanical tester (at Friedrich Alexander University of Erlangen-Nuremberg, Department of Material Science and Engineering), with load cell of 50 N and crosshead speed of 5 mm/min. Samples, in quintuplicate, were prepared and cut in cubic shape (dimension about 7x7x7 mm^3).

Compressive strength tests on chitosan-based foams were performed on cylindrical samples (triplicate, Ø = 5 mm, h = 8 mm) with an Instron instrument (model 3365) with load cell of 10 N at a crosshead speed of 1 mm/min in dry condition. One hysteresis cycle was performed for each sample: load was applied up to 50% deformation and then removed.

2.5.5 Contact angle measurements

The water contact angle was measured by the contact angle meter (Surftens Universal, OEG GmbH, Frankfurt (Oder), Germany) at Friedrich Alexander Universität Erlangen-Nuremberg, Department of Material Science and Engineering. Deionized water was automatically dropped onto the electrospun mats, coated 45S5 bioglass® scaffolds and composite scaffolds. The contact angle was measured three times from different positions on the same sample and an average value was then calculated.

2.5.6 Porosity measurement

Porosity measurements of chitosan-based foams (fabricated with protocol 2 and 3, § 2.4.3) were performed by liquid displacement, accordingly to [8]. Hexane (Sigma Aldrich) was used as displacement liquid because it permeates in the foam structure without generating swelling or shrinking the sample. Measurements were performed by using the following protocol:

1. Weight dried sponge (w0).

2. Measure hexane volume in a graduated cylinder (accuracy 0,1 mL) without sponge (V1: hexane volume without foam).
3. Immerse chitosan foam (weighted at point 1.) in hexane for 5 minutes.
4. Measure the total volume of hexane and sponge immersed in it after 5 minutes (V2: hexane volume with chitosan foam inside).
5. Remove the foam from the hexane.
6. Measure the residual hexane volume (V3: hexane volume after the removal of chitosan foam), without chitosan foam.

It was possible evaluate chitosan foam scaffold total volume and porosity, as follows:
Scaffold total volume: V = (V2 – V1) + (V1 – V3) = V2- V3
Where: (V2 – V1) is the volume of the chitosan foam and (V1 – V3) is the volume of hexane within the scaffold.
The porosity of the scaffold (ε) was obtained by

$$\varepsilon = \frac{V1 - V3}{V2 - V3} \cdot 100$$

2.5.7 Swelling

The swelling studies were performed in DI water at room temperature on chitosan-based foams scaffolds (fabricated by using protocols 2 and 3, §2.4.3). The dry weight of the samples (cut in cylindrical shape, Ø = 6 mm, h = 5 mm) was noted (W0). Scaffolds were placed in DI water and removed at three different time points: after 10, 30 and 60 minutes. The surface adsorbed water was removed by filter paper and wet weight was recorded (Ww). The ratio of swelling was determined by the following formula, according to [9].

$$\text{Swelling Ratio} = \frac{Ww - W0}{W0}$$

2.5.8 pH measurements

In order to assess eventual pH alteration due to chitosan-based foams, the samples (cut in cylindrical shape, Ø = 6 mm, h = 5 mm) were immersed in cell basal medium

(Lonza), to investigate macroscopically eventual color change in the medium due to pH alteration. Only samples fabricated with protocol 2 (§ 2.4.3), showed an instantaneous color change in the medium and for that reason were further investigated, as follows. All kinds of chitosan-based foams (CS, CSHA, CSBG), homogenous in shape and weight, were put in DI water, in order to investigate eventual pH variation induced by the foam itself. pH measurements were performed by the pHmeter pH20 (Hanna Instruments, Smithfield - RI, USA). Foams were cut in cylindrical shape, Ø = 6 mm, h = 5 mm, and their dry weight was about 0,1 g for each kind of foam. The samples were immersed in 40 mL of DI water. pH measurements were performed until the stabilization of pH value.

2.5.9 Bioactivity test (Simulated Body Fluid)

The bioactivity of the samples (electrospun CSHA and CSBG mats and coated 45S5 bioglass® scaffolds) was assessed by samples immersion in a simulated body fluid (SBF) solution, according to [10] and ISO/FDIS 23317:2007(E). Samples were immersed in SBF solution at 37°C for 7 days, with intermediate time points after 1 day and 3 days, for electrospun samples.

2.5.10 Biocompatibility Assay

Electrospun chitosan-based membranes and chitosan-based foams (protocol 3, §2.4.3) were evaluated in terms of cytotoxicity and cell proliferation using hMSCs (passage 2, Lonza, Basel, Switzerland). Prior to cell seeding, crosslinked electrospun membranes were punched into 6 mm diameter discs, neutralized with immersion in NaOH 0.1 M aq. solution, rinsed with PBS three times, and UV sterilized. Chitosan-based foams were cut in a cylindrical shape (Ø = 6 mm, h = 3 mm) and UV sterilized.

For a preliminary cytotoxicity assessment, aiming the evaluation of cell response after the exposure to the scaffolds (this assay is further cited in the text as cell exposure to the scaffolds), hMSCs were seeded into 96-well plates at a density of $3.5 \cdot 10^4$ cells/cm^2 in α-MEM (Lonza), supplemented with 10% fetal bovine serum (FBS, Lonza), 1% L-glutamine and 1% penicillin, streptomycin and amphotericin mixture (Lonza), and

incubated overnight. For each well, a sample disc was added, and cytotoxicity was assayed after 4, 8 and 24 hours using Vybrant Cytotoxicity Assay Kit (Invitrogen). The assay is based on the measurement of Glucose-6-Phosphate Dehydrogenase (G6PD) released in the culture medium by dying or apoptotic cells. Cells alone (without scaffolds) cultured in the same conditions were used as a negative control. The same assay was used also to perform the cytotoxicity assessment aiming the evaluation of scaffolds cytotoxicity after cell seeding on them (this assay is further cited in the text as cytotoxicity test). In fact hMSCs were seeded into 96-well plates at a density of $3.5 \cdot 10^4$ cells/cm^2 directly onto the scaffolds. After cell attachment on the scaffolds (24 hours after the seeding), the same time points (4, 8 and 24 hours) were used for the evaluation of samples cytotoxicity.

Similarly, for cell proliferation assessment, hMSCs were seeded into 96-well plates at a density of $5 \cdot 10^3$ cells/cm^2 directly onto the scaffolds. The medium was changed every 3 days and cultures were maintained in a humidified incubator at 37 °C in a 5% CO_2 atmosphere. Control cultures were not supplemented with samples. Cell proliferation was assayed by MTT assay, based on the activity of mitochondrial dehydrogenase enzymes in cells: at each time point, samples were removed, and 20 µL of 3-(4,5-dimethylthiazol-2-yl)-2,5-diphenyltetrazolium bromide (MTT, Sigma) aqueous solution (5 mg/mL) were added to the culture medium. After incubation for 4 h, 100 µl of dimethyl sulfoxide (Sigma) were added to each well, and absorbance was read at 570 nm using a plate reader (TECAN, Männedorf, Switzerland).

References

[1] Rainer A, Giannitelli SM, Abbruzzese F, Traversa E, Licoccia S, Trombetta M. Fabrication of bioactive glass–ceramic foams mimicking human bone portions for regenerative medicine. Acta Biomaterialia. 2008;4:362-9.

[2] Vallet-Regí M, Romero AM, Ragel CV, LeGeros RZ. XRD, SEM-EDS, and FTIR studies of in vitro growth of an apatite-like layer on sol-gel glasses. Journal of Biomedical Materials Research. 1999;44:416-21.

[3] Klossner RR, Queen HA, Coughlin AJ, Krause WE. Correlation of Chitosan's Rheological Properties and Its Ability to Electrospin. Biomacromolecules. 2008;9:2947-53.

[4] Chen QZ, Thompson ID, Boccaccini AR. 45S5 Bioglass®-derived glass–ceramic scaffolds for bone tissue engineering. Biomaterials. 2006;27:2414-25.

[5] Ho M-H, Kuo P-Y, Hsieh H-J, Hsien T-Y, Hou L-T, Lai J-Y, et al. Preparation of porous scaffolds by using freeze-extraction and freeze-gelation methods. Biomaterials. 2004;25:129-38.

[6] Li Z, Zhang M. Chitosan–alginate as scaffolding material for cartilage tissue engineering. Journal of Biomedical Materials Research Part A. 2005;75A:485-93.

[7] Gu ZY, Xue PH, Li WJ. Preparation of the porous chitosan -membrane by cryogenic induced phase separation. Polymers for Advanced Technologies. 2001;12:665-9.

[8] Tığlı R, Gümüşderelioğlu M. Evaluation of alginate-chitosan semi IPNs as cartilage scaffolds. Journal of Materials Science: Materials in Medicine. 2009;20:699-709.

[9] Peter M, Binulal NS, Soumya S, Nair SV, Furuike T, Tamura H, et al. Nanocomposite scaffolds of bioactive glass ceramic nanoparticles disseminated chitosan matrix for tissue engineering applications. Carbohydrate Polymers. 2010;79:284-9.

[10] Kokubo T, Takadama H. How useful is SBF in predicting in vivo bone bioactivity? Biomaterials. 2006;27:2907-15.

3. Electrospinning of crosslinked pure chitosan membranes

Index

Abstract

Chitosan is a polymer of known biocompatibility and widely investigated for tissue engineering purposes. This chapter deals with the fabrication of defect free pure chitosan nanofibrous meshes by using the electrospinning technique. Pure chitosan nanofibers were obtained without the use of additional copolymers, and crosslinked by using two different methods. The obtained samples were characterized by SEM observations, ATR/FT-IR spectroscopy, tensile test and biocompatible assay. Results showed that the scaffolds were composed of nanosized fibers, forming a non-woven mat. ATR/FT-IR analysis confirmed efficacy of crosslinking and the absence of solvents residual. All these results confirm that the developed chitosan electrospun membranes are biocompatible and potential good candidates for further applications in tissue engineering.

3.1 Chitosan: electrospinning and crosslinking techniques

Electrospinning is a technique to obtain fibrous structures; these are characterized by a very high surface area and good mechanical properties for tissue engineering applications. Electrospun polymeric fibrous meshes also offer a suitable environment for cell attachment, they are easy and inexpensive to fabricate and scale-up [1, 2].

Chitosan, obtained from a deacetylation reaction of chitin, is one of the most promising biopolymers for tissue engineering for orthopedic applications, because of its biocompatibility, biodegradability, and suitability to promote cell adhesion. Moreover, it can be easily processed and tailored in various shapes, including beads, films, sponges, tubes, powders, and fibers [3, 4]. Unfortunately, it is quite difficult to obtain defect-free electrospun meshes starting from chitosan solutions, even if in literature several study reported successful results, sometimes by the introduction of cosolvent or copolymer [5-13].

Electrospun chitosan membranes need to be crosslinked in order to enhance their resistance to physiological environment. In literature are reported several studies about the different crosslinking techniques, by using appropriate crosslinker for chitosan electrospun membranes [14-16]. In particular, in this work, the use of glutaraldehyde (GA) and genipin (GEN) as chitosan crosslinkers is evaluated. Schematically, the crosslinking process by the effect of glutaraldehyde could occur by several mechanisms, as Michael-type adducts with terminal aldehydes, which lead to the formation of carbonyl groups (Figure 3.1.b) [17], and by Schiff base formation, that leads to imine-type functionality (Figure 3.1.a) [18].

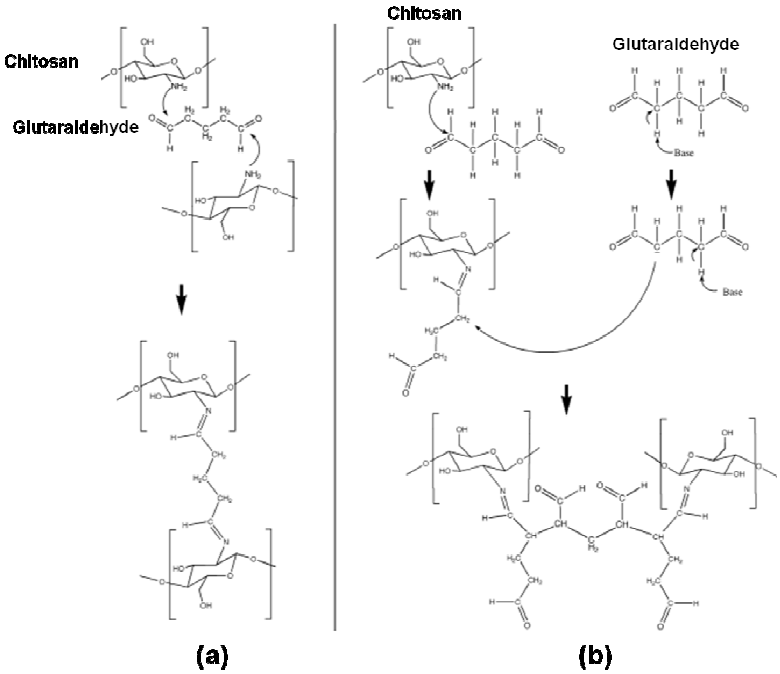

Figure 3.1 Glutaraldehyde-Chitosan crosslinking mechanisms: Schiff Base imine functionality (a) and Michael-type adducts with terminal aldehydes (b) [14].

For what concerns genipin-chitosan crosslinking mechanisms, it could be briefly described as follows, and reported in figure 3.2. In acidic environment, a nucleophilic attack of an amino groups of chitosan to carbon 3 (C-3) of genipin occurs, followed by the opening of the dihydropyran ring and the formation of a tertiary amine [19].

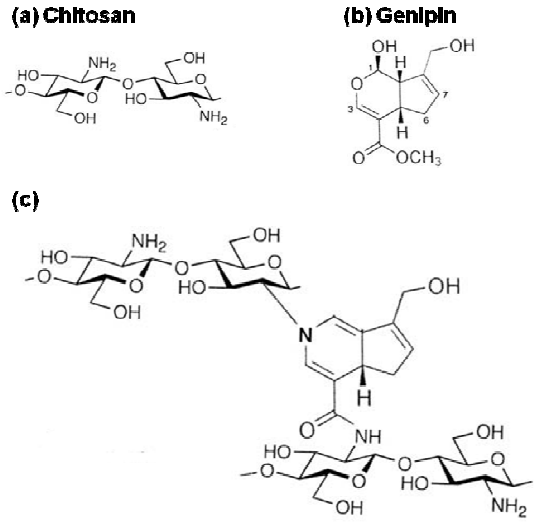

Figure 3.2 Genipin-chitosan crosslinking mechanism (c), chitosan structural units (a) and genipin (b).[19]

The aim of this work is the optimization of the electrospinning process of pure chitosan meshes in combination with the proper choice of both crosslinking process and crosslinker agent.

Starting from the data and parameters reported in chapter 2, the outline of the present chapter comprehends an initial part dealing with the electrospinning of pure chitosan dissolved in several solvents and its related optimization of the electrospinning parameters. For what concerns the crosslinking process, two methods are presented, called two steps and one-step, depending on the time of the introduction of crosslinker into chitosan solution/sample and two different crosslinkers have been evaluated (glutaraldehyde and genipin). Results reported a comparison among the obtained sample properties.

3.2 Results and Discussion

In this section the results obtained from the electrospinning of pure chitosan and then the results obtained from the two crosslinking methods applied to the electrospun membranes are presented. The paragraph is divided in subsections devoted to the explanation of different outcomes from several characterization analyses.

3.2.1 Morphological analysis

Optimization of pure chitosan electrospun membrane

Chitosan is usually electrospun in association with copolymers as polyethylenoxide, polyvinyalcohol, polylactide, silk fibroin and collagen; moreover, as an alternative approach to improve the solubility and processability of chitosan, several chitosan derivatives, including hexanoyl chitosan, quaternized chitosan, N-carboxyethyl chitosan, and block copolymers of chitosan and L-lactide or polyethyleneglycol oligomer, were synthesized and electrospun with or without polymeric additives [20].

Trifluoroacetic acid (TFA) is commonly used as a solvent for chitosan solutions for the electrospinning [6-9], and dichloromethane (DCM) is also used as a cosolvent to optimize the net of fibers and reduce the presence of beads and artifacts [6, 8].

In order to optimize the electrospinning of pure chitosan, several chitosan solutions and combinations of electrospinning parameters were tested and previously reported in § 2.4.1. In the following table (similar to table 2.6 in chapter 2), the tested chitosan solutions, the related electrospinning parameters and SEM micrographs (obtained according to § 2.5.1) are reported.

	Solutions	Electrospinning parameters and comments	SEM micrographs
1	**4 % w/v chitosan in AA (aq. solution 30%v/v)**	Distance tip-target: range between 5 to 15 cm. Solution feed rate: range between1.5 to 5 mL/h. Voltage: range between 10 to 25 kV. *Note: Only drops on the target (electrospraying). Electrospraying phenomena reduced by increasing polymeric solution feed rate (i.e. 5 mL/h). No samples preserved for further investigations.*	--
2	**2.5 % w/v chitosan in AA (aq. solution 90% v/v)**	*Fibers and drops on the target.* Distance tip-target: tested range from 5 to 15 cm, good results (target covered by white layer) with 5-7 cm. Solution feed rate: too high value (i.e. 5 mL/h) or too low value (i.e. 1 mL/h) lead to drops deposition on the target. Good range between 3 and 4 mL/h, evaluated in terms of deposition of white layer on the target (it was not possible separate the white layer from the Al substrate). Voltage: tested the range between 15 and 30 kV (increasing 1 kV, for each test). The others parameters were fixed at the following values: distance tip-target: 7 cm; solution feed-rate: 4 mL/h. Good results (target covered by white layer) for the range 20-25 kV.	--
3	**4 % w/v chitosan in AA (aq. solution 90% v/v)**	*It was not possible to electrospin that solution.*	--
4	**2 % w/v chitosan in AA (aq. solution 90% v/v)/DCM (80:20)**	Drops on the target. Distance tip-target: range: 7 -10 cm. Solution feed rate: range: 1.0 – 3.0 mL/h. Voltage: range: 10-25 kV. *No samples preserved for further investigations.*	--
5	**2.6% w/v chitosan in AA/DCM (80:20)**	*It was not possible to electrospin that solution.*	--
6	**4 % w/v chitosan in AA/DCM (70:30)**	*It was not possible to electrospin that solution.*	--
7	**3% w/v chitosan in aq. lactic**	*Only drops on the target (electrospraying)*	--

	acid solution (2% v/v in DI water)		
8	**2.7% w/v chitosan in TFA**	Distance tip-collector / voltage / solution feed rate / needle diameter 15 cm / 15 kV / 2 mL/h / 23G 7 cm / 26 kV / 1.2 mL/h / 23G **SEM** *Not fibers collected on the target. (it was not possible separate the white layer from the Al substrate)*	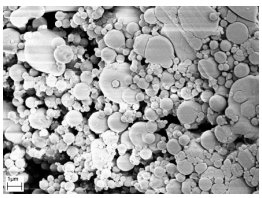
9	**5% w/v chitosan in TFA**	Distance tip-collector / voltage / solution feed rate / needle diameter 5 cm / 20 kV / 0.05 mL/h / 21G / No fibers 5 cm / 20 kV / 0.1 mL/h / 21G / No fibers 4 cm / 18 kV / 0.15 mL/h / 21G / No fibers 4 cm / 18 kV / 0.15 mL/h / 21G / **SEM** 10 cm / 18 kV / 0.2 mL/h / 21G / **SEM**	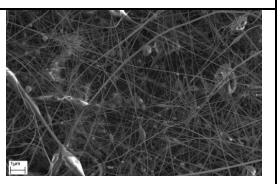 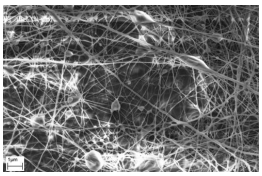
10	**6% w/v chitosan in TFA**	Distance tip-collector / voltage / solution feed rate / needle diameter 8 cm / 17 kV / 0.5 mL/h / 21G / **SEM** 10 cm / 17 kV / 0.5 mL/h / 21G / No fibers 8 cm / 17 kV / 0.2 mL/h / 21G / **SEM** 10 cm / 17 kV / 0.3 mlLh / 21G	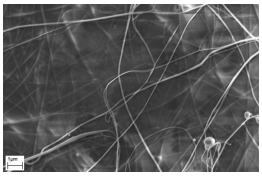 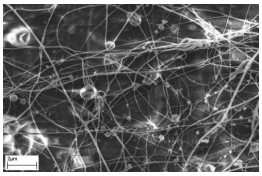
11	**8% w/v chitosan in TFA**	Distance tip-collector / voltage / solution feed rate / needle diameter 10 cm / 17 kV / 0.8 mL/h / 21G 10 cm / 20 kV / 0.8 mL/h / 21G / No fibers 10 cm / 20 kV / 0.5 mL/h / 21G 10 cm / 23 kV / 0.5 mL/h / 21G Only drops on the target (electrospraying)	--
12	**4% w/v chitosan in TFA/DCM (80:20)**	Distance tip-collector / voltage / solution feed rate / needle diameter 15 cm / 15 kV / 0.03 mL/h / 21G / No fibers 10 cm / 15 kV / 0.03 mL/h / 21G / No fibers 15 cm / 15 kV / 0.10 mL/h / 21G / No fibers 10 cm / 15 kV / 0.10 mL/h / 21G / **SEM** 10 cm / 15 kV / 0.05 mL/h / 21G / **SEM** 10 cm / 15 kV / 0.20 mL/h / 21G / **SEM** 15 cm / 15 kV / 0.15 mL/h / 21G / **SEM** 10 cm / 20 kV / 0.10 mL/h / 21G / **SEM** 10 cm / 20 kV / 0.05 mL/h / 21G / **SEM** 10 cm / 20 kV / 0.15 mL/h / 21G / **SEM**	 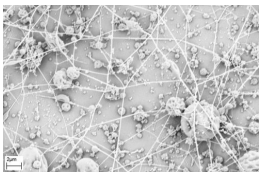

			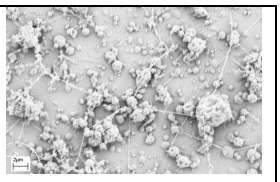 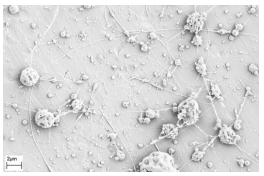 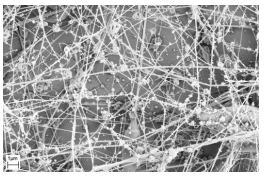 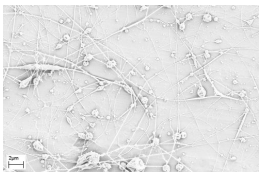 
13	**8% w/v chitosan in TFA/DCM (80:20)**	Distance tip-collector / voltage / solution feed rate / needle diameter 15 cm / 15 kV / 0.10 mL/h / 21G **SEM** 15 cm / 15 kV / 0.15 mL/h / 21G **SEM** 15 cm / 20 kV / 0.10 mL/h / 21G **SEM**	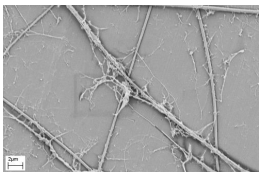 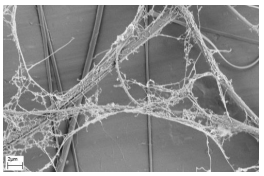 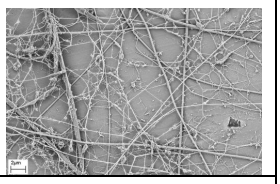
14	**10% w/v chitosan in TFA/DCM (80:20)**	Distance tip-collector / voltage / solution feed rate / needle diameter 15 cm / 15 kV / 0.10 mL/h / 23G **SEM** 15 cm / 15 kV / 0.15 mL/h / 23G **SEM**	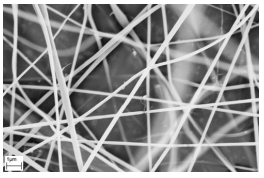

			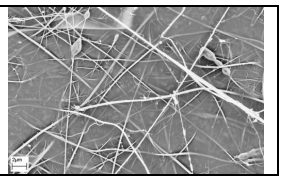

Table 3.1 Chitosan solutions, electrospinning parameters and related SEM micrographs.

As reported in the SEM micrographs, showed in table 3.1, the electrospun membranes fabricated starting from the solution 14, according to the list § 2.1.1, (with the following process parameters: distance tip-collector: 15 cm; voltage: 15 kV; solution feed rate: 0.10 mL/h; needle diameter: 23 G) showed the best results and were characterized by a mesh of continuous, homogeneous and defect-free fibers, having an average fiber diameter of 450 ± 110 nm.

Crosslinking processes: Two-steps method (ref § 2.1.2)

As previously reported, the optimized pure chitosan electrospun membranes, before crosslinking (ESCS, for sample labels ref. to table 2.1 in § 2.1.2) are characterized by the morphology of a net of continuous, randomly oriented and beads-free fibers, as showed in the SEM micrograph in figure 3.3.a (starting from chitosan solution n.14, reported in table 3.1). The calculated average fiber diameter was 450 ± 110 nm.

In two-steps crosslinking method, polymer chains crosslinking was achieved by exposure of chitosan electrospun membranes to GA vapors at room temperature. The absence of GA residuals was observed by the following ATR/FT-IR characterization. In order to identify the appropriate sample time of exposure on GA vapors, several time points were evaluated. Figure 3.3.b displays SEM micrographs of electrospun chitosan membrane after crosslinking in GA vapors for 3 hours (ESCSXL3 sample, for sample labels ref. to table 2.1 in § 2.1.2). After crosslinking, fibers averaged 440 ± 210 nm. The effect of crosslinking process did not modify membrane average fiber diameter. The effect of exposure time to crosslinker agent on fibers morphology was also evaluated. Figure 3.3.c and 3.3.d show SEM micrographs of a chitosan membrane after crosslinking by exposure to GA vapors for 18 (ESCSXL18) and 24 (ESCSXL24) hours, respectively. As it can be observed, fibrous morphology was gradually deformed, indicating that a prolonged exposure to GA was not suitable for the preservation of the fibrillar structure.

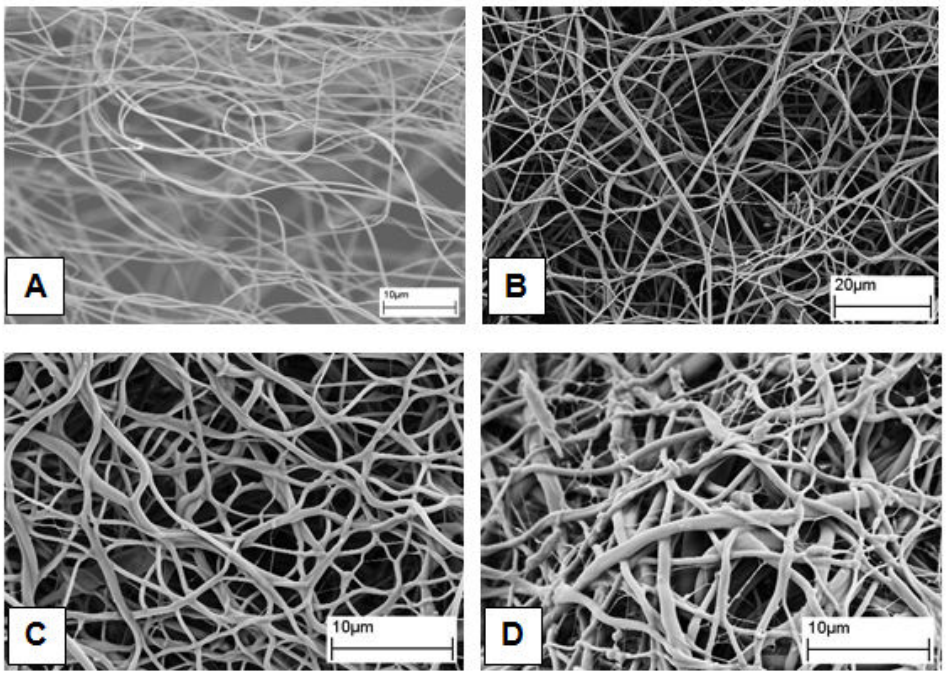

Figure 3.3 SEM micrographs of electrospun chitosan fibers before (ESCS, fig.1.a) and after crosslinking at different exposure time to GA solution (ESCSXL3, fig.1.b; ESCSXL18, fig.1.c; ESCSXL24 fig.1.d).

In literature, other studies have evaluated a similar crosslinking process for chitosan-based electrospun membrane [8, 14], and in the present work, a process optimization, in terms of GA solution concentration, GA solution amount respect to sample effective area and time of exposure to GA vapors, was performed. The optimized parameters were a GA aq. solution of 25% v/v, GA solution amount of 0.2 mL/cm^2, considering sample effective exposed area, and 3 hours as exposure time.

Crosslinking processes: One-step method

One-step crosslinking method was performed by using two different crosslinker agents: glutaraldehyde (GA) and genipin (GEN), by the addition of crosslinker solution directly to chitosan solution before the electrospinning process. This paragraph is divided in two subsections devoted to each crosslinker.

Glutaraldehyde

The use of the same crosslinker made possible a comparison between the two different crosslinking methods. Also in this case, the crosslinking efficacy and the absence of GA residuals were investigated and confirmed by ATR/FT-IR characterization (§ 3.2.2).

In one-step method (§ 2.1.2), GA at two different solution concentrations was added to chitosan solution (GA aq. solution of 10% v/v (ESCSXLGA10 sample) and 50% v/v (ESCSXLGA50 sample, for sample labels ref to table 2.1 in § 2.1.2)).

Differences in morphology, between the two methods and between the two added GA solutions in the same one-step method, are highlighted in figure 3.4 and concern the average diameter of the obtained fibers. In fact, crosslinked membranes by two-steps method (after 3 hours of exposure to GA vapors) had an average fiber diameter of 440 ± 210 nm (ESCSXL3, figure 3.4.b), while a reduction in fiber diameter was observed in one-step method samples. In particular, in figure 3.4.c the one-step method sample ESCSXLGA10 is showed, the calculated average fiber diameter was 167 ± 43 nm and some defects were observed in the fibrillar structure. For what concerns the other crossliked sample ESCSXLGA50, the calculated average fiber diameter was 202 ± 66 nm. That sample showed a more homogeneous, defect-free fibrous structure.

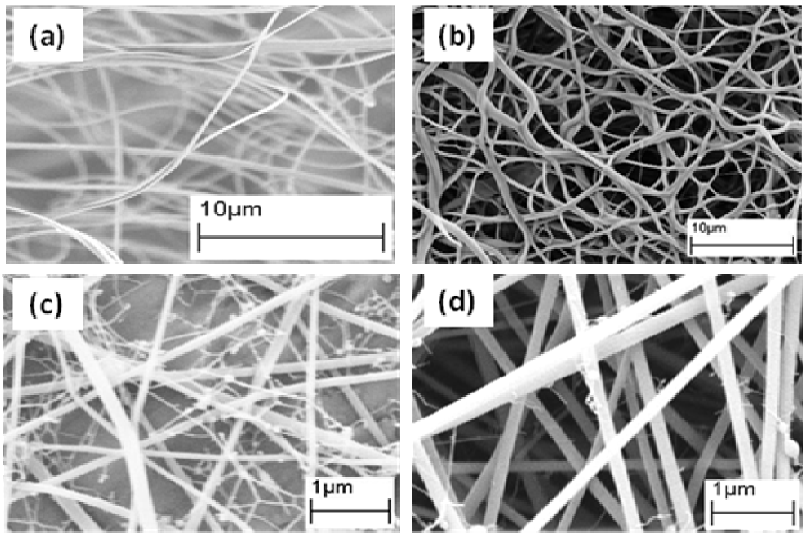

Figure 3.4 SEM micrographs of electrospun chitosan fibers before crosslinking process (a); two-steps method crosslinked sample (b); one-step method crosslinked samples, obtained from a starting solution containing glutaraldehyde at 10% v/v and 50% v/v, respectively (c, d).

In conclusion, both crosslinking methods allowed to obtain homogeneous chitosan nanofibrous membranes. These results demonstrate how the direct addition of the crosslinker into the chitosan starting solution gave rise to the formation of very narrow fibers.

Genepin

One-step crosslinking method was also used to evaluate the effect of genipin, as chitosan crosslinker in combination with the electrospinning process. The efficacy and the mechanisms of crosslinking was investigated by using ATR/FT-IR analysis (§ 3.2.2).

The use of genipin as crosslinker for biomedical applications was already the focus of previous studies [21-24]. In particular, in combination with the electrospinning process, the genipin was already used as gelatin crosslinker by Panzavolta *et al.* [21], even if, in that work, the amount of genipin introduced in the gelatin solution before the electrospinning was not sufficient to produce an effective membrane crosslinking, demonstrated by the membrane solubility in aqueous environment, so it was necessary to immerse the electrospun genipin-gelatin membrane in a genipin solution for 7 days to obtain electrospun genipin-crosslinked membranes insoluble in aqueous solution.

In this study two different amounts of genipin solution (1.25% w/v in DI water/EtOH), respect to chitosan solution total volume (8% v/v (ESCSXLGEN8, for sample labels ref. to table 2.1 in § 2.1.2) and 20% v/v (ESCSXLGEN20)) were evaluated. The sample ESCSXLGEN8 resulted not completely crosslinked and partially soluble in aqueous solution, while the sample ESCSXLGEN20 resulted insoluble in aqueous solution, showing an homogenous, defect-free fibrous mesh, and having an average fiber diameter of 273 ± 72 nm, as reported in figure 3.5.b.

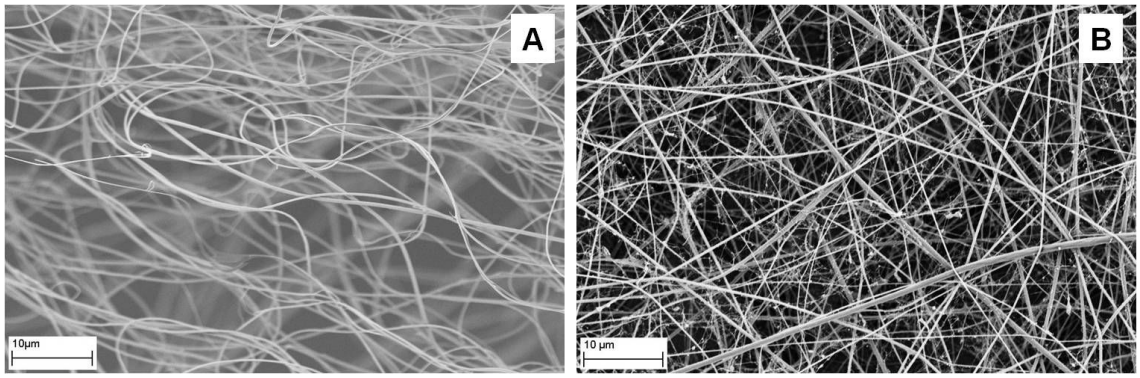

Figure 3.5 SEM micrographs of electrospun chitosan fibers before crosslinking process (a) and genipin-crosslinked sample by one-step method (ESCSGEN20).

3.2.2 ATR/FT-IR analysis

Glutaraldehyde crosslinking

Crosslinking processes: Two-steps method

ATR/FT-IR analysis was performed, as reported in § 2.5.2, in order to assess the degree of deacetylation of the sample, to evaluate the effects of crosslinking process, identifying the type of mechanism by which the crosslinking occurred and to investigate the presence of toxic solvent residues.

The ATR/FT-IR spectra in the OH stretching region of the electrospun chitosan samples before (ESCS) and after crosslinking with GA vapors (ESCSXL3, ESCSXL18, ESCSXL24) are reported in figure 3.6.

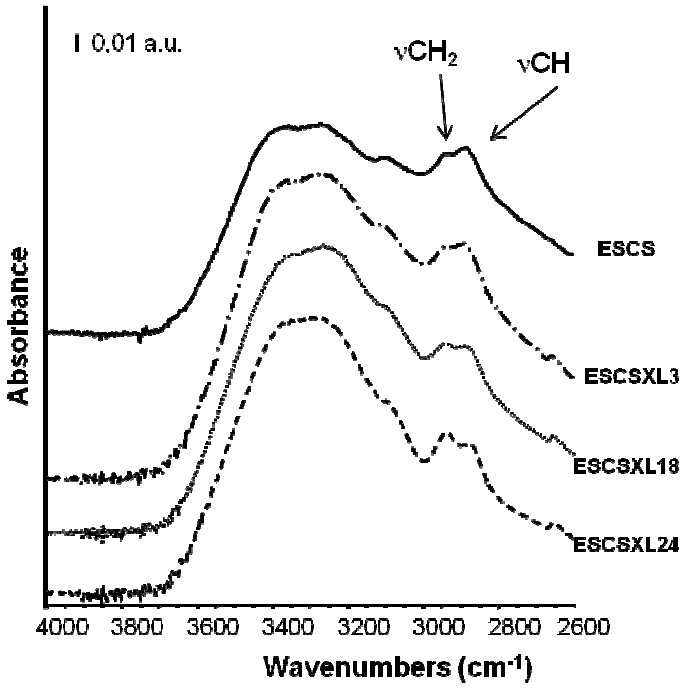

Figure 3. 6 ATR/FT-IR spectra in the region 4000 – 2600 cm^{-1} of chitosan electrospun membrane before (ESCS sample) and after crosslinking (ESCSXL3, ESCSXL18, ESCSXL24 samples), respectively after 3, 18 and 24 hours of exposure to GA vapors.

All the spectra were dominated by chitosan absorption. In the -OH stretching region ESCS spectrum was characterized by a broad band with two components centered at 3370 and 3260 cm^{-1}, while all the crosslinked samples spectra showed a main component at about 3330 cm^{-1}. Differences among the samples were also reported in the -NH stretching region. ESCS presented an absorption at 3100 cm^{-1} due to νNH stretching vibrations of primary amine ($-NH_2$) group. In all crosslinked samples this signal was lower in intensity, confirming that crosslinking process has occurred. In ESCS sample, a broad band with two components at 2940 and 2880 cm^{-1} due to stretching νCH_2 and νCH, respectively, were present. The intensity of the latter signal was higher. In crosslinked samples, νCH_2 became gradually predominant (it increases proportionally to exposure time), confirming an increase of methylenic groups, reliably associated to GA backbone. In crosslinked samples the absence of free glutaraldehyde is confirmed by the nonappearance of signals of νCH typical of aldehydic groups.

The spectra of all samples in the fingerprint region are reported in figure 3.7. In order to point out and confirm that crosslinking process had occurred, the spectrum arisen from

the subtraction of ESCS spectrum from the ESCSXL3 one is reported in the same figure.

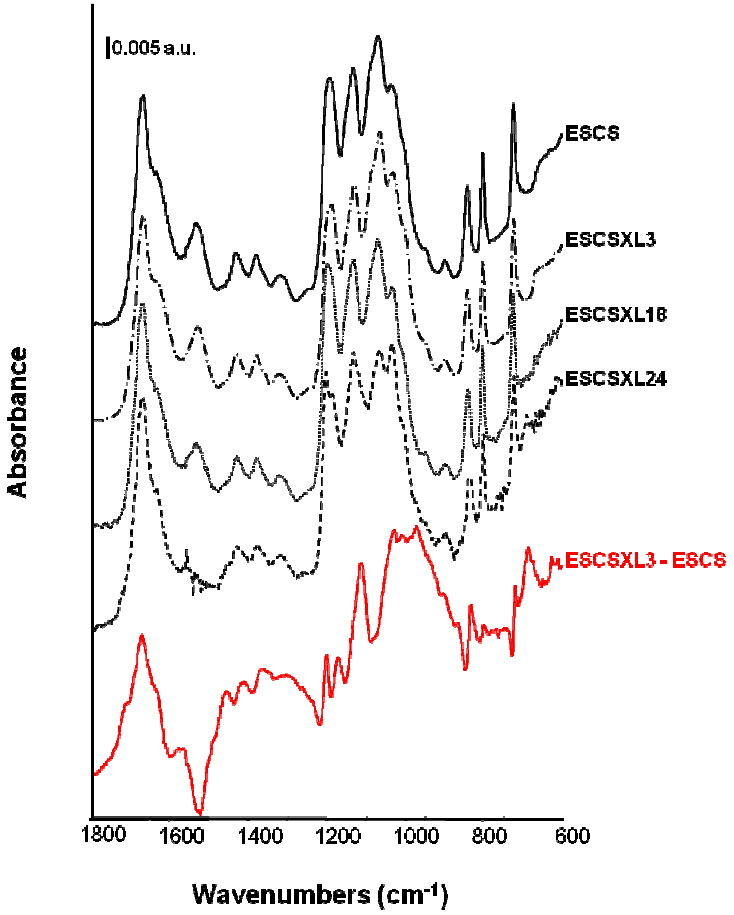

Figure 3.7 ATR/FT-IR spectra in the fingerprint region of chitosan electrospun membrane before (ESCS sample) and after crosslinking (ESCSXL3, ESCSXL18, ESCSXL24 samples), respectively after 3, 18 and 24 hours of exposure to GA vapors; and the subtraction spectrum ESCSXL3 – ESCS.

All spectra were dominated by chitosan absorption. A shoulder at 1720 cm^{-1} in the subtraction spectrum, due to stretching vibration of carbonyl group was present, confirming that Michael-type adducts with terminal aldehydes crosslinking occurred, according to [14]. The two components at 1670 and 1530 cm^{-1}, showed in ESCS sample, due to νNH_2 of primary amine ($-NH_2$) group, became lower in intensity in crosslinked samples. In particular, the peak at 1530 cm^{-1} in ESCS sample, disappeared in crosslinked samples. The loss of primary amines confirmed occurrence of the crosslinking process. This process modified the ESCS spectrum in the region of stretching vibrations of chitosan saccharide structure. In crosslinked samples an increased intensity of these bands was observed, due to electron attractive effect of C=N

bond exerted on C-O-C group. This effect was observed at 1110 and at 970 cm^{-1} (weak). A signal at 1170 cm^{-1} due to νC=N, was present, confirming the crosslinking process.

The above reported results strongly confirm that this method led to the preparation of crosslinked chitosan in two conformations: Michael-type adducts with terminal aldehydes, which led to the formation of carbonyl groups, and by Schiff base imine functionality.

Moreover, a change in color associated to crosslinking process was observed, and showed in figure 3.8. The crosslinked samples tuned from white to pale yellow after exposure to GA, confirming the formation of a imine Schiff base, as previously described [17].

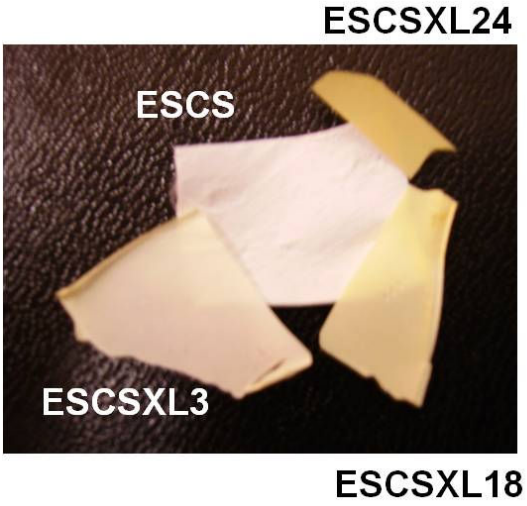

Figure 3.8 Color change of glutaraldehyde-crosslinked chitosan electrospun membranes after two-steps process, at different time of exposure.

The degree of deacetylation of the ESCS sample was estimated by calculating the ratio between the intensity of the absorption bands of νNH_2 and νC-O, according to the literature [14]. Samples showed a 70% of deacetylation.

Crosslinking processes: One-step method

Glutaraldehyde was also used during the other crosslinking process (one-step method, ref. § 2.1.2). Two solution concentrations of GA was tested and samples were called according to this (ESCSXLGA10 and ESCSXLGA50, respectively).

All the considerations reported above, about the ATR/FT-IR spectra analysis could be applied also to these samples. All sample spectra, before (ESCS sample) and after (ESCSXLGA10 and ESCSXLGA50 samples) crosslinking are showed in figure 3.9.

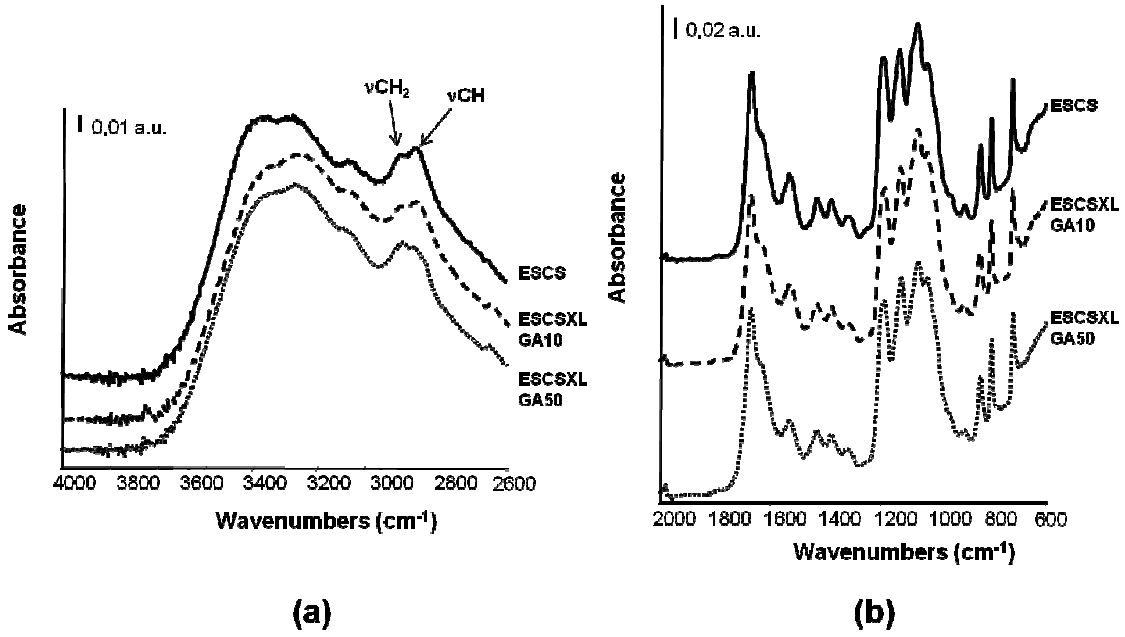

Figure 3.9 ATR/FT-IR spectra of chitosan electrospun membranes before (ESCS) and after (ESCSXLGA10,ESCSXLGA50) crosslinking: in the region 4000 – 2600 cm^{-1} (a); and in the fingerprint region (b).

Also in this case a membranes color change due to crosslinking process occurred, as showed in figure 3.10.

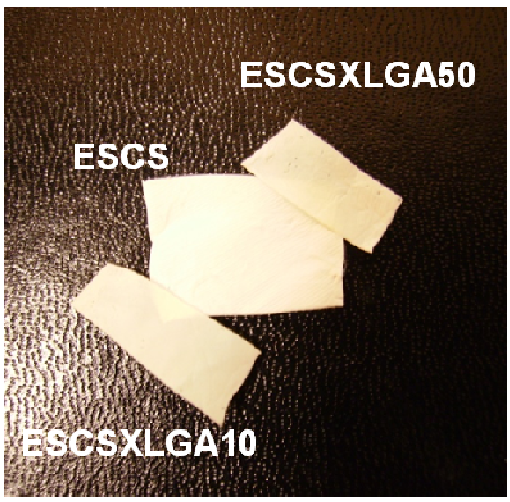

Figure 3.10 Color change of glutaraldehyde-crosslinked chitosan electrospun membranes by one-step method.

Genipin crosslinking

Crosslinking processes: One-step method

ATR/FT-IR analysis was performed, as reported in § 2.5.2, in order to evaluate the effects of crosslinking process. The ATR/FT-IR spectra in the fingerprint region of the electrospun chitosan samples before (ESCS) and after crosslinking with genipin (ESCSXLGEN20), and pure genipin are reported in figure 3.13.a. In the same region, the subtraction spectrum (ESCSXLGEN20 – ESCS) and pure genipin spectrum are showed in figure 3.13.b.

Both uncrosslinked and crosslinked samples spectra were dominated by chitosan absorption.

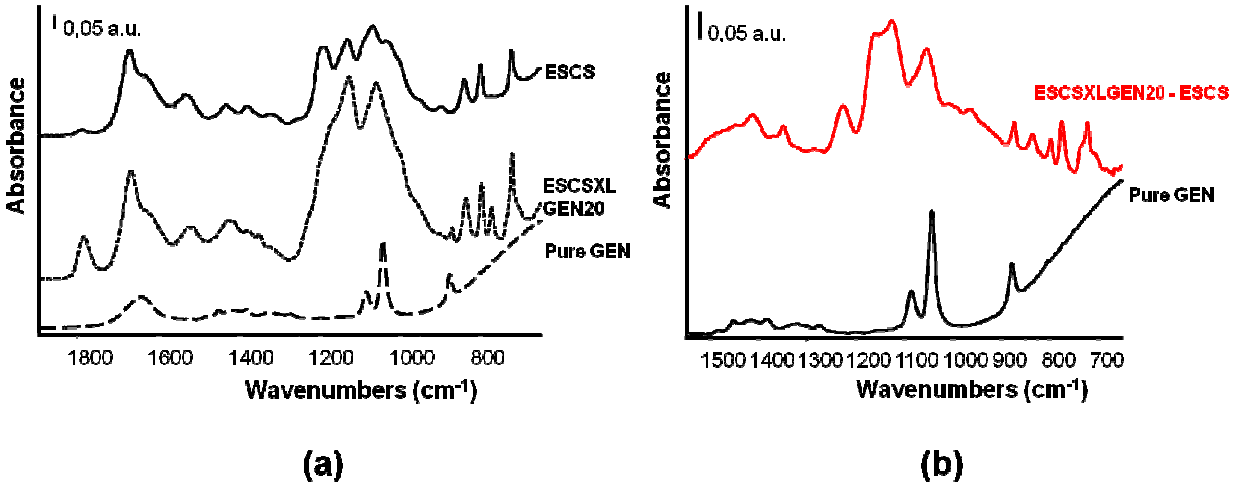

Figure 3.11 ATR/FT-IR spectra of chitosan electrospun membranes before (ESCS) and after (ESCSXLGEN20) crosslinking, and pure genipin in the fingerprint region (a); the subtraction spectrum (ESCSXLGEN20 – ESCS) and pure genipin spectrum (b).

Some modifications in typical chitosan saccharide structure (visible in the C-O-C stretching vibration region around 1100 cm^{-1}) were showed in crosslinked sample (figure 3.13.a). A new band centered at 1550 cm^{-1} was observed in the subtraction spectrum (figure 3.13.b), due to amine and amide N–H bending vibrations, according to previous investigation [24]. That band was absent in pure genipin spectrum, underlying that it is only due to genipin-chitosan interaction, confirming the occurrence of crosslinking process. In figure 3.13.b, in the subtraction spectrum, three peaks at 875, 835 and 795 cm^{-1}, due to the resonance of the crosslinked genipin-chitosan structure (according to figure 3.2) were observed, confirming that the crosslinking was occurred.

3.2.3 Mechanical properties

Sample mechanical properties were investigated by tensile test. The protocols of sample preparation and test were previously described in §2.5.4.

Crosslinking process affected sample mechanical properties as reported in the following tables. In particular, in table 3.2, the mechanical properties values of ESCS and crosslinked samples, after two-steps method, are recorded. The reported average Young's modulus was determined from the slope of the linear elastic region of the stress-strain curve and averaged among the samples. The Young's modulus of the ESCS and crosslinked samples was found to be 7 ± 3 MPa for ESCS sample, and 17 ± 7 MPa, 144 ± 21 MPa, 63 ± 13 MPa, respectively for ESCSXL3, ESCSXL18 and ESCSXL24 samples. An increase in Young's modulus was observed in all crosslinked samples, and it was combined also with an increase in sample brittleness for ESCSXL18 and ESCSXL24 samples, making difficult sample handling.

	Young's modulus [MPa]	**Ultimate tensile strength [MPa]**	**Break strain [mm/mm]**
ESCS	7 ± 3	0.31 ± 0.08	0.07 ± 0.01
ESCSXL3	17 ± 7	0.7 ± 0.4	0.07 ± 0.03
ESCSXL18	144 ± 21	2.4 ± 0.6	0.04 ± 0.01
ESCSXL24	63 ± 13	0.8 ± 0.4	0.029 ± 0.005

Table 3.2 Mechanical properties values of ESCS and glutaraldehyde crosslinked samples after two-steps method.

In table 3.3, the mechanical properties values of ESCS and crosslinked samples, after one-step method, are recorded. The Young's modulus of the ESCS and crosslinked samples was found to be 7 ± 3 MPa for ESCS sample, 12 ± 2 MPa, and 18 ± 9 MPa, respectively for ESCSXLGA10 and ESCSXLGA50 samples. As previously reported for

the other investigated crosslinking method, an increase in Young's modulus value was observed in all crosslinked samples.

	Young's modulus [MPa]	Ultimate tensile strength [MPa]	Break strain [mm/mm]
ESCS	7 ± 3	0.31 ± 0.08	0.07 ± 0.01
ESCSXLGA10	12 ± 2	0.5 ± 0.1	0.08 ± 0.02
ESCSXLGA50	18 ± 9	0.48 ± 0.09	0.046 ± 0.009

Table 3.3 Mechanical properties values of ESCS and glutaraldehyde crosslinked samples after one-step method.

For what concerns genipin-crosslinked sample, mechanical properties values were close to uncrosslinked sample, as recorded in table 3.4, showing that the crosslinking process did not affect sample mechanical properties.

	Young's modulus [MPa]	Ultimate tensile strength [MPa]	Break strain [mm/mm]
ESCS	7 ± 3	0.31 ± 0.08	0.07 ± 0.01
ESCSXLGEN20	7 ± 4	0.10 ± 0.02	0.06 ± 0.02

Table 3.4 Mechanical properties values of ESCS and genipin crosslinked samples.

3.2.4 Biocompatibility assay

Considering that electrospun derived nanofibrous scaffolds are suitable for hMSCs applications [25] and that chitosan has been already used to host MSCs for experimental applications both *in vitro* and *in vivo* [26], preliminary tests, aimed to investigate cell viability of the obtained chitosan electrospun samples, were performed. Biocompatibility tests were performed only on two-steps crosslinked samples

(ESCSXL3) (protocols details are reported in §2.5.10). Cell viability (cells exposure to electrospun fibers) of those samples was higher than 90%. Moreover, the proliferation assay was performed on ESCSXL3 samples in triplicate and cells without scaffolds were cultured in the same conditions and used as control. Results showed a progressive increase in the number of cells, that was higher than the control, as showed in figure 3.12.

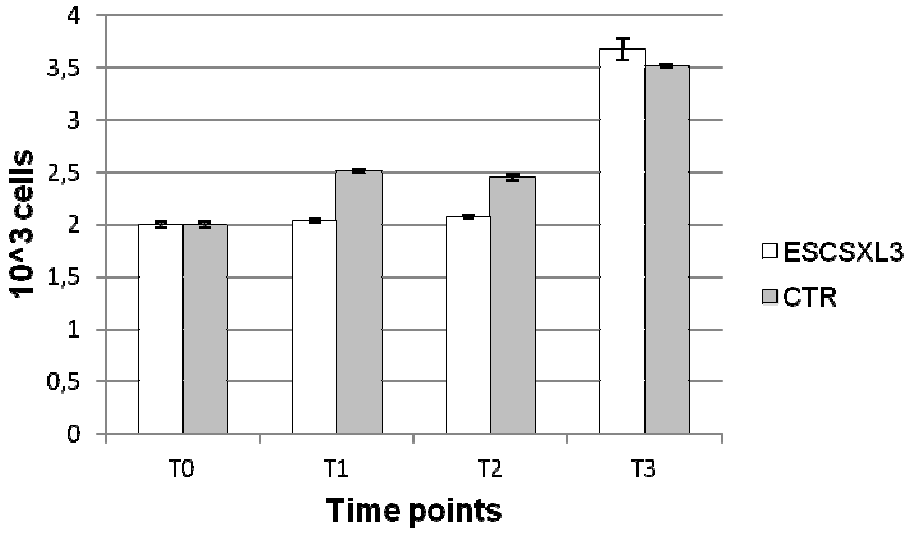

Figure 3.12 Graphic of proliferation assay results performed on chitosan electrospun membrane GA-crosslinked by two-steps method (ESCSXL3) at several time points: d1 (T1), d3 (T2) and d7 (T3).

These results suggested that the electrospinning process did not modify the biocompatibility of chitosan polymer confirming the absence of organic solvent residues on the synthesized scaffolds as already evidenced by ATR/FT-IR results. Further detailed biological assessments are mandatory in order to evaluate the effects of different crosslinkers on samples biological properties.

3.3 Conclusions

In this chapter, an optimization of pure chitosan electrospinning process, without the addition of copolymer was achieved, and homogeneous defect-free nanofibrous electrospun meshes of pure chitosan were obtained.

Moreover, the investigation and optimization of crosslinking processes for pure chitosan electrospun membranes, were performed, in particular two different crosslinking methods were evaluated, by using two chitosan crosslinker. All the obtained chitosan electrospun crosslinked samples were characterized in terms of morphology, chemical structure and mechanical properties.

Both the investigated methods allowed performing successful crosslinking of electrospun chitosan nanofibers. Samples obtained by one-step process were characterized by smaller diameter fibers. Glutaraldehyde-based crosslinking techniques affected sample mechanical properties, instead of the genipin-based crosslinking method.

References

[1] Huang Z-M, Zhang YZ, Kotaki M, Ramakrishna S. A review on polymer nanofibers by electrospinning and their applications in nanocomposites. Composites Science and Technology. 2003;63:2223-53.

[2] Teo W-E, Inai R, Ramakrishna S. Technological advances in electrospinning of nanofibers. Science and Technology of Advanced Materials. 2011;12:013002.

[3] Di Martino A, Sittinger M, Risbud MV. Chitosan: A versatile biopolymer for orthopaedic tissue-engineering. Biomaterials. 2005;26:5983-90.

[4] Jayakumar R, Prabaharan M, Nair SV, Tamura H. Novel chitin and chitosan nanofibers in biomedical applications. Biotechnol Adv. 2010;28:142-50.

[5] De Vrieze S, Westbroek P, Van Camp T, Van Langenhove L. Electrospinning of chitosan nanofibrous structures: feasibility study. Journal of Materials Science. 2007;42:8029-34.

[6] Ohkawa K, Cha D, Kim H, Nishida A, Yamamoto H. Electrospinning of Chitosan. Macromolecular Rapid Communications. 2004;25:1600-5.

[7] Desai K, Kit K, Li J, Zivanovic S. Morphological and Surface Properties of Electrospun Chitosan Nanofibers. Biomacromolecules. 2008;9:1000-6.

[8] Duan B, Wu L, Yuan X, Hu Z, Li X, Zhang Y, et al. Hybrid nanofibrous membranes of PLGA/chitosan fabricated via an electrospinning array. Journal of Biomedical Materials Research Part A. 2007;83A:868-78.

[9] Schiffman JD, Stulga LA, Schauer CL. Chitin and chitosan: Transformations due to the electrospinning process. Polymer Engineering & Science. 2009;49:1918-28.

[10] Klossner RR, Queen HA, Coughlin AJ, Krause WE. Correlation of Chitosan's Rheological Properties and Its Ability to Electrospin. Biomacromolecules. 2008;9:2947-53.

[11] Sangsanoh P, Supaphol P. Stability Improvement of Electrospun Chitosan Nanofibrous Membranes in Neutral or Weak Basic Aqueous Solutions. Biomacromolecules. 2006;7:2710-4.

[12] Teng S-H, Wang P, Kim H-E. Blend fibers of chitosan–agarose by electrospinning. Materials Letters. 2009;63:2510-2.

[13] Schiffman JD, Schauer CL. A Review: Electrospinning of Biopolymer Nanofibers and their Applications. Polymer Reviews. 2008;48:317-52.

[14] Schiffman JD, Schauer CL. Cross-Linking Chitosan Nanofibers. Biomacromolecules. 2007;8:594-601.

[15] Schiffman JD, Schauer CL. One-Step Electrospinning of Cross-Linked Chitosan Fibers. Biomacromolecules. 2007;8:2665-7.

[16] Chen ZG, Wang PW, Wei B, Mo XM, Cui FZ. Electrospun collagen-chitosan nanofiber: a biomimetic extracellular matrix for endothelial cell and smooth muscle cell. Acta Biomater. 2010;6:372-82.

[17] Tual C, Espuche E, Escoubes M, Domard A. Transport properties of chitosan membranes: Influence of crosslinking. Journal of Polymer Science Part B: Polymer Physics. 2000;38:1521-9.

[18] Koyama Y, Taniguchi A. Studies on chitin X. Homogeneous cross-linking of chitosan for enhanced cupric ion adsorption. Journal of Applied Polymer Science. 1986;31:1951-4.

[19] Muzzarelli RAA. Genipin-crosslinked chitosan hydrogels as biomedical and pharmaceutical aids. Carbohydrate Polymers. 2009;77:1-9.

[20] Lee KY, Jeong L, Kang YO, Lee SJ, Park WH. Electrospinning of polysaccharides for regenerative medicine. Advanced Drug Delivery Reviews. 2009;61:1020-32.

[21] Panzavolta S, Gioffrè M, Focarete ML, Gualandi C, Foroni L, Bigi A. Electrospun gelatin nanofibers: Optimization of genipin cross-linking to preserve fiber morphology after exposure to water. Acta Biomaterialia. 2011;7:1702-9.

[22] Yan L-P, Wang Y-J, Ren L, Wu G, Caridade SG, Fan J-B, et al. Genipin-cross-linked collagen/chitosan biomimetic scaffolds for articular cartilage tissue engineering applications. Journal of Biomedical Materials Research Part A. 2010;95A:465-75.

[23] Moura MJ, Figueiredo MM, Gil MH. Rheological Study of Genipin Cross-Linked Chitosan Hydrogels. Biomacromolecules. 2007;8:3823-9.

[24] Chiono V, Pulieri E, Vozzi G, Ciardelli G, Ahluwalia A, Giusti P. Genipin-crosslinked chitosan/gelatin blends for biomedical applications. Journal of Materials Science: Materials in Medicine. 2008;19:889-98.

[25] Nisbet DR, Forsythe JS, Shen W, Finkelstein DI, Horne MK. Review Paper: A Review of the Cellular Response on Electrospun Nanofibers for Tissue Engineering. Journal of Biomaterials Applications. 2009;24:7-29.

[26] Breyner NM, Hell RCR, Carvalho LRP, Machado CB, Peixoto Filho IN, Valério P, et al. Effect of a Three-Dimensional Chitosan Porous Scaffold on the Differentiation of Mesenchymal Stem Cells into Chondrocytes. Cells Tissues Organs. 2010;191:119-28.

Appendix

Optimization of pure chitosan electrospun membrane: process improvement

In order to improve the yield of the electrospinning process, the effects of the addition of several salts to chitosan solution (ref. § 2.1.3) were investigated in terms of improvement of solution spinnability and solution preservation before the electrospinning process (as previously reported in literature [10]). The selected salts were sodium chloride, calcium chloride and magnesium chloride, they were added to chitosan solution (solution n.14, list § 2.1.1) just before the electrospinning process. The amount of salt concentration was fixed at 1.67 % w/w respect to chitosan. For what concerns sodium chloride, also a double concentration was tested. In the following table, salt amount, SEM micrographs (obtained according to § 2.5.1) and calculated average fiber diameter are recorded.

Salt type	Amount of salt	Sample name	SEM micrograph	Average fiber diameter [nm]
NaCl	1.67 % w/w respect to chitosan	ESCSNa1	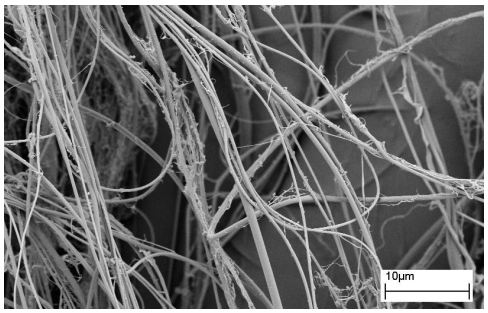	290 ± 100
	3.33 % w/w respect to chitosan	ESCSNa3	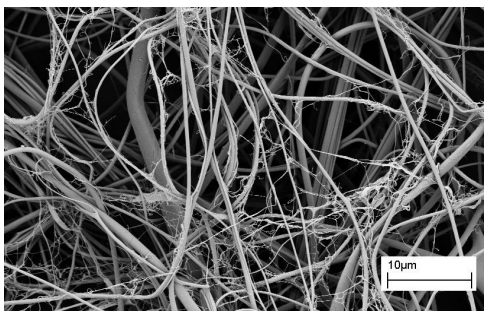	320 ± 110

$CaCl_2$	1.67 % w/w respect to chitosan	ESCSCa	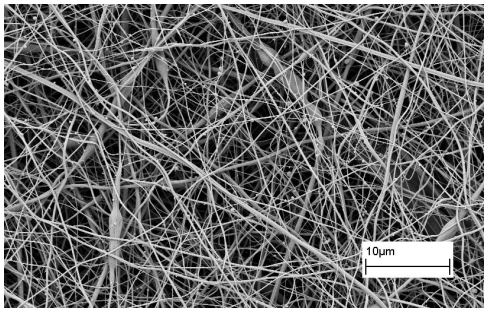	230 ± 110
$MgCl_2$	1.67 % w/w respect to chitosan	ESCSMg	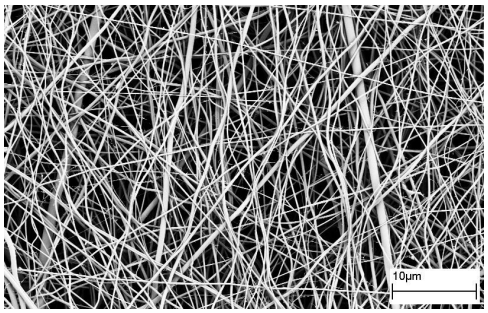	210 ± 40

Table 3.5 Salts amount, SEM micrographs and average fiber diameter.

For all salts added, an improvement in terms of increase in the electrospun membrane thickness (after the same time of electrospinning) was observed. All the samples were characterized by a reduction in average fiber diameter, respect to chitosan electrospun sample without any salts. The ATR/FT-IR analysis, performed according to §2.5.2, on those samples confirmed that the addition of salts did not modify the chemical structure of chitosan electrospun sample, as showed in the following figure.

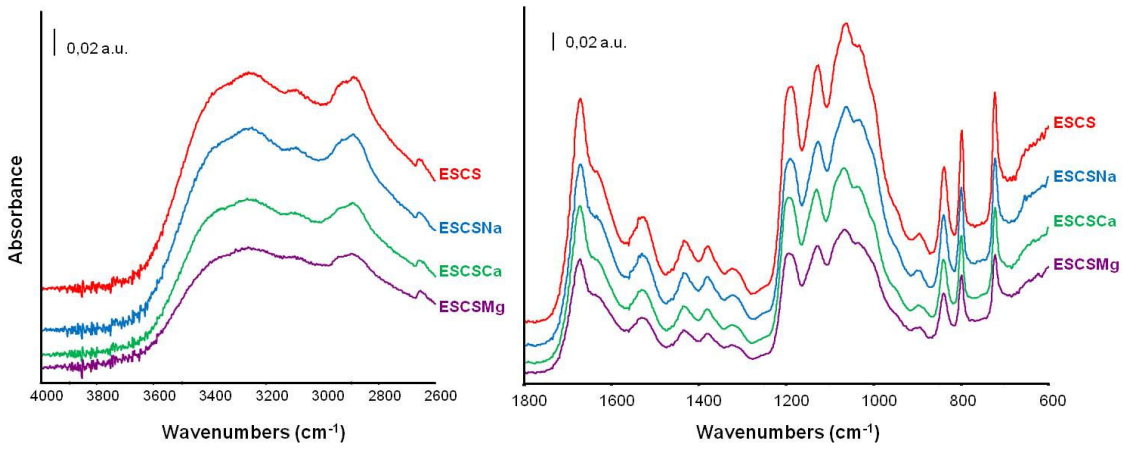

Figure 3.13 ATR/FT-IR spectra of chitosan electrospun samples after the addition of salts.

4. Electrospinning of hydroxyapatite-chitosan nanofibers

Index

Abstract

A biomimetic approach aiming to the fabrication of scaffolds with structure and composition similar to natural bone, was pursued, in this chapter, by the introduction of hydroxyapatite (HA) nanopowder within the polymeric fibers. The addition of HA was evaluated in terms of modifications in the chitosan solution spinnability, in the electrospinning parameters and crosslinking process. All the obtained chitosan/HA electrospun uncrosslinked and crosslinked samples were characterized in terms of morphology, chemical structure, mechanical properties and bioactivity. Positive results were obtained in terms of yield of the electrospinning process, fabrication of homogeneous nanofibrous sample morphology, preservation of HA structure in the obtained samples, and samples bioactivity.

4.1 Addition of nanopowder of hydroxyapatite for biomimetic aims

The electrospinning technique is a well-established method for the fabrication of nano- and microfibrous meshes based on the application of a high electric field between a positively charged electrode (tip of syringe containing a polymeric solution or melt) and a grounded (or negatively charged) fiber collector. Several evolutions of the standard setup have been developed, such as the design of specific collectors and the presence of multiple nozzle configurations which enable the fabrication of composite fibrous membranes by feeding different biomaterials at the same time [1-5].

Several studies have been focused on biomimetic approaches aiming to the fabrication of electrospun scaffolds with structure and composition similar to natural bone, by the introduction of inorganic phases within the polymeric fibers [6-9]. In fact, Ko *et al.* developed nanofibrous organic/inorganic composite electrospun scaffolds containing nano-sized demineralized bone powders (DBPs) with poly(L-lactide) (PLA), targeting bone regeneration, demonstrating that PLA/DBP scaffolds have better performance, with respect to bare PLA controls, in terms of early mineralization *in vitro* and new bone formation in critical size defects in rats [10]. Another example is the use of poly(L-lactic acid) blended with HA particles. Several concentrations of HA were evaluated and results showed that the presence of HA promoted the attachment and the proliferation of murine preosteoblastic cells MC3T3-E1, improving the extent of mineralization after 14 and 21 days of cell culture on these electrospun scaffolds [11]. Prabhakaran *et al*. fabricated and compared a PLA, a PLA/HA, and a PLA/collagen/HA electrospun scaffolds. *In vitro* experiments, after seeding with human fetal osteoblast cells (hFOBs), demonstrated that the synergic effect of PLA, collagen and HA enhanced mineral deposition, even respect to the PLA/HA scaffold [12]. An example of *in vivo* application of electrospun PLA/HA scaffolds in rabbit model was reported by Rainer *et al*. [13] They used, for sternal bone healing, an acellular microfibrous electrospun scaffold and inserted it directly in the site of rib fracture. After sternal repair evaluation, positive results were obtained in terms of fracture healing.

Several studies were focused on the use of chitosan in combination with HA particles [14-16]. In particular the use of chitosan/HA in combination with the electrospinning

technique was reported by Zhang *et al.* [14]. They fabricated a nanofibrous electrospun chitosan scaffold, mixed with poly(ethylene oxide) (PEO), loaded with HA nanoparticles, by combining an *in situ* co-precipitation synthesis approach with the electrospinning process. *In vitro* results, after seeding with hFOBs revealed that chitosan/HA scaffold improved bone formation with respect to the control, represented by chitosan-based scaffold without HA. This work highlighted also the importance of the preservation of HA crystalline structure after its dispersion in acid environment, that could induce HA structural modifications.

In the present chapter, different amount of commercial HA nanopowder was dispersed in chitosan solution before the electrospinning process. After the addition of HA nanopowder, the homogeneous chitosan/HA suspension was immediately electrospun. Different amount of HA were tested, until reaching a limit of HA concentration in optimized spinnable pure chitosan solution. This limit was represented by the solution at 30% w/w HA, respect to chitosan, and it was not spinnable. The obtained composite chitosan/HA membranes were crosslinked by two-steps process for 3 hours, by using GA 25% v/v aq. solution. Protocols details about synthesis, electrospinning and crosslinking processes are reported in § 2.1.3 and § 2.4.1.

4.2 Results and Discussion

In this section the results obtained from the electrospinning of chitosan with the addition of nanopowder of HA and the characterization of those samples are presented. The paragraph is divided in subsections devoted to the explanation of different outcomes from several characterization analyses.

4.2.1 Morphological analysis

SEM analysis was performed according to § 2.5.1. The presence of HA modified solution spinnability and also the yield of the process, for both tested HA concentrations. Moreover, an improvement in terms of increase in the electrospun membrane thickness (after the same time of electrospinning), respect to pure chitosan electrospun samples, was observed.

The addition of HA to chitosan solution modify the average fiber diameter, respect to pure chitosan, as recorded in table 4.1 (similar to table 2.2, containing sample name explanation). This reduction was observed in both samples, with the addition of 5% and 10% w/w respect to chitosan, and was preserved also after the crosslinking process.

Amount of hydroxyapatite	Crosslinking process	Crosslinker	Sample name	Note	Average fiber diameter [nm]
None	None	None	ESCS		450 ± 110
None	Two-steps (3 hours)	GA (aq. sol. 25% v/v)	ESCSXL3		440 ± 210
5% w/w respect to chitosan	None	None	ESCSHA5		200 ± 50
5% w/w respect to chitosan	Two-steps (3 hours)	GA (aq. sol. 25% v/v)	ESCSHA5XL		210 ± 70
10% w/w respect to chitosan	None	None	ESCSHA10		240 ± 70
10% w/w respect to chitosan	Two-steps (3 hours)	GA (aq. sol. 25% v/v)	ESCSHA10XL		220 ± 50
30% w/w respect to chitosan	None	None	ESCSHA30	It was not possible to electrospin that solution	
30% w/w respect to chitosan	Two-steps (3 hours)	GA (aq. sol. 25% v/v)	ESCSHA30XL	It was not possible to electrospin that solution	

Table 4.1 Summary about amount of HA, crosslinking process, sample name, note related to the electrospinning process and fiber average diameter, calculated by SEM image analysis (by using the software Image J (NIH, US), as previously reported in §2.5.1).

The addition of HA did not modify the homogeneous fibrillar structure already observed in pure chitosan electrospun samples. SEM analysis was used also to investigate eventual morphological modifications due to the crosslinking process. In fact, in figure 4.1, SEM micrographs of ESCSHA5 sample, before and after crosslinking, were reported. As showed, there were not visible differences in terms of

fibrillar structure and calculated average diameter (values recorded in table 4.1), referable to the crosslinking process.

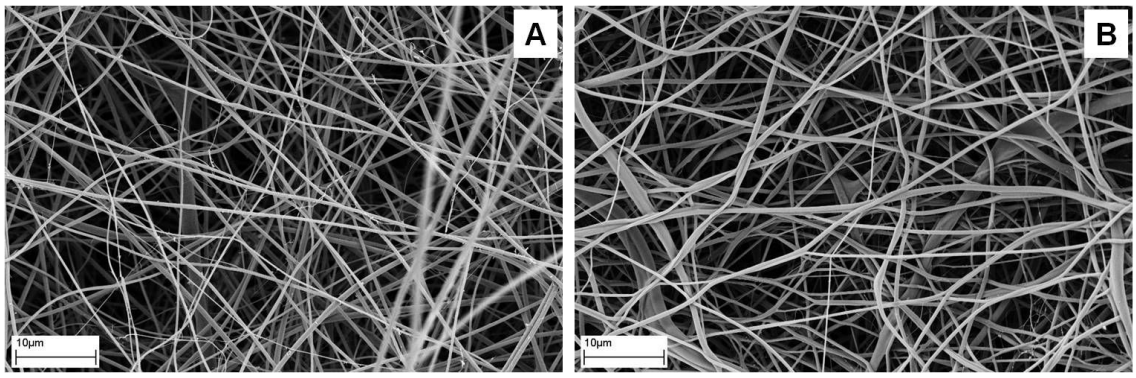

Figure 4.1 SEM micrographs of ESCSHA5 before (a) and after crosslinking process (b).

Same observations could be performed on ESCSHA10 samples. In fact, in figure 4.2 SEM micrographs of ESCSHA10 sample, before and after crosslinking, were reported. Also for those samples, there were not visible differences in terms of fibrillar structure and calculated average fiber diameters (values recorded in table 4.1), referable to the crosslinking process.

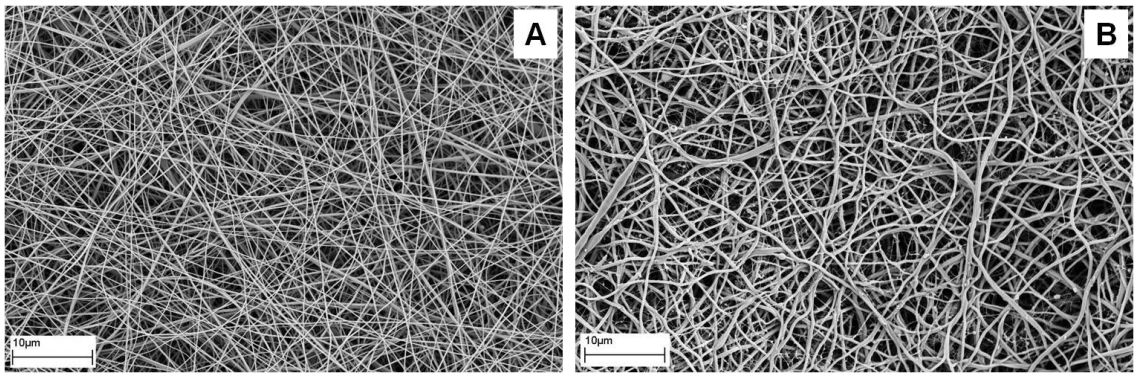

Figure 4.2 SEM micrographs of ESCSHA10 before (a) and after crosslinking process (b).

As showed in figure 4.1 and 4.2, no HA clusters were observed on fibers surface, indicating that the HA was homogeneously dispersed in the suspensions. Moreover, it was not possible to identify HA particles on single fibers, because the size of HA nanopowder was comparable with the average fiber diameter of the obtained meshes.

Results of EDS analysis, associated with SEM observations, are reported in figure 4.3. Spectrum recorded on the ESCSHA10 (not crosslinked) surface showed the presence of Ca and P. Semi-quantitative analysis on this sample gave a Ca/P ratio of 1.6, compatible with hydroxyapatite.

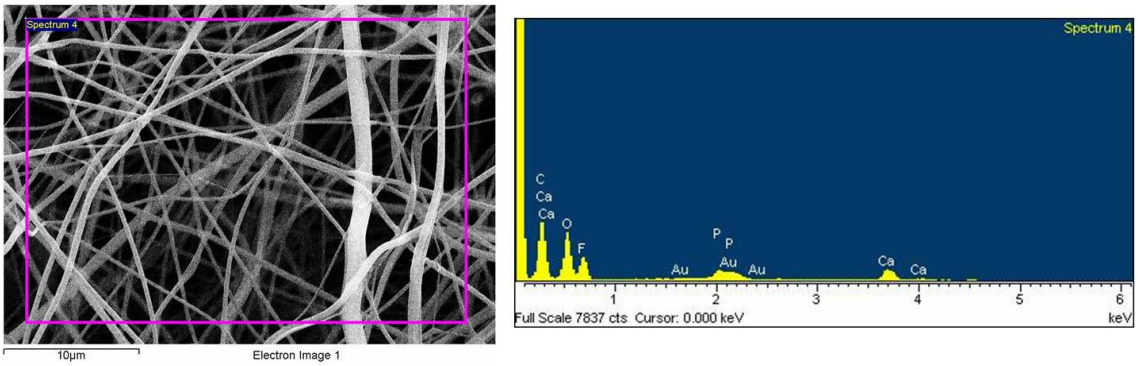

Figure 4.3 EDS spectrum, associated with SEM micrograph of ESCSHA10 sample.

4.2.2 ATR/FT-IR analysis

ATR/FT-IR analysis was performed, according to § 2.5.2, in order to evaluate the presence of HA in chitosan/HA samples, eventual interactions chitosan-HA and the effects of crosslinking process on these samples. Considering that the only difference between ESCSHA5 and ESCSHA10 samples was the amount of HA, here is reported the ATR/FT-IR analysis only on ESCAHA10 sample.

The spectra of ESCSHA10 and ESCS samples in the fingerprint region are reported in figure 4.4. In order to point out the differences introduced by the presence of HA, the spectrum arisen from the subtraction of ESCS spectrum from the ESCSHA10 one is reported in the same figure.

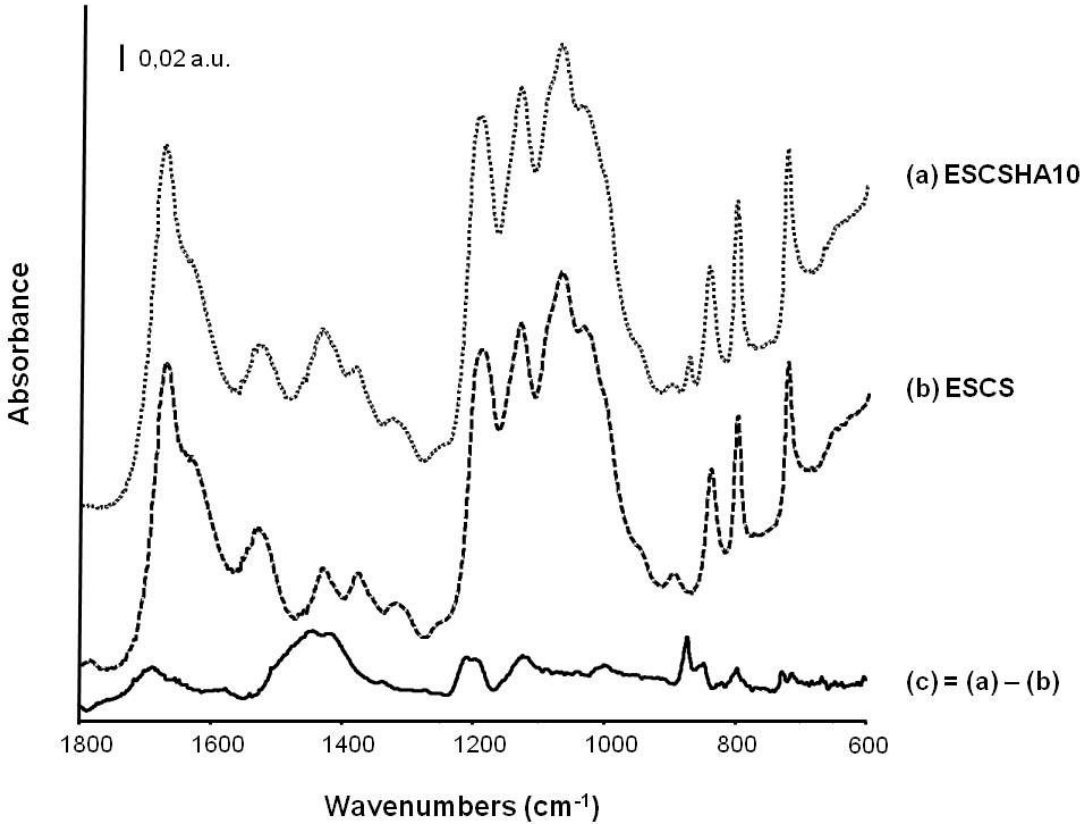

Figure 4.4 ATR/FT-IR spectra in the fingerprint region of ESCSHA10 (a), ESCS (b) samples, and the subtraction spectrum ESCSHA10 – ESCS (c).

All spectra were dominated by chitosan absorption. A component centered at 1340 cm^{-1} in the subtraction spectrum, due to stretching vibration of P=O group was present. This functional group P=O, belonging to the phosphate group, was involved in the formation of two different hydrogen bonding: one with the hydroxyl group and the other one with the amino group of chitosan structure. In fact, in the subtraction spectrum, a component centered at 1680 cm^{-1}, also observable in ESCSHA10 spectrum as a shoulder, was due to primary amine bending vibration. The increase of that component confirmed the hypothesis of hydrogen bonding between P=O and amino group.

In the subtraction spectrum, a broad band with two components centered at 1200 cm^{-1}, can be assigned to stretching vibration of P=O group involved in hydrogen bonding with hydroxyl group, confirming the hypothesis reported above.

A band with two components centered at 1120 cm^{-1} and a band centered at 1000 cm^{-1}, in the subtraction spectrum, were observed and due to the two components of ionic group PO_3^{2-} of phosphate group.

The presence of two categories of phosphate groups coordinated with chitosan chain confirmed the well dispersion of HA nanopowder, without clusters formation, as confirmed also by SEM micrographs, reported in § 4.2.1.

The presence of free HA in the sample was confirmed by the nonappearance of signals due to P-O-C aliphatic group, according to previous investigation [15].

For what concerns the evaluation of crosslinking process, the subtraction spectra of ESCSXL3 – ESCS (a) and ESCSHA10XL – ESCSHA10 (b) in the fingerprint region, are reported in figure 4.5. In both subtraction spectra the same main components were observed. Some modification in HA containing sample (and the shift of some bands), were due to the chitosan-HA interaction.

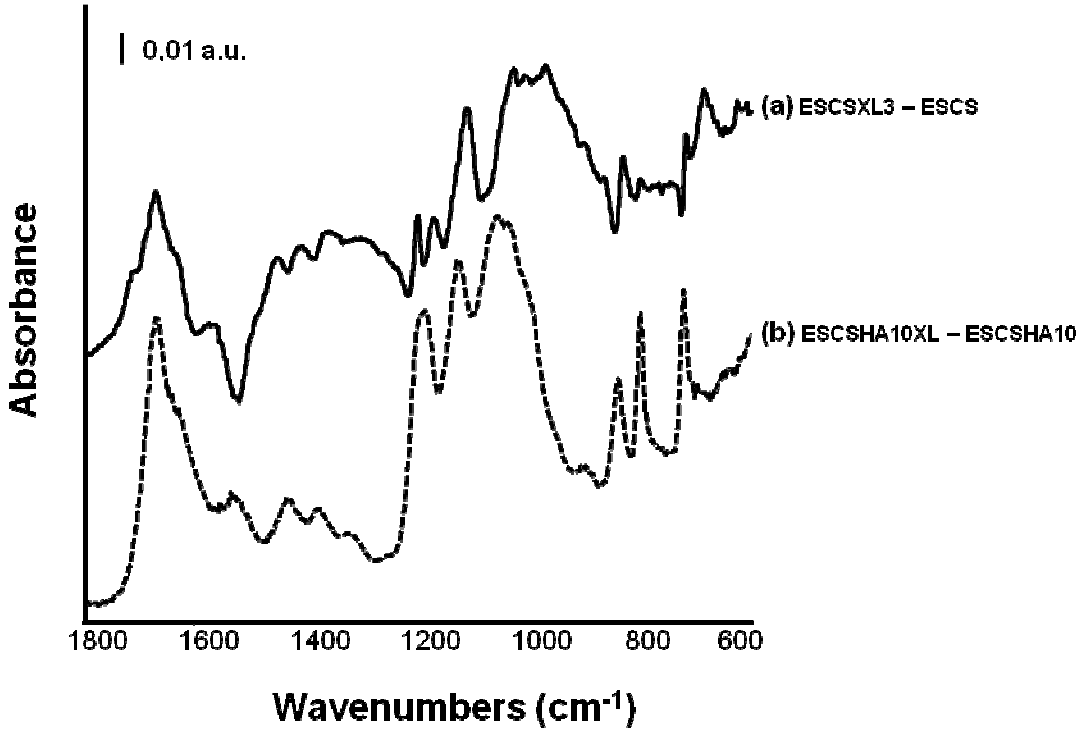

Figure 4.5 ATR/FT-IR Subtraction spectra of ESCSXL3 – ESCS (a) and ESCSHA10XL – ESCSHA10 (b) in the fingerprint region.

4.2.3 XRD analysis

XRD pattern (obtained according to § 2.5.3) reported in figure 4.6, showed both typical structural parameters of glutaraldehyde-chitosan crosslinked electrospun membranes,

according to [17] and confirmed the HA crystalline nature, as reported in a previous study by Zhang *et al.* [14].

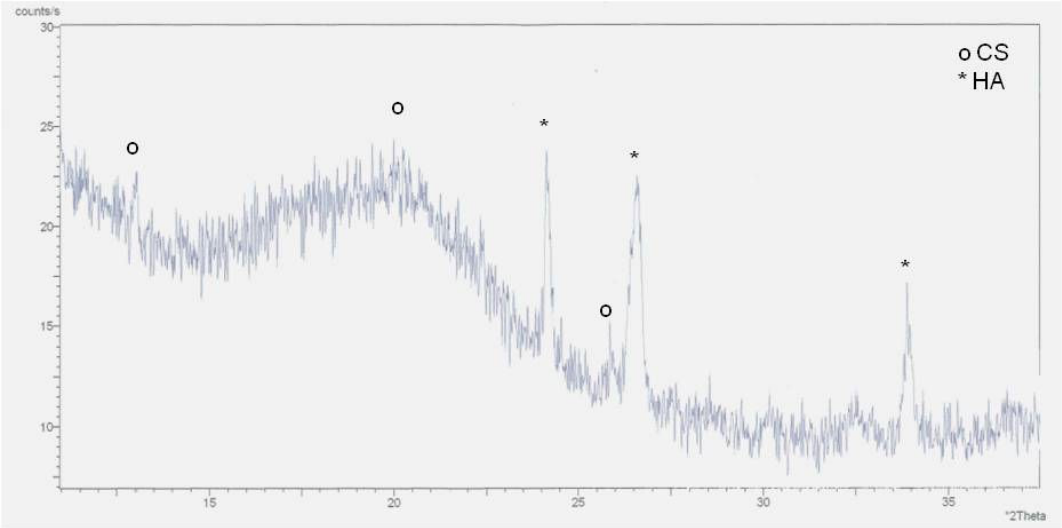

Figure 4.6 XRD pattern of ESCSHA10XL sample.

4.2.4 Mechanical properties

Sample mechanical properties were investigated by tensile test. The protocols of samples preparation and tests were previously described in §2.5.4.

The addition of HA in chitosan electrospun membrane affected sample mechanical properties as reported in the following table, in which the mechanical properties values of ESCS, ESCSHA10 and ESCSHA10XL, are recorded.

The Young's modulus of the ESCS and chitosan/HA samples was found to be 7 ± 3 MPa, 15 ± 3 MPa, and 39 ± 7 MPa, respectively for ESCS, ESCSHA10 and ESCSHA10XL samples. An increase in Young's modulus was observed in ESCSHA10 sample and a further increase was observed in crosslinked sample, according to previous results (§ 3.2.3).

	Young's modulus [MPa]	Ultimate tensile strength [MPa]	Break strain [mm/mm]
ESCS	7 ± 3	0.31 ± 0.08	0.07 ± 0.01
ESCSHA10	15 ± 3	0.7 ± 0.2	0.13 ± 0.03
ESCSHA10XL	39 ± 7	1.1 ± 0.4	0.09 ± 0.04

Table 4.2 Mechanical properties values of ESCS, ESCSHA10 and ESCSHA10XL.

These results highlighted another effect of the addition of HA nanoparticles dispersed in chitosan nanofibers. In fact, although the interface HA/chitosan is weak, as previously reported in the ATR/FT-IR analysis (i.e. two kind of hydrogen bonds between HA and chitosan), the mechanical properties (e.g. Young's modulus) resulted affected by the addition of HA, demonstrating the toughening effect of the dispersed HA nanopowder.

4.2.5 Bioactivity test (Simulated Body Fluid)

The bioactivity of the samples containing HA was assessed by samples immersion in a simulated body fluid (SBF) solution, according to [18], as reported in § 2.5.9. Samples modifications were evaluated by SEM analysis and ATR/FT-IR spectroscopy.
SEM analysis confirmed that after the immersion in SBF solution the electrospun samples preserved their fibrillar structure, as showed in figure 4.7.a. Some deposits precipitated on fibers surface since the first time point, as observed in figure 4.7.b. further investigations on these deposits were performed by ATR/FT-IR analysis.

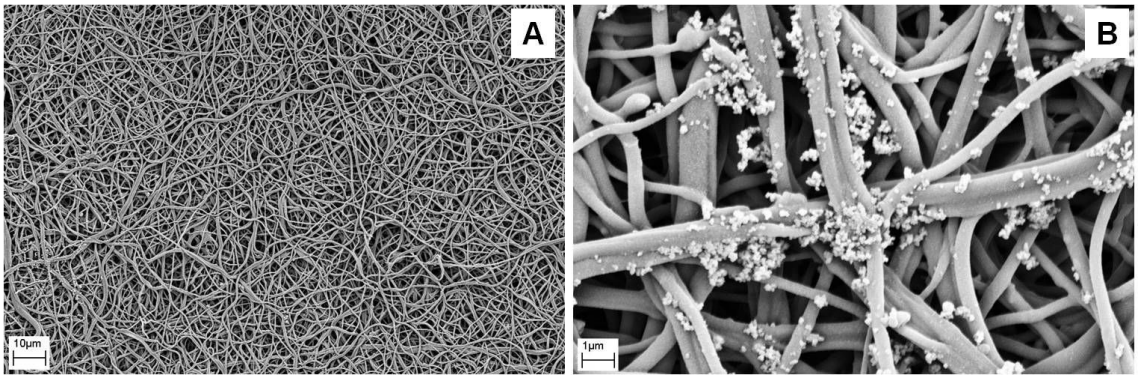

Figure 4.7 SEM micrographs of ESCSHA10 sample after 7 days of immersion in SBF solution (a) and a zoom view of the same sample after 1 day of immersion, confirming some deposits since the first time point.

ATR/FT-IR spectra in the fingerprint region of ESCSHA10XL samples before immersion (d0), and after immersion at each time points: after 1 day (d1), 3 days (d3), and 7 days (d7), are reported in figure 4.8. Some modifications were observed, in particular in the region of phosphate group vibration, in each time point spectrum.

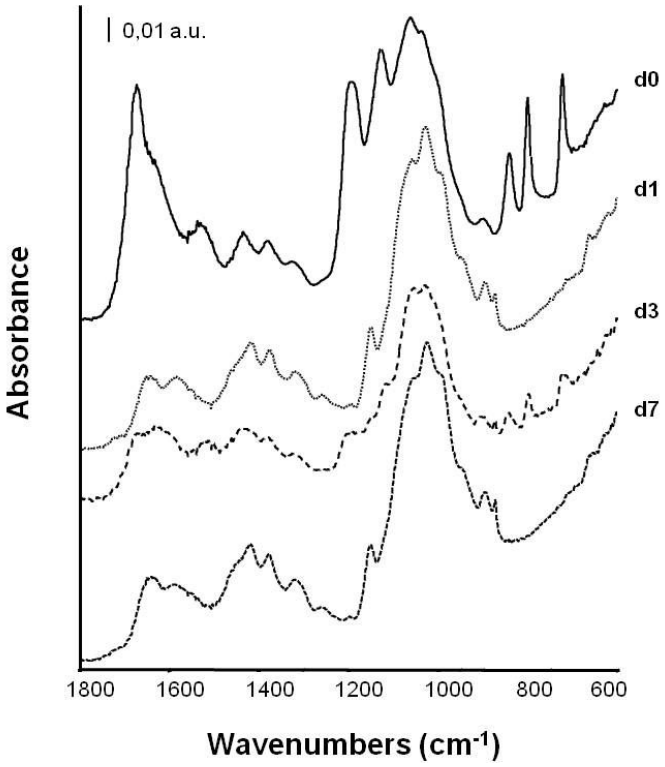

Figure 4.8 ATR/FT-IR spectra of ESCSHA10XL sample before immersion (d0),and after 1 day (d1), 3 days (d3) and 7 days (d7) of immersion in SBF solution.

The differences between d0 and d1, could be referred to the effect of the immersion in SBF solution on electrospun sample. For this reason, in order to eliminate the contribution of sample swelling and the HA contributions, presented in all samples and previously investigated in § 4.2.2, two subtraction spectra: d3 – d1 (figure 4.9.a) and d7 – d1 (figure 4.9.b), are reported. In particular, an increase in the band centered at 1050 cm^{-1}, due to the activity of phosphate group, referable only to the sample bioactivity after immersion in SBF solution, was showed.

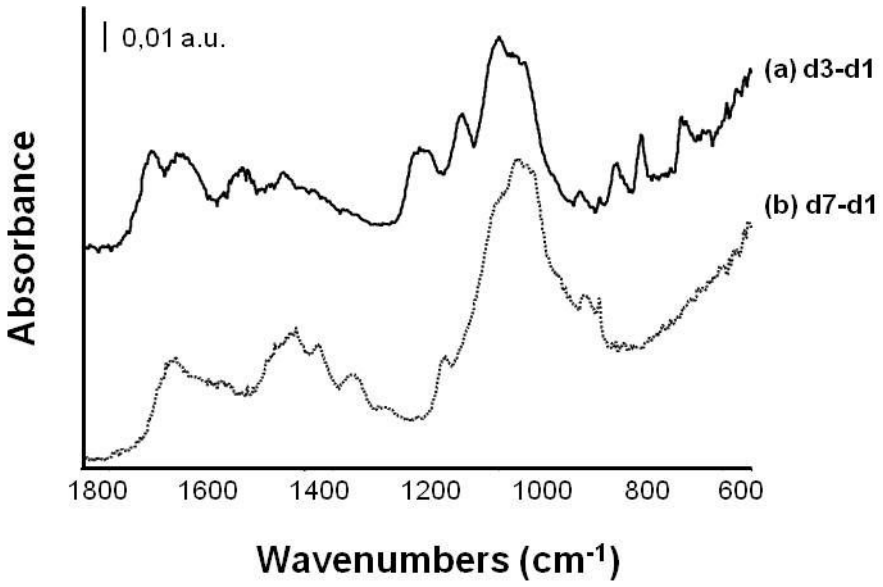

Figure 4.9 ATR/FT-IR subtraction spectra in the fingerprint region, between different timepoints of samples immersion in SBF solution: d3-d1 (a) and d7-d1 (b).

4.3 Conclusions

In this chapter, a biomimetic approach aiming to the fabrication of scaffolds with structure and composition similar to natural bone, was pursued by the introduction of inorganic phase (hydroxyapatite (HA) nanopowder) within the polymeric fibers. The addition of HA was evaluated in terms of modifications in the chitosan solution

spinnability and in the electrospinning parameters. All the obtained chitosan/HA electrospun uncrosslinked and crosslinked samples were characterized in terms of morphology, chemical structure, mechanical properties and bioactivity. In particular an accurate investigation was performed to confirm that HA preserved its typical structure after the introduction in chitosan solution, the electrospinning and crosslinking processes. Positive results were obtained in terms of yield of electrospinning process, fabrication of homogeneous nanofibrous sample morphology, preservation of HA structure in the obtained samples, and samples bioactivity.

In HA-containing samples, a decrease in fiber average diameter, and an increase in sample mechanical properties were observed.

References

[1] Secasanu VP, Giardina CK, Wang Y. A novel electrospinning target to improve the yield of uniaxially aligned fibers. Biotechnology Progress. 2009;25:1169-75.

[2] Park SA, Park K, Yoon H, Son J, Min T, Kim GH. Apparatus for preparing electrospun nanofibers: designing an electrospinning process for nanofiber fabrication. Polym Int. 2007;56:1361-6.

[3] Agarwal S, Wendorff JH, Greiner A. Progress in the Field of Electrospinning for Tissue Engineering Applications. Advanced Materials. 2009;21:3343-51.

[4] Kalra V, Lee JH, Park JH, Marquez M, Joo YL. Confined assembly of asymmetric block-copolymer nanofibers via multiaxial jet electrospinning. Small. 2009;5:2323-32.

[5] Kim GH, Min T, Park SA, Kim WD. Coaxially electrospun micro/nanofibrous poly(epsilon-caprolactone)/eggshell-protein scaffold. Bioinspir Biomim. 2008;3:16006.

[6] Olszta MJ, Cheng X, Jee SS, Kumar R, Kim Y-Y, Kaufman MJ, et al. Bone structure and formation: A new perspective. Materials Science and Engineering: R: Reports. 2007;58:77-116.

[7] Kim GM, Asran A, Michler GH, Simon P, Kim JS. Electrospun PVA/HAp nanocomposite nanofibers: biomimetics of mineralized hard tissues at a lower level of complexity. Bioinspir Biomim. 2008;3:046003.

[8] Kim H-W, Lee H-H, Chun G-S. Bioactivity and osteoblast responses of novel biomedical nanocomposites of bioactive glass nanofiber filled poly(lactic acid). Journal of Biomedical Materials Research Part A. 2008;85A:651-63.

[9] Ren L, Wang J, Yang F-Y, Wang L, Wang D, Wang T-X, et al. Fabrication of gelatin-siloxane fibrous mats via sol-gel and electrospinning procedure and its application for bone tissue engineering. Materials Science and Engineering: C. 2010;30:437-44.

[10] Ko EK, Jeong SI, Rim NG, Lee YM, Shin H, Lee B-K. In Vitro Osteogenic Differentiation of Human Mesenchymal Stem Cells and In Vivo Bone Formation in Composite Nanofiber Meshes. Tissue Engineering Part A. 2008;14:2105-19.

[11] Chuenjitkuntaworn B, Supaphol P, Pavasant P, Damrongsri D. Electrospun poly(L-lactic acid)/hydroxyapatite composite fibrous scaffolds for bone tissue engineering. Polymer International. 2010;59:227-35.

[12] Prabhakaran MP, Venugopal J, Ramakrishna S. Electrospun nanostructured scaffolds for bone tissue engineering. Acta Biomater. 2009;5:2884-93.

[13] Rainer A, Spadaccio C, Sedati P, De Marco F, Carotti S, Lusini M, et al. Electrospun Hydroxyapatite-Functionalized PLLA Scaffold: Potential Applications in Sternal Bone Healing. Annals of Biomedical Engineering. 2011;39:1882-90.

[14] Zhang Y, Venugopal JR, El-Turki A, Ramakrishna S, Su B, Lim CT. Electrospun biomimetic nanocomposite nanofibers of hydroxyapatite/chitosan for bone tissue engineering. Biomaterials. 2008;29:4314-22.

[15] Depan D, Venkata Surya PKC, Girase B, Misra RDK. Organic/inorganic hybrid network structure nanocomposite scaffolds based on grafted chitosan for tissue engineering. Acta Biomaterialia. 2011;7:2163-75.

[16] Kalpana SK, Dinesh RK, Rajalaxmi D. Synthesis and characterization of a novel chitosan/montmorillonite/hydroxyapatite nanocomposite for bone tissue engineering. Biomedical Materials. 2008;3:034122.

[17] Schiffman JD, Stulga LA, Schauer CL. Chitin and chitosan: Transformations due to the electrospinning process. Polymer Engineering & Science. 2009;49:1918-28.

[18] Kokubo T, Takadama H. How useful is SBF in predicting in vivo bone bioactivity? Biomaterials. 2006;27:2907-15.

5. Electrospinning of bioactive glass-chitosan nanofibers

Index

Abstract

In this chapter, a biomimetic approach, having the goal of the fabrication of scaffolds with structure and composition similar to natural bone, was pursued, by the introduction of bioactive glass (BG) particles, fabricated by sol-gel method, within the polymeric fibers. BG-loaded chitosan fibers were synthesized after the optimization of the electrospinning process. The addition of BG was evaluated in terms of modifications in the chitosan solution spinnability and stability, in the electrospinning parameters, and in the crosslinking process. All the obtained chitosan/BG electrospun samples were characterized in terms of morphology, chemical structure, mechanical properties and *in vitro* bioactivity. Positive results were obtained in terms of yield of the electrospinning process, fabrication of homogeneous nanofibrous sample morphology, and samples bioactivity.

5.1 Bioactive glass-chitosan system: a new couple of electrospinnable biomaterials

The major part of the bone extracellular matrix (ECM) contains calcium phosphates mineral phases which requires a mineralization step that is essential in the bone regeneration process. The existence of bone bioactive inorganic components within polymeric scaffold generally favors calcium phosphate mineralization followed by an osteogenic differentiation process. Therefore, several studies have focused on introducing a range of inorganic phases within the polymeric nanofibers with the ultimate aim of achieving both bone-specific bioactivity and improved mechanical properties [1, 2].

Recently, bone-bioactive inorganic materials (i.e. calcium phosphates and bioactive glasses/glass ceramics) have been used to obtain biomimetic electrospun constructs.

Nanofibrous inorganic materials were usually investigated in the role of nanofillers for the production of nanocomposite scaffolds with degradable polymers [3-8].

In particular, electrospun nanofibrous bioactive glass, was well homogenized with collagen or a PLLA solution with the aim to produce uniform and homogenous scaffolds, for improving the bone-bioactivity of the organic phase, the osteogenic differentiation and the cellular mineralization. Positive results, related to coupling bone-bioactivity of the inorganic component with shape-formability of the organic phase, led to the considerations that this kind of approach is very useful and promising for further applications [3, 4].

The matching of sol–gel processing and electrospinning technique, was used by Ren *et al.* for gelatin/siloxane hybrids fabrication. Bone marrow-derived mesenchymal stem cells (BMSCs) were seeded on these hybrid constructs. The results indicated that by varying the viscosity of gelatin/siloxane precursor solution it was possible to regulate the porous structure and fiber size of the gelatin/siloxane fibrous mats. Additionally, gelatin/siloxane fibrous mats biomimetically deposited apatite in a simulated body fluid (SBF), as well as stimulating BMSCs proliferation and differentiation *in vitro* [9].

Another way of combining bioactive glass and the polymeric electrospun meshes was represented by the use of the electrospun meshes as external coating for bioactive glass

scaffolds. In particular, bioactive glass scaffolds were used as target fiber collector during the electrospinning process [10-12].

Chitosan is considered as one of the most attractive natural biopolymers for biomedical and biotechnological applications [13, 14]. The combined use of chitosan and bioactive glass was already focus of previous studies [7, 8]. In particular, Peter *et al.* fabricated composite scaffolds, by disseminating bioactive glass nanoparticles in chitosan solution before the freeze drying process, obtaining positive results in terms of nanoparticles dispersion, scaffold swelling and degradation properties, *in vitro* bioactivity and cell viability [8]. Tuzlakoglu *et al.* presented a simply method of combining Bioglass® and chitosan fibrous scaffolds, obtained by wet spinning. In fact, that method was based on spraying a Bioglass®/water suspension on the surface of the scaffolds. That spraying methodology allows the coating of the bulk of the scaffold. Samples were, then, dried under air flow and immersed in simulated body fluid (SBF) for 7 days. Positive outcomes in terms of cell (human osteoblast-like cell line SaOs-2) adhesion and viability were obtained [7].

Moreover, it is important to consider the potentiality of ionic dissolution products of bioactive glass in biological environment [15], evaluating also the versatile applications, beyond the bone tissue engineering, of those composite scaffolds.

In the present chapter, the combining use of bioactive glass (BG) particles and chitosan with the electrospinning process was reported. In particular, BG particles were homogeneously dispersed in chitosan solution (solution n.14, list in § 2.1.1) before the electrospinning process. BG powder was obtained by sol-gel process, accordingly to Rainer *et al.* [16]. The obtained homogeneous suspension was immediately electrospun. The obtained composite chitosan/BG membranes were crosslinked by two-steps process for 3 hours, by using GA 25% v/v aq. solution. Protocols details about synthesis, electrospinning and crosslinking processes are reported in § 2.1.3 and § 2.4.1.

5.2 Results and Discussion

In this section the results obtained from the electrospinning of chitosan with the addition of BG particles and the characterization of the produced samples, are reported. The paragraph is divided in subsections devoted to the explanation of different outcomes from several characterization analyses.

5.2.1 Morphological analysis

SEM analysis was performed on the obtained samples according to § 2.5.1. It was performed the electrospinning of two different solution concentrations, the first one contained 2 wt% of BG powder respect to chitosan, was used to investigate the suspension stability before, during and after the process of electrospinning. After checking solution stability, conductivity and effects on the yield of the electrospinning process respect to electrospun pure chitosan, the other solution, containing 15 wt% of BG powder respect to chitosan, was tested. A summary of the amount of BG, crosslinking process, sample name, and fiber average diameter, calculated by SEM image analysis, as previously reported in §2.5.1, is recorded in the following table (table 5.1 is similar to table 2.3, containing sample name explanation).

Amount of BG	Crosslinking process	Crosslinker	Sample name	Note	Average fiber diameter [nm]
None	None	None	ESCS		450 ± 110
None	Two-steps (3 hours)	GA (aq. sol. 25% v/v)	ESCSXL3		440 ± 210
2% w/w respect to chitosan	None	None	ESCSBG2		855 ± 54
2% w/w respect to chitosan	Two-steps (3 hours)	GA (aq. sol. 25% v/v)	ESCSBG2XL	Not performed	--
15% w/w respect to chitosan	None	None	ESCSBG15		176 ± 29
15 % w/w respect to chitosan	Two-steps (3 hours)	GA (aq. sol. 25% v/v)	ESCSBG15XL		280 ± 73

Table 5.1 Summary about amount of BG, crosslinking process, sample name, and fiber average diameter, calculated by SEM image analysis, as previously reported in § 2.5.1.

The first solution with 2 wt% of BG, led to the fabrication of a inhomogeneous net of fibers (as showed in figure 5.1.a), for that reason this sample was not crosslinked. An increase in average fiber diameter, respect to pure chitosan electrospun sample, was also observed and reported in table 5.1. A detail of BG particles embedded on chitosan fiber' surface was showed in figure 5.1.b.

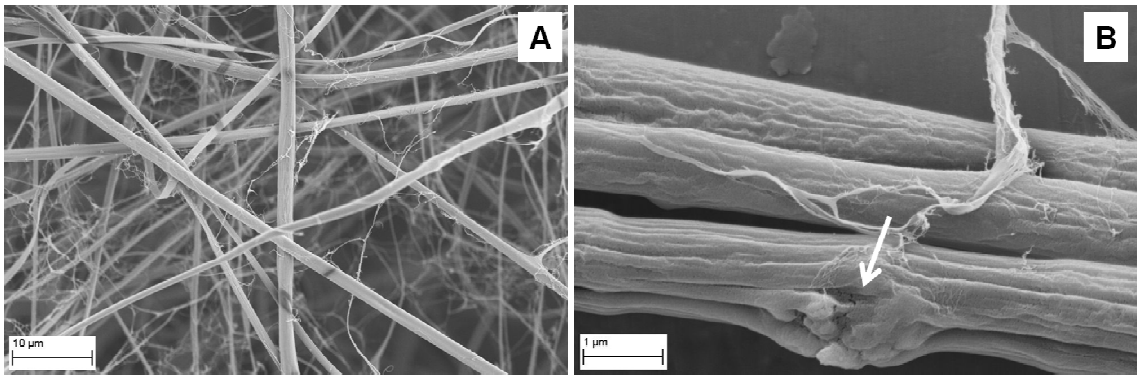

Figure 5.1 SEM micrographs of ESCSBG2 sample (a) and a zoom view of the same sample, underlying the presence of BG particle on fiber surface, as indicated by the red arrow (b).

The electrospinning of the chitosan solution containing 15 wt% of BG, produced an homogeneous mesh of nanofiber, as showed in figure 5.2.a, with an average fiber diameter of 176 ± 29 nm, as recorded in table 5.1. Moreover, an improvement in terms of increase in the electrospun membrane thickness (after the same time of electrospinning), respect to pure chitosan electrospun samples, was observed.

The crosslinking process (two-steps method, previously described in § 2.1.2) did not affect the fibrous morphology of chitosan/BG sample, as showed in figure 5.2.b, and also the average fiber diameter was comparable to the same sample before the crosslinking.

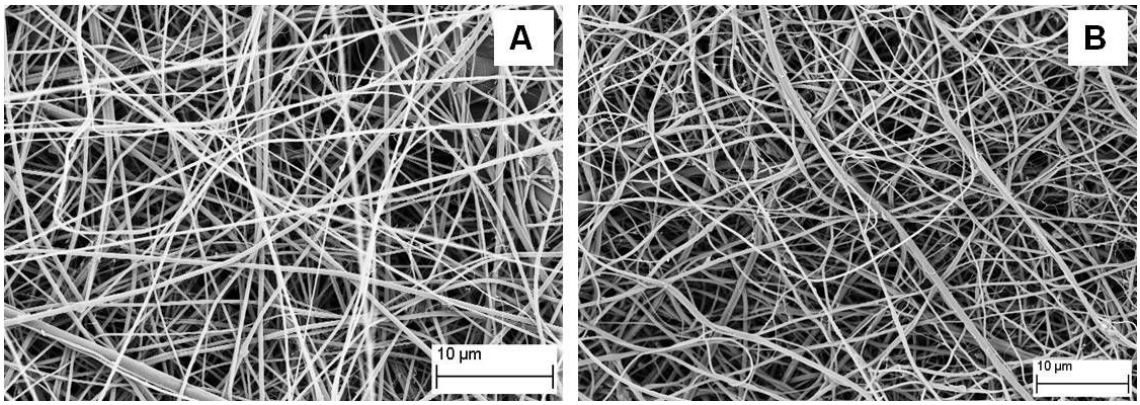

Figure 5.2 SEM micrographs of ESCSBG15 before (a) and after crosslinking process (b).

5.2.2 ATR/FT-IR analysis

ATR/FT-IR analysis, performed according to § 2.5.2, had the role to evaluate the presence of BG in chitosan/BG samples, eventual interactions chitosan-BG and the effects of crosslinking process on these samples.

ATR/FT-IR spectra of the electrospun chitosan membrane ESCS (without BG); the electrospun chitosan/BG membrane, pure BG powder, and the subtraction of ESCS spectrum from the ESCSBG15 one are reported in the same figure 5.3.

Both spectra (a) and (b), in figure 5.3, were dominated by chitosan absorption, and the presence of BG was observed in the subtraction spectrum (c), confirming the presence of BG after the electrospinning process. In particular, the peak at 1050 cm^{-1} was due to stretching vibration of Si-O-Si, according to [16] and the peak shift, respect to the BG powder spectrum, was due to BG-chitosan interaction.

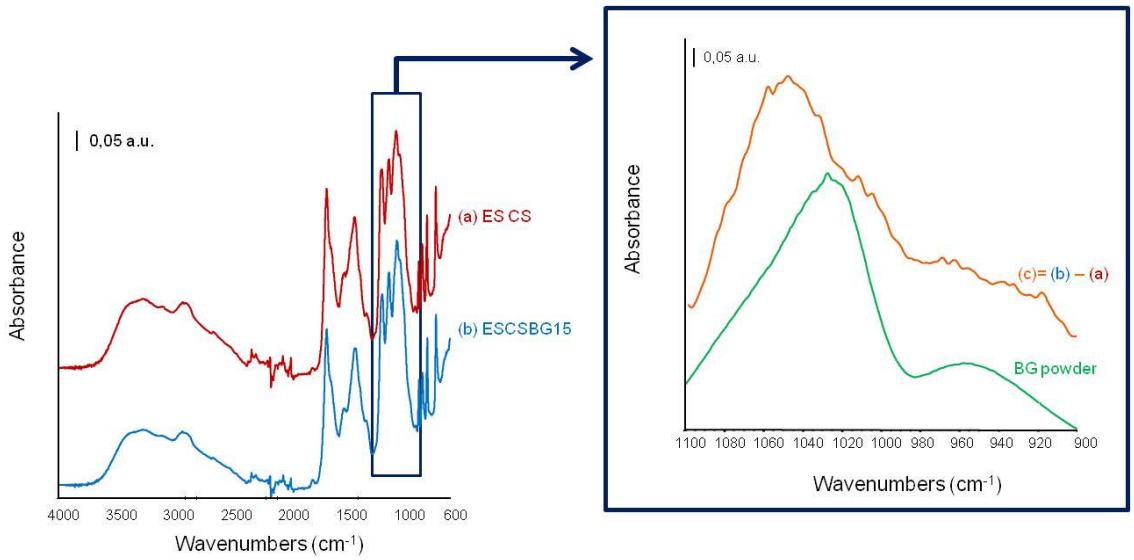

Figure 5.3 ATR/FT-IR spectra of the electrospun chitosan membrane ESCS (without bioglass) in (a); electrospun chitosan/BG membrane ESCSBG15 (b), subtraction spectrum: (c) = (b) – (a), and BG powder.

After the crosslinking process, it was necessary to evaluate the effects of this process on chitosan/BG samples. ATR/FT-IR samples are showed in figure 5.4. Spectral evidence of the crosslinking in chitosan/BG sample are reported in figures 5.4.a and 5.4.b. The crosslinking process did not modify bioglass structure, as showed in the ATR/FT-IR spectra in figure 5.4.c and 5.4.d. In fact the peak at 1050 cm^{-1} due to stretching vibration of Si-O-Si, and the same peak shift reported above, were observed.

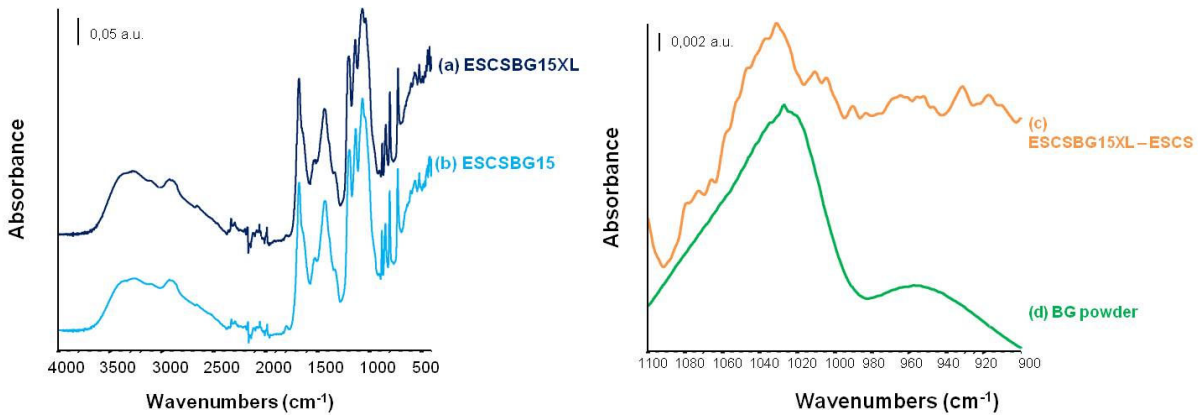

Figure 5.4 ATR/FT-IR spectra of ESCSBG15XL (a), ESCSBG15 (b) samples, the subtraction spectrum ESCSBG15XL – ESCS (c), and the BG powder (d).

5.2.3 Mechanical properties

Sample mechanical properties were investigated by tensile test. The protocols of samples preparation and tests were previously described in §2.5.4.

The addition of BG in chitosan electrospun membrane did not affect sample mechanical properties as reported in the following table, in which the mechanical properties values of ESCS, ESCSXL3, ESCSBG15 and ESCSBG15XL, are recorded.

The Young's modulus of the chitosan and chitosan/BG samples was found to be 7 ± 3 MPa, 17 ± 7 MPa, 6 ± 2 MPa, and 10 ± 4 MPa respectively for ESCS, ESCSXL3, ESCSBG15 and ESCSBG15XL samples.

	Young's modulus [MPa]	**Ultimate tensile strength [MPa]**	**Break strain [mm/mm]**
ESCS	7 ± 3	0.31 ± 0.08	0.07 ± 0.01
ESCSXL3	17 ± 7	0.7 ± 0.4	0.07 ± 0.03
ESCSBG15	6 ± 2	0.27 ± 0.06	0.069 ± 0.007
ESCSBG15XL	10 ± 4	0.34 ± 0.08	0.04 ± 0.02

Table 5.2 Mechanical properties values of ESCS, ESCSXL3, ESCSBG15 and ESCSBG15XL.

An increase in Young's modulus value was observed for crosslinked sample (ESCSBG15XL value respect to ESCSBG15 value), according to previous results (§ 3.2.3). The amount of BG particles was not enough to induce modifications in mechanical properties, e.g. an increase in Young's modulus, as previously observed for the addition of HA to chitosan nanofibers. The absence of modifications in samples mechanical properties could be ascribable not only to the scarcity of dispersed BG, but also to the weak interface BG/chitosan.

5.2.4 Bioactivity test (Simulated Body Fluid)

The bioactivity of the samples containing BG was assessed by samples immersion in a simulated body fluid (SBF) solution, according to [17], as reported in § 2.5.9. Samples modifications were evaluated by SEM analysis and ATR/FT-IR spectroscopy.

SEM analysis confirmed that after the immersion in SBF solution the electrospun samples preserved their fibrillar structure at each time point (after 1, 3 and 7 days of immersion), as showed in figure 5.5.

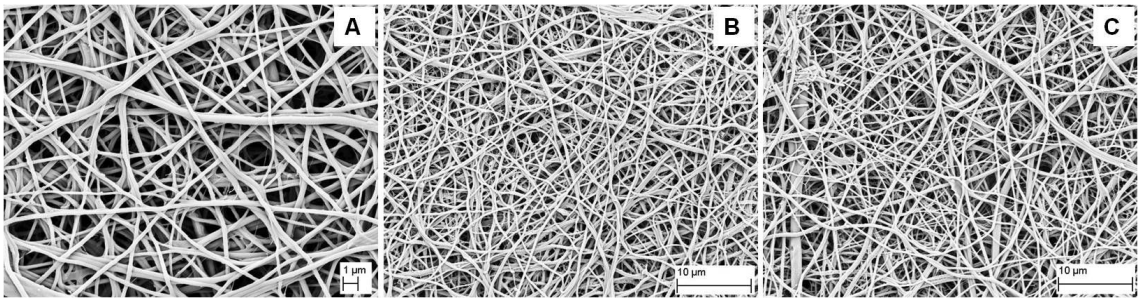

Figure 5.5 SEM micrographs of ESCSBG15XL sample after 1 (a), 3 (b), and 7 (c) days of immersion in SBF solution.

ATR/FT-IR spectra of ESCSBG15XL samples after immersion at each time points: after 1 day (d1), 3 days (d3), and 7 days (d7), are reported in figure 5.6.a. Some modifications were observed, in particular in the region of phosphate group vibration, in each timepoint spectrum.

Considering that the immersion in aqueous solution modify samples ATR/FTIR spectra, in order to eliminate the contribution of sample swelling and the BG contributions, presented in all samples, two subtraction spectra: d3 – d1 and d7 – d1 are reported in figure 5.6.b. In particular in those spectra, a progressive increase in a broad band centered at 900 cm^{-1} due to stretching vibration of phosphate group, was showed and ascribable to the sample bioactivity after immersion in SBF solution.

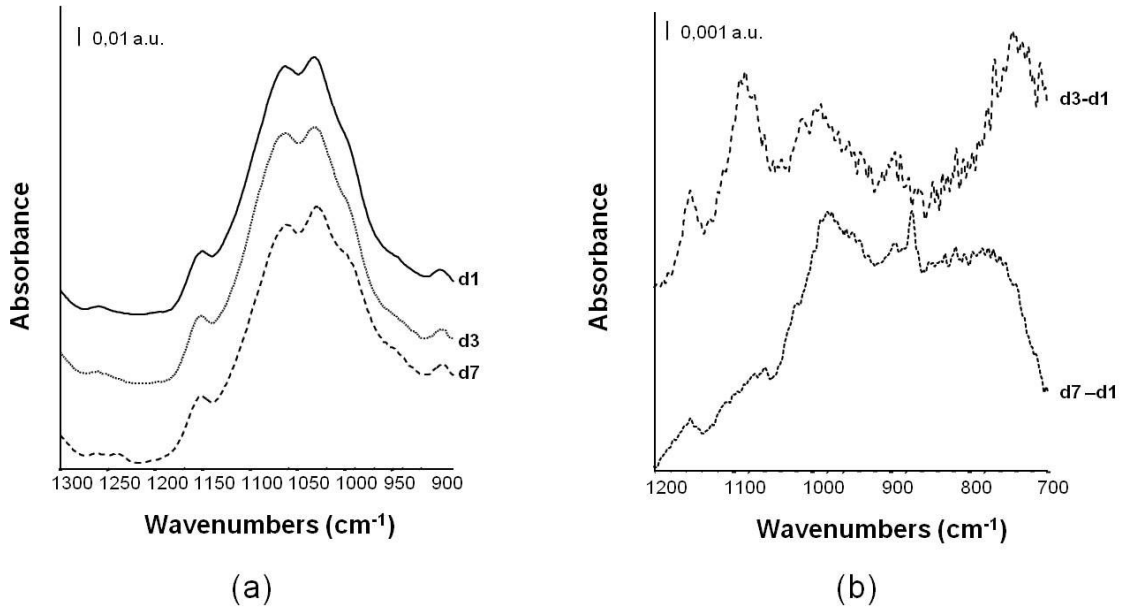

Figure 5.6 ATR/FT-IR spectra of ESCSBG15XL sample after 1 day (d1), 3 days (d3) and 7 days (d7) of immersion in SBF solution (a) and ATR/FT-IR subtraction spectra, between different timepoints of samples immersion in SBF solution: d3-d1 and d7-d1.

5.2.5 Biocompatibility assay

Samples characterization was completed by a preliminary cell viability assay. Biocompatibility tests were performed on ESCSBG15XL samples (in triplicate), and ESCSXL3 samples (in triplicate) were used as control (protocols detail are reported in § 2.5.10). Cell viability of those samples was higher than 80%, as showed in figure 5.7.

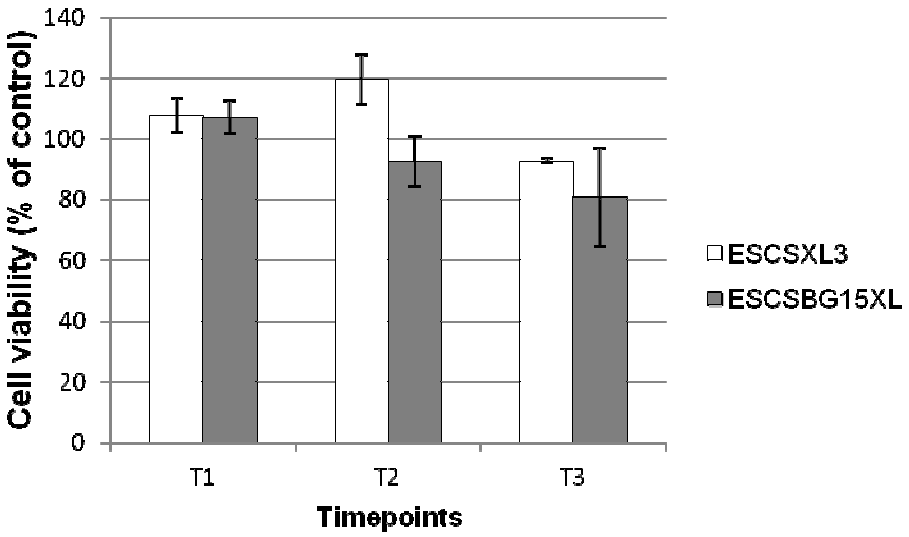

Figure 5.7 Cell viability of ESCSXL3 (chitosan) and ESCSBG15XL (chitosan BG) samples, evaluated by MTT assay with 3 timepoints: 4h (T1), 8h (T2) and 24h (T3).

These preliminary positive results showed the potential suitability of the obtained scaffolds for tissue engineering applications, even if further assessments (e.g. differentiation assay) are mandatory because they could highlight the presence of specific differentiative stimuli due to the BG particles dispersion in chitosan nanofibers.

5.3 Conclusions

In conclusion, BG-loaded chitosan fibers were synthesized after the optimization of the electrospinning process. All the obtained chitosan/BG electrospun uncrosslinked and crosslinked samples were characterized in terms of morphology, chemical structure, mechanical properties and bioactivity. Composite scaffolds showed homogeneous fibrous structure, and a decrease in fiber average diameter with respect to pure chitosan meshes. Moreover, the addition of the ceramic phase increased *in vitro* bioactivity of pure chitosan.

References

[1] Olszta MJ, Cheng X, Jee SS, Kumar R, Kim Y-Y, Kaufman MJ, et al. Bone structure and formation: A new perspective. Materials Science and Engineering: R: Reports. 2007;58:77-116.

[2] Di Martino A, Liverani L, Rainer A, Salvatore G, Trombetta M, Denaro V. Electrospun scaffolds for bone tissue engineering. Musculoskeletal Surgery. 2011;95:69-80.

[3] Kim H-W, Song J-H, Kim H-E. Bioactive glass nanofiber-collagen nanocomposite as a novel bone regeneration matrix. Journal of Biomedical Materials Research Part A. 2006;79A:698-705.

[4] Kim H-W, Lee H-H, Chun G-S. Bioactivity and osteoblast responses of novel biomedical nanocomposites of bioactive glass nanofiber filled poly(lactic acid). Journal of Biomedical Materials Research Part A. 2008;85A:651-63.

[5] Boccaccini AR, Erol M, Stark WJ, Mohn D, Hong Z, Mano JF. Polymer/bioactive glass nanocomposites for biomedical applications: A review. Composites Science and Technology. 2010;70:1764-76.

[6] Rezwan K, Chen QZ, Blaker JJ, Boccaccini AR. Biodegradable and bioactive porous polymer/inorganic composite scaffolds for bone tissue engineering. Biomaterials. 2006;27:3413-31.

[7] Tuzlakoglu K, Reis R. Formation of bone-like apatite layer on chitosan fiber mesh scaffolds by a biomimetic spraying process. Journal of Materials Science: Materials in Medicine. 2007;18:1279-86.

[8] Peter M, Binulal NS, Soumya S, Nair SV, Furuike T, Tamura H, et al. Nanocomposite scaffolds of bioactive glass ceramic nanoparticles disseminated chitosan matrix for tissue engineering applications. Carbohydrate Polymers. 2010;79:284-9.

[9] Ren L, Wang J, Yang F-Y, Wang L, Wang D, Wang T-X, et al. Fabrication of gelatin-siloxane fibrous mats via sol-gel and electrospinning procedure and its application for bone tissue engineering. Materials Science and Engineering: C. 2010;30:437-44.

[10] Bretcanu O, Misra SK, Yunos DM, Boccaccini AR, Roy I, Kowalczyk T, et al. Electrospun nanofibrous biodegradable polyester coatings on Bioglass®-based glass-ceramics for tissue engineering. Materials Chemistry and Physics. 2009;118:420-6.

[11] Yunos DM, Ahmad Z, Boccaccini AR. Fabrication and characterization of electrospun poly-DL-lactide (PDLLA) fibrous coatings on 45S5 Bioglass® substrates for bone tissue engineering applications. Journal of Chemical Technology & Biotechnology. 2010;85:768-74.

[12] Yunos DM, Ahmad Z, Salih V, Boccaccini AR. Stratified scaffolds for osteochondral tissue engineering applications: Electrospun PDLLA nanofibre coated Bioglass®-derived foams. Journal of Biomaterials Applications. 2011.

[13] Jayakumar R, Prabaharan M, Nair SV, Tamura H. Novel chitin and chitosan nanofibers in biomedical applications. Biotechnol Adv. 2010;28:142-50.

[14] Schiffman JD, Schauer CL. A Review: Electrospinning of Biopolymer Nanofibers and their Applications. Polymer Reviews. 2008;48:317-52.

[15] Hoppe A, Güldal NS, Boccaccini AR. A review of the biological response to ionic dissolution products from bioactive glasses and glass-ceramics. Biomaterials. 2011;32:2757-74.

[16] Rainer A, Giannitelli SM, Abbruzzese F, Traversa E, Licoccia S, Trombetta M. Fabrication of bioactive glass–ceramic foams mimicking human bone portions for regenerative medicine. Acta Biomaterialia. 2008;4:362-9.

[17] Kokubo T, Takadama H. How useful is SBF in predicting in vivo bone bioactivity? Biomaterials. 2006;27:2907-15.

6. Electrospun chitosan membranes as a component of multilayer composite for osteochondral tissue engineering

Index

The experimental activities reported in this chapter were designed and performed at Institute for Biomaterials, Department of Material Science and Engineering, Friedrich Alexander University of Erlangen-Nuremberg (Germany), during the candidate's PhD visiting period, under the direct supervision of Prof. Aldo R. Boccaccini.

Abstract

A straightforward method for manufacturing stratified scaffolds for osteochondral tissue engineering is reported. The method integrates three different techniques widely used for scaffold fabrication: the sponge replica method, freeze drying and freeze gelation,

and electrospinning. 45S5 Bioglass® was used for the fabrication of the rigid bioactive substrate intended to be in contact with bone tissue, chitosan and alginate based solutions were used for building the interface between the Bioglass®-based scaffold and the soft cartilage side of the construct. Finally a chitosan-based electrospun nanofibrous membrane (previously described in chapter 3) was selected for the upper layer of the scaffold. In this design, the intermediate layer had multiple functions providing adherence between the other scaffold components, preventing delamination and acting as soft coating for the rigid Bioglass® substrate. Morphological analysis, bioactivity tests in simulated body fluid (SBF), as well as mechanical and wettability tests were performed on all samples to assess the optimal stratified scaffold combination. Key results are presented and discussed in the context of the potential application of these novel scaffolds in osteochondral tissue engineering.

6.1 Introduction

In this chapter, a particular application of chitosan-based electrospun membranes, previously described in chapters 3, 4 and 5, is reported.

Biomimetic approaches to functional tissue engineering focusing on tissue-to-tissue interface regeneration are based on stratified or layered scaffolds in order to reproduce the native interface structure [1]. Depending on the particular kind of tissue interface and in order to reproduce the native tissue complexity, in terms of biology, structure and functionality, several strategies (materials or cell-dependent) are being adopted [1-3]. One of the most widely investigated tissue interfaces is the cartilage-bone or osteochondral interface. Many studies have been carried out focusing on multilayer scaffolds fabrication involving a superficial cartilaginous layer mimicking the articular cartilage and an underlying mineralized layer reproducing the subchondral bone tissue [4-7].

The aim of the present work was to develop a simple method for the fabrication of stratified composite scaffolds by the deposition of a thin polymer (chitosan) nanofibrous layer on a porous bioactive glass foam-like substrate, fabricated by foam replica method (according to [8]), for osteochondral segment regeneration. These two layers were assembled through a polymeric solution which should act as a functional "glue" to

effectively join the nanofibrous membrane to the porous glass substrate, acting also as a coating for the Bioglass®-based scaffold, thereby improving its mechanical properties without modifying the porous structure. A scheme of the proposed techniques integration for the fabrication of multilayered stratified scaffold is reported in Figure 6.1.

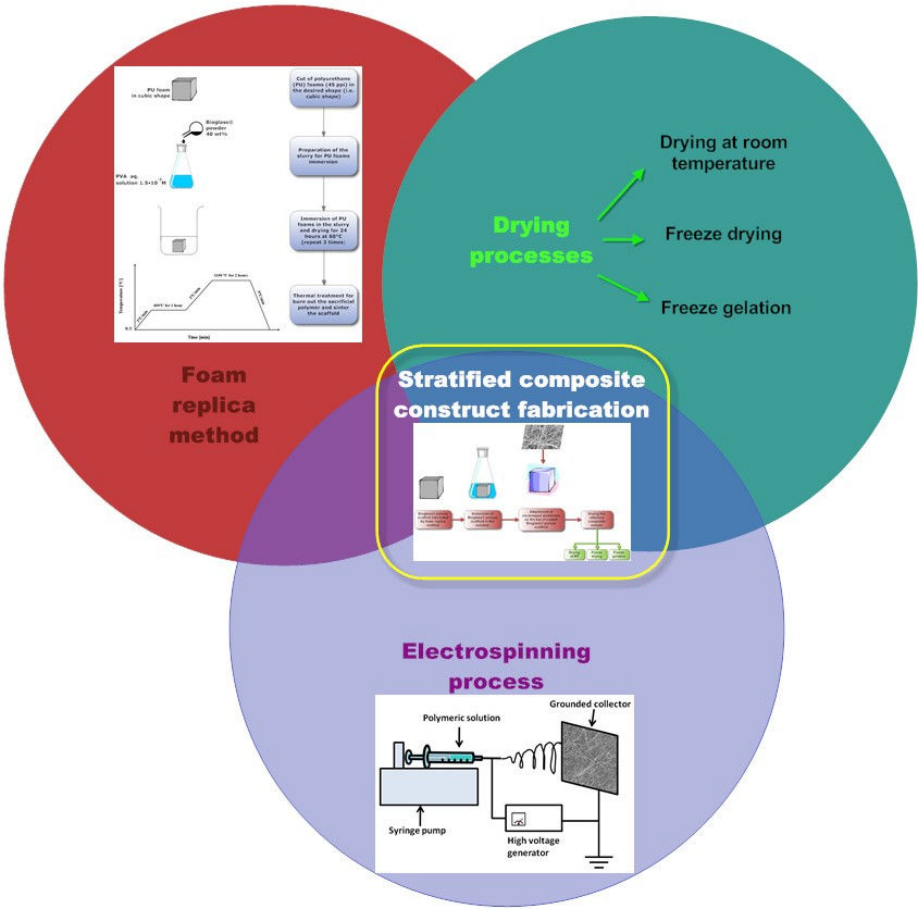

Figure 6.1 Scheme of the proposed techniques integration for the fabrication of multilayered stratified scaffold.

The manufacturing techniques involved a combination of methods, including: electrospinning for the fabrication of the upper cartilage-contact nanofibrous layer, freeze drying and freeze gelation methods for the synthesis of the intermediate layer and the foam replica method for bioactive glass scaffold fabrication.

It is well known that electrospinning enables fabrication of fibrous structures suitable for tissue engineering applications [9-12]. Previous investigations leading to composite

constructs having electrospun meshes at the top of a scaffold for tissue engineering [13] and for filtering applications [14] have been carried out using the substrate as grounded collector during the electrospinning process. It has been considered however that a soft interlayer would be beneficial to improve the adherence between the polymeric electrospun mesh and the underlying rigid scaffold [15].

Freeze drying and gelation methods are well-established techniques for controlled porous scaffolds fabrication using biodegradable polymers [16, 17], thus in this study these methods were considered for developing the interface layer in the stratified scaffold structure.

As indicated above, the aim of the present investigation was to develop novel stratified scaffolds for osteochondral tissue engineering where a soft intermediate layer is incorporated between the rigid bone scaffold (Bioglass®-based) and the cartilage-contact electrospun chitosan mesh, in order to provide strong bonding at the interface and to prevent delamination. Having this final aim in mind, different polymeric solutions, based on chitosan, alginate, gelatin and sucrose, were tested. These natural polymers were selected because of their well-known properties, biocompatibility and applications in the biomedical field [18]. Qualitative preliminary tests regarding the ability of preventing layer delamination were performed by the samples immersion in DI water and the tape test, after these tests, the selected samples were further investigated, as reported in the following paragraph.

6.2 Results and Discussion

In this section the results obtained from the fabrication of the stratified composite constructs, (showed in figure 6.2, starting from the fabrication of the Bioglass® scaffolds, by foam replica method, the coating process, and the final composite structure), and the characterization of those samples are presented. The paragraph is divided in subsections devoted to the explanation of different outcomes from several characterization analyses.

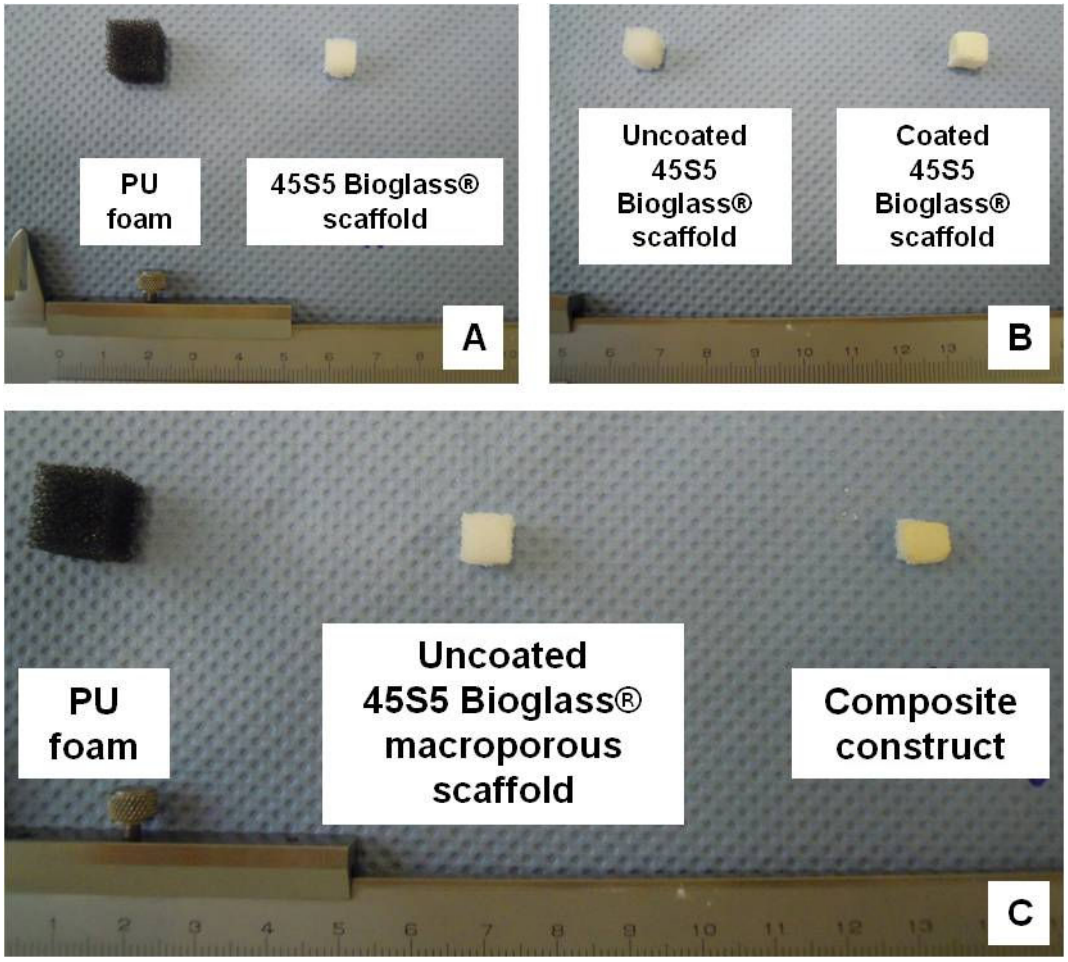

Figure 6.2 Digital camera images showing PU foam and 45S5 Bioglass® scaffold fabricated by foam replica method (A), uncoated and coated 45S5 Bioglass® scaffolds (B), and PU foam, uncoated Bioglass® scaffold and composite construct (coated Bioglass® with electrospun membrane on the top) (C).

6.2.1 Resistance to delamination tests: immersion in aq. solution and tape test

Two qualitative tests were performed in order to investigate the resistance to layer delamination in the obtained stratified composite constructs. In fact, this property was initially evaluated by sample immersion in DI water at room temperature (RT) and then at 37 °C, and by using the tape test (Elcometer 107, Cross Hatch Cutter, Manchester, UK). These tests were considered as selection criteria among the several polymeric solutions and drying techniques used for the fabrication of the intermediate layer. In particular, the samples immersion in DI water was performed to evaluate samples

response to aqueous environment and test failure was highlighted by the total or partial detachment of the electrospun membrane from the top of the stratified composite structure. While, the tape adhesion test is usually perform on coatings to quantify the strength of the bond between substrate and coating and it is based on a qualitative and macroscopic evaluation of samples surface after the removal of the adhesive tape from the sample coating.

Immersion in DI water

All samples immersed in DI water were put at RT for 2 days (40 mL of DI water for each sample), and then put at 37 °C for 7 days, in order to evaluate the effect of the immersion in aqueous solution on the stratified composites samples. In the following tables (tables 6.1 and 6.2) samples name, intermediate layer solution and performance after immersion in DI water are recorded. Data are divided in two tables, according to the intermediate solution lists, previously reported in § 2.4.2.2 (ref. to tables 2.11 and 2.12 also for sample labels).

This test was not performed to all the obtained samples, in fact, considering that it was an evaluation of the "glue" action of the intermediate layer, it was sufficient performed the test only on the samples having different intermediate solutions, without taking account of the kind of the electrospun membrane put on the top.

Solution	Sample name	Immersion in DI water
DI water	DIW_1	Macroscopically not good.
	DIW_2	When it becomes dry, the electrospun membrane comes off.
Acetic Acid (2% v/v aq. sol)	AA_1	--
	AA_2	Test failed (the electrospun membrane came off the composite during the immersion).

Table 6.1 Intermediate solutions, sample name and outcomes from sample immersion in DI water.

Solution	Sample name	Immersion in DI water
Chitosan (4% w/v chitosan in 2%v/v AA aq. sol)	D._C4_1	--
	D._C4_2	--
	D._C4_3	--
	D._C4_4	--
	D._C4_5	Positive result (no layer delamination).
	F.D.5_C4_6	Positive result (no layer delamination).
	F.D.5_C4_7	--
	F.D.5_C4_8	--
Chitosan (2%w/v chitosan in 2%v/v AA aq. sol)	F.D.24_C2_2_1	--
	F.D.24_C2_2_2	Positive result (no layer delamination).
	F.D.24_C2_2_3	--
Chitosan (2%w/v chitosan in 5%v/v AA aq. sol)	F.D.90_C2_5_1	Positive result (no layer delamination).
	F.D.90_C2_5_2	--
	F.G._C2_5_3	Positive result (no layer delamination).
	F.G._C2_5_4	--
Gelatin (2% w/v gelatin in DI water)	D._G2_1	Positive result (no layer delamination).
	D._G2_2	--
	D._G2_3	Positive result (no layer delamination).
	D._G2_4	--
Gelatin (1% w/v gelatin in dH_2O)	D._G1_1	Test failed (the electrospun membrane came off the composite during the immersion).
Sucrose (10% w/v sucrose in DI water)	D._S10_1	--
	D._S10_2	--
	D._S10_3	Test failed (the electrospun membrane came off the composite during the immersion).
Sodium alginate (2% w/v sodium alginate in DI water)	F.D.24_A2_1	Positive result (no layer delamination).
	F.D.90_A2_2	Positive result (no layer delamination).
	F.D.90_A2_3	--
	F.G._A2_4	Positive result (no layer delamination).
Chitosan/Alginate (4.8 % w/v chitosan:alginate (1:1))	F.D.90_CA_1	Positive result (no layer delamination).

Table 6.2 Intermediate polymeric solutions, sample name and outcomes from sample immersion in DI water.

Tape test

Only the samples showing positive results after immersion in DI water, were evaluated by using tape test. The test was performed by well-attaching the sticky layer of the strip (adhesive tape) on the top of the sample (from the side of the electrospun layer), the strip was then quickly removed with a proper angle (according to the protocol of Elcometer 107). A qualitative evaluation of the electrospun membrane that was removed from the composite sample and remained attached on the strip was performed. The presence of the electrospun membrane and in some cases of small residues of the rigid Bioglass® substrate on the strip were considered as test failure. This qualitative evaluation was simplified by the fact that all the electrospun crosslinked samples were yellow (as previously reported in § 3.2.2), while the strip was white. Results from the tape test are recorded in the following tables (tables 6.3 and 6.4, ref. to tables 2.11 and 2.12, as previously indicated also for tables 6.1 and 6.2).

Solution	Sample name	Tape test
DI water	DIW_1	Not performed because of the failure after immersion in DI water.
	DIW_2	--
Acetic Acid (2% v/v aq. sol)	AA_1	--
	AA_2	Not performed because of the failure after immersion in DI water.

Table 6.3 Intermediate solutions, sample name and outcomes from tape test.

Solution	Sample name	Tape test
Chitosan (4% w/v chitosan in 2%v/v AA aq. sol)	D._C4_1	--
	D._C4_2	--
	D._C4_3	--
	D._C4_4	--
	D._C4_5	Positive result (no layer delamination).
	F.D.5_C4_6	Test failed

	F.D.5_C4_7	--
	F.D.5_C4_8	--
Chitosan (2%w/v chitosan in 2%v/v AA aq. sol)	F.D.24_C2_2_1	--
	F.D.24_C2_2_2	Positive result (no layer delamination).
	F.D.24_C2_2_3	--
Chitosan (2%w/v chitosan in 5%v/v AA aq. sol)	F.D.90_C2_5_1	Positive result (no layer delamination).
	F.D.90_C2_5_2	--
	F.G._C2_5_3	Positive result (no layer delamination).
	F.G._C2_5_4	--
Gelatin (2% w/v gelatin in DI water)	D._G2_1	Test failed
	D._G2_2	--
	D._G2_3	Test failed
	D._G2_4	--
Gelatin (1% w/v gelatin in DI water)	D._G1_1	Not performed because of the failure after immersion in DI water.
Sucrose (10% w/v sucrose in DI water)	D._S10_1	--
	D._S10_2	--
	D._S10_3	Not performed because of the failure after immersion in DI water.
Sodium alginate (2% w/v sodium alginate in DI water)	F.D.24_A2_1	Test failed
	F.D.90_A2_2	Positive result (no layer delamination).
	F.D.90_A2_3	--
	F.G._A2_4	Test failed
Chitosan/Alginate (4.8 % w/v chitosan:alginate (1:1))	F.D.90_CA_1	Positive result (no layer delamination).

Table 6.4 Intermediate polymeric solutions, sample name and outcomes from sample immersion in DI water.

Summarizing the obtained results from the resistance to delamination tests (immersion in DI water and tape test), the intermediate layer solutions that showed unsatisfactory performances were:

- DI water.
- Acetic Acid (2% v/v aq. sol).
- Gelatin (2% w/v gelatin in DI water).
- Gelatin (1% w/v gelatin in DI water).
- Sucrose (10% w/v sucrose in DI water).

While further investigated intermediate layer polymeric solutions were:

- Chitosan (4% w/v chitosan in 2%v/v AA aq. sol).
- Chitosan (2%w/v chitosan in 2%v/v AA aq. sol).
- Chitosan (2%w/v chitosan in 5%v/v AA aq. sol).
- Sodium alginate (2% w/v sodium alginate in DI water).
- Chitosan/Alginate (4.8 % w/v chitosan:alginate (1:1)).

These results highlighted that both the intermediate layer solutions (DI water and acetic acid solution) were not suitable for the role of the intermediate layer. For what concerns the polymeric solutions the results showed the crucial importance of the combination of the two following factors: the kind of polymer and the applied drying method. For example, sodium alginate resulted a good candidate, but not all tested drying methods were suitable for that aim, in fact, only the freeze drying technique for 90 hours applied to the sodium alginate samples resulted adequate, respect to freeze drying technique for 24 hours and freeze gelation. On the other hand, other materials, as gelatin and sucrose resulted completely unsuitable independently from the drying techniques used. Although these results, all the samples were evaluated by using light microscope, and results are reported in the following section, but the SEM analysis was performed only on selected samples that overcame the immersion in DI water, tape test and showed interesting morphology at light microscopy evaluation in terms of preserved substrate porous structure and top layer adhesion.

6.2.2 Morphological analysis

Samples morphological analysis was performed by using light microscopy and field emission scanning electron microscopy (SEM) analyses, as described in § 2.5.1. The obtained results are divided in the two following subsections.

Light Microscopy

Although light microscopy (LM) is an unsuitable technique to investigate the structure of 3D samples with an inhomogeneous superficial roughness, this technique was used at first to evaluate the eventual pore obstruction (due to the Bioglass®-substrate coating) and the electrospun membrane attachment. Samples presenting a preserved porosity and a proper electrospun membrane position were further investigated by SEM analysis.

In the following tables (tables 6.5 and 6.6) are listed the LM pictures and short discussion and comments on each sample. Samples names were assigned according to the tables 2.11 and 2.12, in which are also recorded samples fabrication protocols.

In figure 6.3 is reported the LM image of the uncoated 45S5 Bioglass® porous substrate.

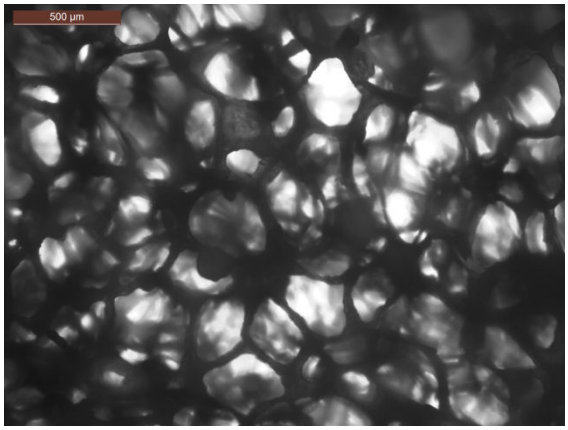

Figure 6.3 Structure of uncoated 45S5 Bioglass® scaffold, used as composite construct substrate, observed at LM.

Solution	Sample name	Light Microscopy
DI water	DIW_1	Macroscopically not good
	DIW_2	When it becomes dry, the ES membrane comes off.

Acetic Acid (2% v/v aq. sol)	AA_1	Many folding on the surface. Empty BG pores. 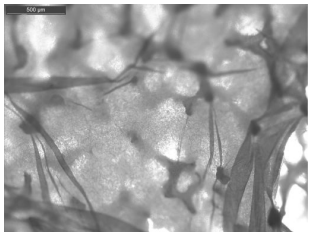 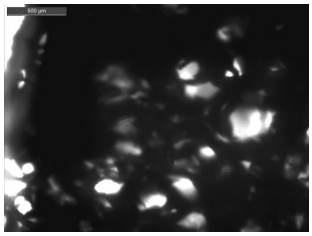
	AA_2	Empty BG pores. 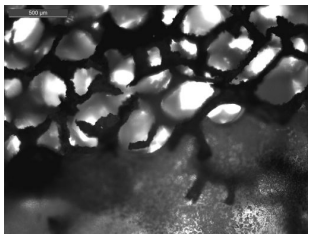 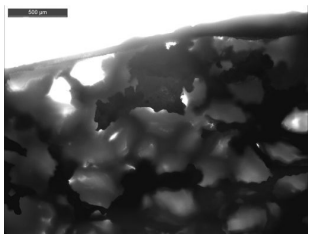

Table 6.5 Light Microscope images of composite constructs, obtained by using the solutions reported in Table 2.11.

Polymeric solution	Sample name	Light Microscopy
Chitosan (4% w/v chitosan in 2%v/v AA aq. sol)	D._C4_1	Excess of polymeric solution, BG pores are closed.
	D._C4_2	In the opposite side of ES membrane, the BG porosity is preserved.
	D._C4_3	Difficulties in image focus, because of the irregular surface of the composite.
	D._C4_4	Pore observed in section view are closed.
	D._C4_5	Same sample to D._C4_4
	F.D.5_C4_6	Residues of polymeric solution in the BG pores.  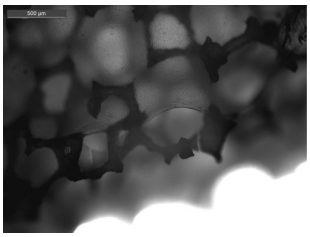
	F.D.5_C4_7	Same consideration of previous sample. Broken structures due to the freeze drying process.

		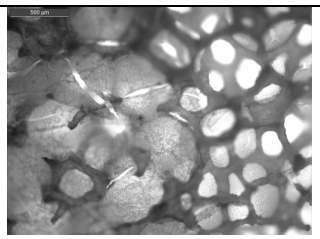 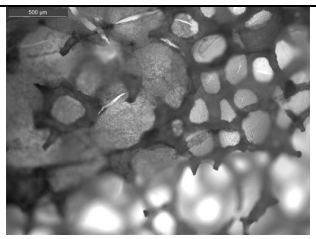 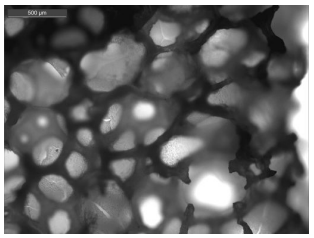
	F.D.5_C4_8	The parafilm coating collapsed on the specimens during the freeze drying process, it was not possible to characterize this sample.
Chitosan (2%w/v chitosan in 2%v/v AA aq. sol)	F.D.24_C2_2_1	The parafilm coating collapsed on the specimens during the freeze drying process, it was not possible to characterize this sample.
	F.D.24_C2_2_2	 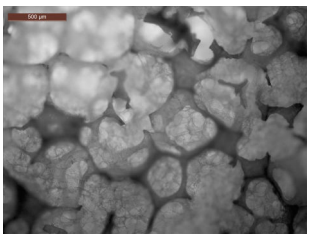
	F.D.24_C2_2_3	The only difference with F.D.24_C2_2 sample was the kind of the electrospun membrane, for this reason this sample was not analyzed at L.M.
Chitosan (2%w/v chitosan in 5%v/v AA aq. sol)	F.D.90_C2_5_1	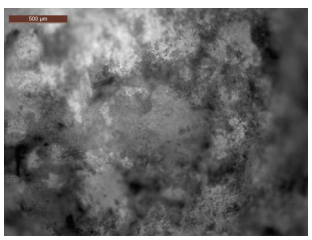 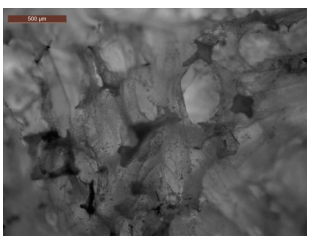
	F.D.90_C2_5_2	The only difference with F.D.90_C2_5_1 sample was the kind of the electrospun membrane, for this reason this sample was not analyzed at L.M.

	F.G._C2_5_3	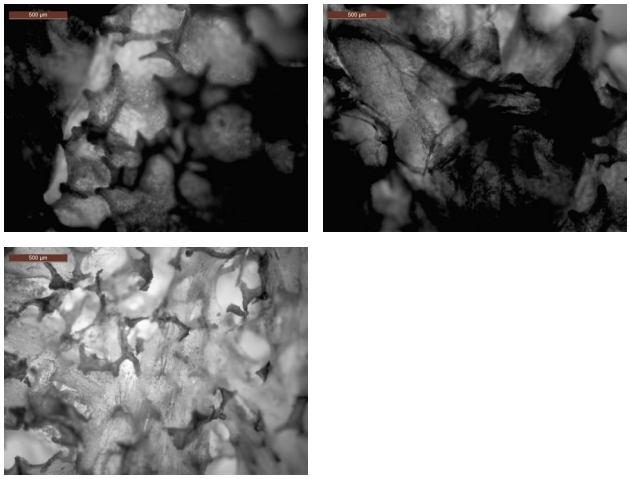
	F.G._C2_5_4	The only difference with F.G._C2_5_3 sample was the kind of the electrospun membrane, for this reason this sample was not analyzed at L.M.
Gelatin (2% w/v gelatin in DI water)	D._G2_1	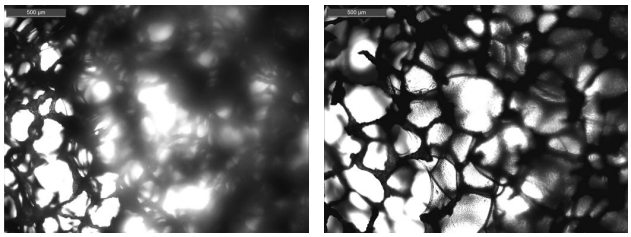
	D._G2_2	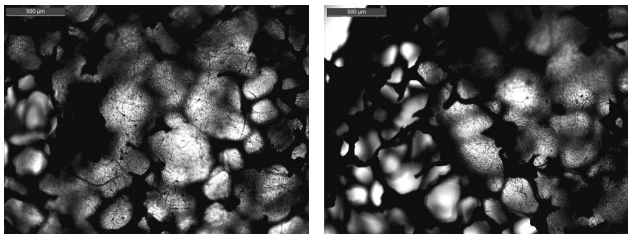
	D._G2_3	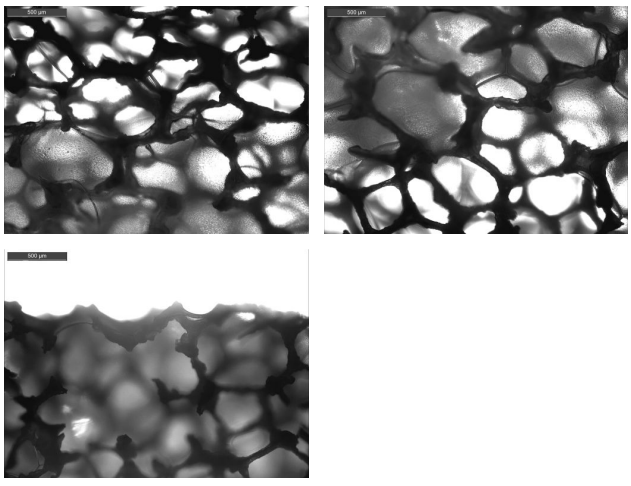
	D._G2_4	Surface and section images. BG pores are empty also

		without the final rinsing. 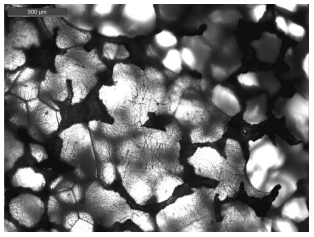 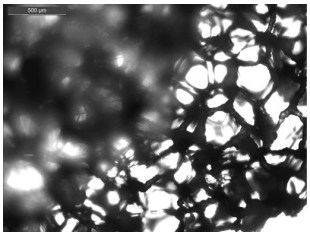
Gelatin **(1% w/v gelatin in DI water)**	D._G1_1	Sample failed immersion in DI water and was not analyzed at LM.
Sucrose (10% w/v sucrose in DI water)	D._S10_1	Surface and section images. BG pores are empty. 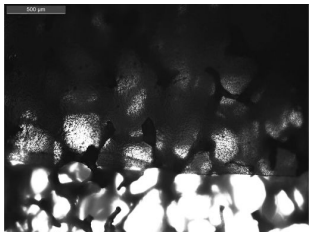 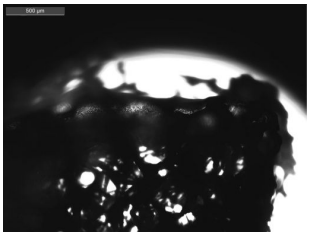 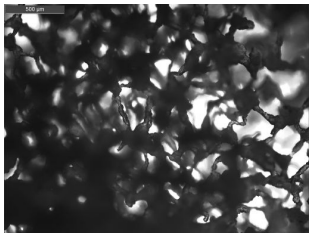
	D._S10_2	Surface and section images. BG pores are empty. 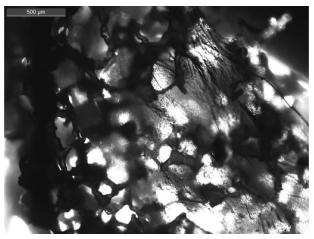 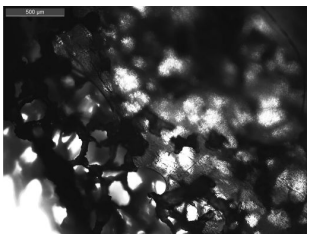 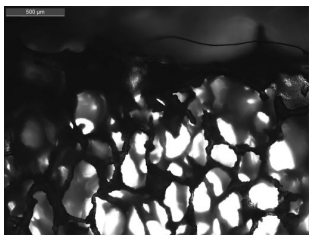 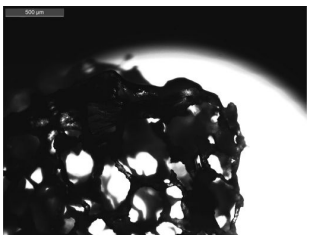
	D._S10_3	Sample failed immersion in DI water and was not analyzed at LM.

Sodium alginate (2% w/v sodium alginate in DI water)	F.D.24_A2_1	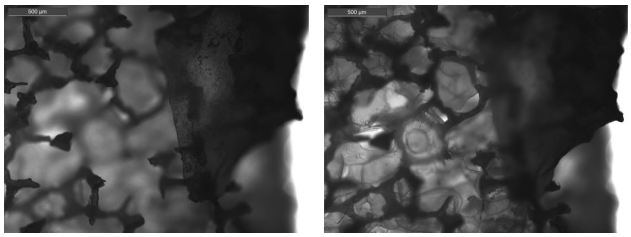
	F.D.90_A2_2	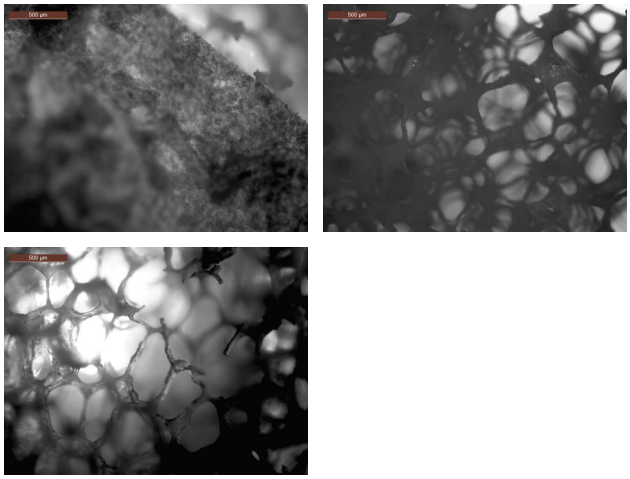
	F.D.90_A2_3	The only difference with F.D.90_A2_2 sample was the kind of the electrospun membrane, for this reason this sample was not analyzed at L.M.
	F.G._A2_4	Sample failed tape test and was not analyzed at LM.
Chitosan/Alginate (4.8 % w/v chitosan:alginate (1:1))	F.D.90_CA_1	Directly investigated by SEM.

Table 6.6 Light Microscope images of composite constructs, obtained by using the polymeric solutions reported in table 2.12.

SEM analysis

SEM analysis was performed on the selected samples, in order to investigate the preservation of Bioglass® substrate porosity and to evaluate the adhesion of the upper layer, by analyzing the sample interface area. SEM micrographs are reported in the following table.

Solution	Sample name	SEM micrographs
Chitosan (4% w/v chitosan in 2%v/v AA aq. sol)	D._C4_5	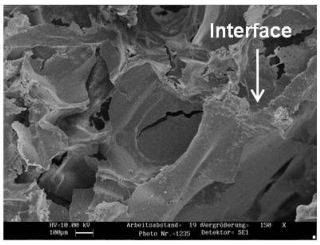 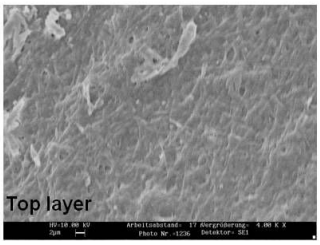 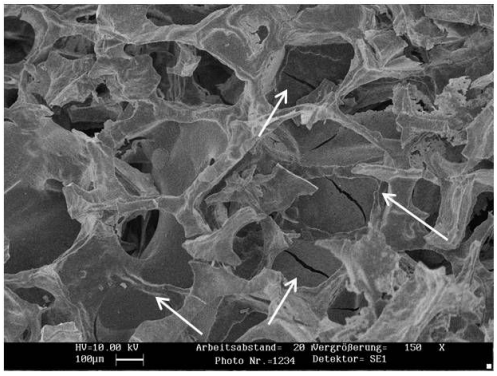 As showed in the cross section substrate pore resulted closed (as highlighted by white arrows).
Chitosan (2%w/v chitosan in 2%v/v AA aq. sol)	F.D.24_C2_2_2	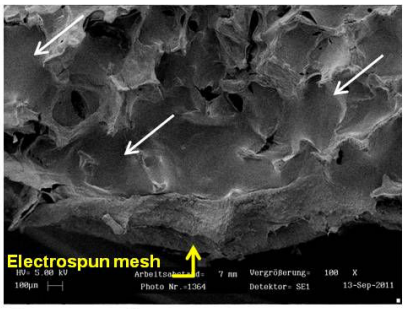 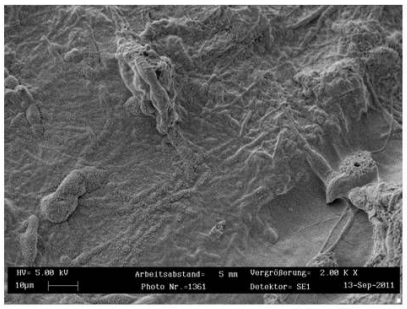 Cross section Top layer As showed in the cross section substrate pore resulted partially closed (as highlighted by white arrows).

Chitosan (2%w/v chitosan in 5%v/v AA aq. sol)	F.D.90_C2_5_1	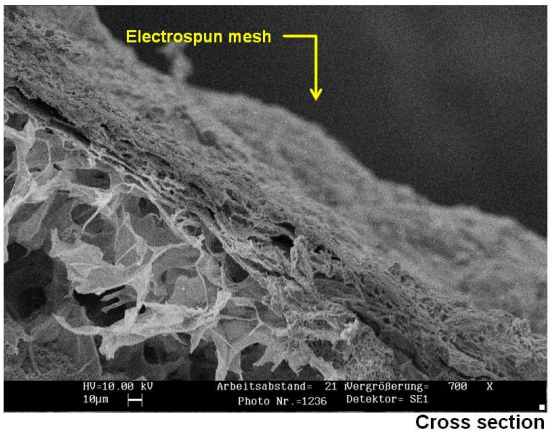 Cross section 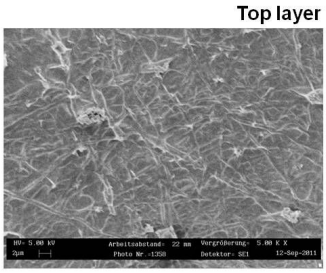 Top layer 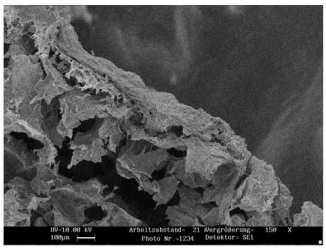 Substrate porosity preserved, as showed in cross section and in the zoom view of the same area.
	F.G._C2_5_3	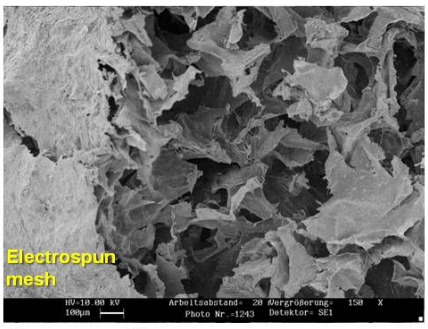 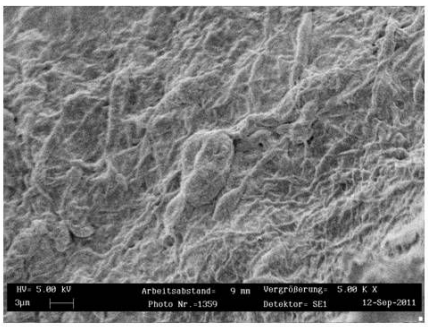 Cross section Top layer Substrate porosity preserved, as showed in cross section.
Sodium alginate (2% w/v sodium alginate in DI water)	F.D.90_A2_2	 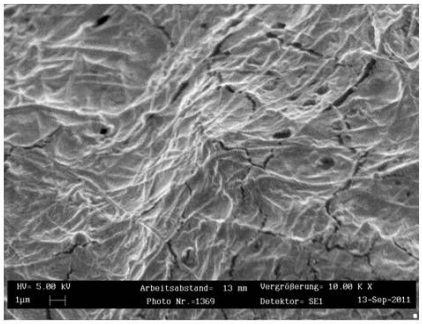 Cross section Top layer Substrate porosity preserved, as showed in cross section.

Chitosan/ Alginate (4.8 % w/v chitosan:alginate (1:1))	F.D.90_CA_1	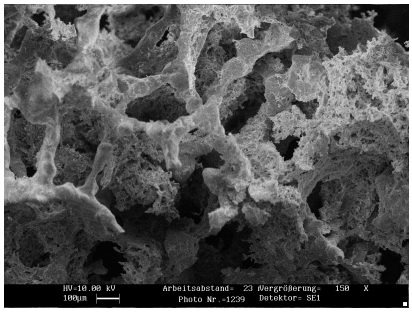 The sample was very brittle and it resulted partially broken during the stub preparation before SEM analysis.

Table 6.7 SEM micrographs of composite constructs, obtained by using the selected polymeric solutions for the intermediate layer.

After SEM analysis, it was possible to consider unsatisfactory the use of chitosan solution at 4% w/v in AA aq. solution (at 2% v/v) for the composite intermediate layer, because SEM micrographs showed that the substrate pore were closed, and also the use of the chitosan/alginate solution, because of the sample intrinsic inability to be handled, in fact it broke during stub preparation for SEM analysis. The further evaluated samples had as the intermediate layer, the following polymeric solution and were fabricated by using the following drying techniques (all data are summarized in the following table).

Polymeric solution	Rinsing solution	Drying technique	Sample name
Chitosan (2%w/v chitosan in 2%v/v AA aq. sol)	--	Freeze drying for 24 hours	F.D.24_C2_2
Chitosan (2%w/v chitosan in 5%v/v AA aq. sol)	0,75%w/v NaOH/ethanol aqueous solution precooled at -20°C	Freeze drying for 90 hours	F.D.90_C2_5
		Freeze gelation	F.G._C2_5
Sodium alginate (2% w/v sodium alginate in DI water)	4% w/v $CaCl_2$/ethanol aqueous solution precooled at -20°C	Freeze drying for 90 hours	F.D.90_A2

Table 6.8 Summary of selected polymeric solution used as intermediate layer, rinsing solution for samples, drying techniques and sample names.

In SEM micrographs of the top layer, for each sample, it was possible to distinguish the fibrillar structure of the electrospun membrane, even if some cracks are visible on the top surface (like in sample F.D.90_A2_2), which are likely the result of the drying process. The influence of the freeze drying process on the electrospun membrane, without the presence of the interface layers, was evaluated by freezing an electrospun membrane at -20°C overnight, and then by freeze drying it for 90 hours. SEM evaluation of that membrane showed that the freeze drying process itself did not affect its morphology (it is possible to compare these SEM micrographs with the ESCSHA10XL ones reported in chapter 4), like reported in figure 6.4, confirming that modifications observed in the top side of the composites were due to the influence of the intermediate layers and not due to the freeze-drying process itself.

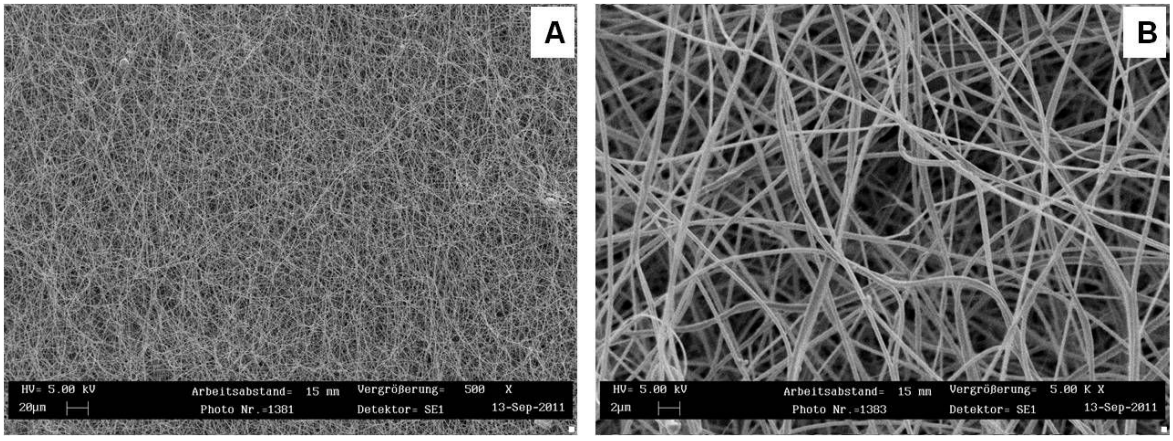

Figure 6.4 SEM micrographs of electrospun membrane ESCSHA10XL after freezing at -20°C and freeze drying for 90 hours at different magnifications: 500X (a) and 5000X (b).

6.2.3 Bioactivity test (Simulated Body Fluid)

SEM analysis

The immersion in SBF was important in order to evaluate possible changes in the substrate (Bioglass® scaffold) bioactivity induced by the coating layer (it was performed as previously described in § 2.5.9). The morphological alterations of the cross section after 7 days of immersion in SBF are reported in figure 6.5. There is evidence of crystal deposition on the surfaces of bioactive glass-based scaffold in all

samples investigated (Figure 6.5.a and 6.5.b). Apart from the sample shown in Fig 6.5.c (alginate-based sample), there was, however, no evidence of crystal deposition on the electrospun membrane (the electrospun membrane used was ESCSXL (sample name explanation reported in table 2.1), without HA or BG particles), which is a convenient result regarding the intended application of these composites for osteochondral regeneration, e.g. considering that the top electrospun layer should be devoted to cartilage regeneration, and therefore no mineral/hydroxyapatite deposition is desired on this layer.

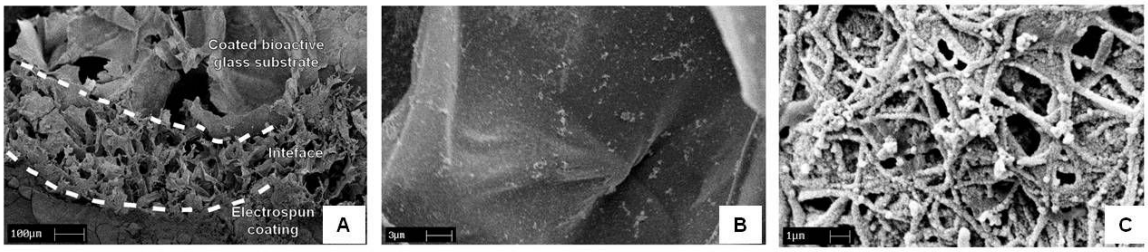

Figure 6.5 Morphological analysis after SBF bioactivity test by SEM: representative cross section of chitosan-based sample (F.D.90_C2_5) (A), zoom view of crystals inside the pore structure of the same sample (F.D.90_C2_5) (B), example of crystals on the sample top side (F.D.90_A2) (C).

6.2.4 Contact angle measurements

Contact angle measurements were performed on each layer and on the entire composites, according to the protocol described in § 2.5.5. For what concerns the electrospun membrane alone and the coated substrates (without external electrospun coating), it was not possible to perform any measurements because the dispensed water drop was not stable, wetting completely and instantaneously the sample surface. While for the entire composites, the results showed a different behavior respect to each single layer, in fact for two samples (F.D.24_C2_2 and F.D.90_A2) the contact angle values were 46 ± 6° and 36 ± 9°, respectively. This different behavior could be justified by the fact that in these two samples the composite structure presented an undesired reduction in porosity that allowed to perform the measurement, without showing hydrophobic behavior.

6.2.5 Evaluation of Bioglass® scaffold coating

6.2.5.1 Mechanical properties

Concerning the evaluation of the different polymer coatings for the Bioglass® scaffolds (without the electrospun membrane on the top), the compressive strength test results (see protocol in § 2.5.4), performed on all the samples listed in Table 6.8, underlined that their Young's modulus values were very similar. These values were calculated from the initial linear slope of the stress-strain curve; samples stress-strain curves are reported in Figure 6.6.

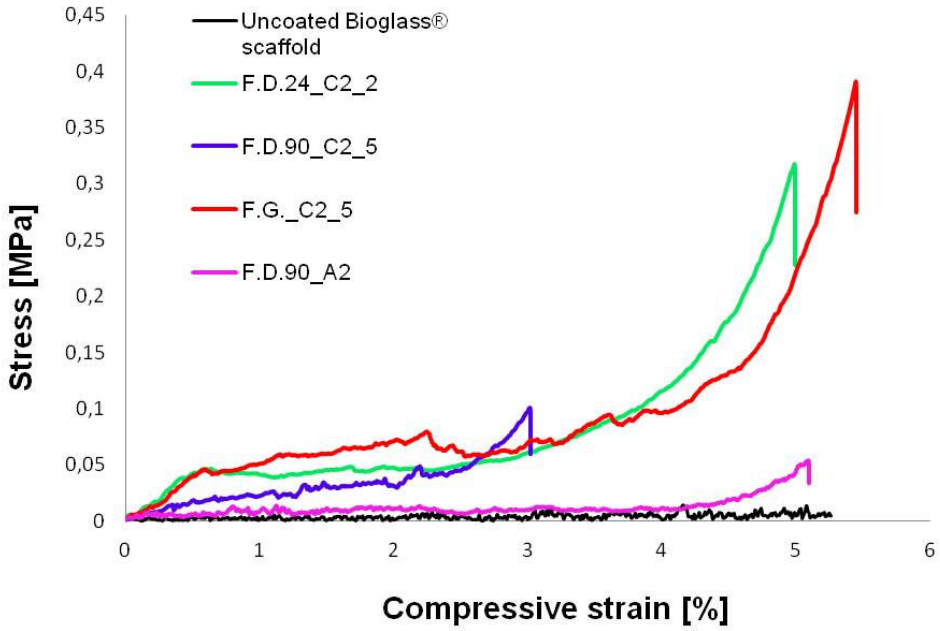

Figure 6.6 Stress-strain curves in compression of uncoated and all coated Bioglass® scaffolds.

The Young's modulus values were in the range 1–5 MPa, while, for what concerns the compressive strength, the F.G._C2_5 sample showed the best result (0.35 ± 0.05 MPa). All measured values of samples listed in Table 6.8, i.e. Young's modulus, maximum load and compressive strength, are reported in Table 6.9.

Sample	Young's modulus [MPa]	Max Load [N]	σ [MPa]
F.D.24_C2_2	4 ± 2	12 ± 4	0.28 ± 0.09
F.D.90_C2_5	3 ± 2	4 ± 2	0.10 ± 0.04
F.G._C2_5	5 ± 1	15 ± 5	0.35 ± 0.05
F.D.90_A2	1.1 ± 0.5	1.2 ± 0.9	0.03 ± 0.02

Table 6.9 Summary of mechanical properties values of samples listed in table 6.8 (Young's modulus, maximum load and compressive strength) measured during compressive strength test.

Figures 6.7 and 6.8 show digital camera images of uncoated and coated scaffolds before and after mechanical test, clearly indicating that, apart from F.D.90_A2 sample, the structural integrity of the scaffold had dramatically improved, i.e. the presence of the polymer layer has toughened the otherwise brittle scaffold.

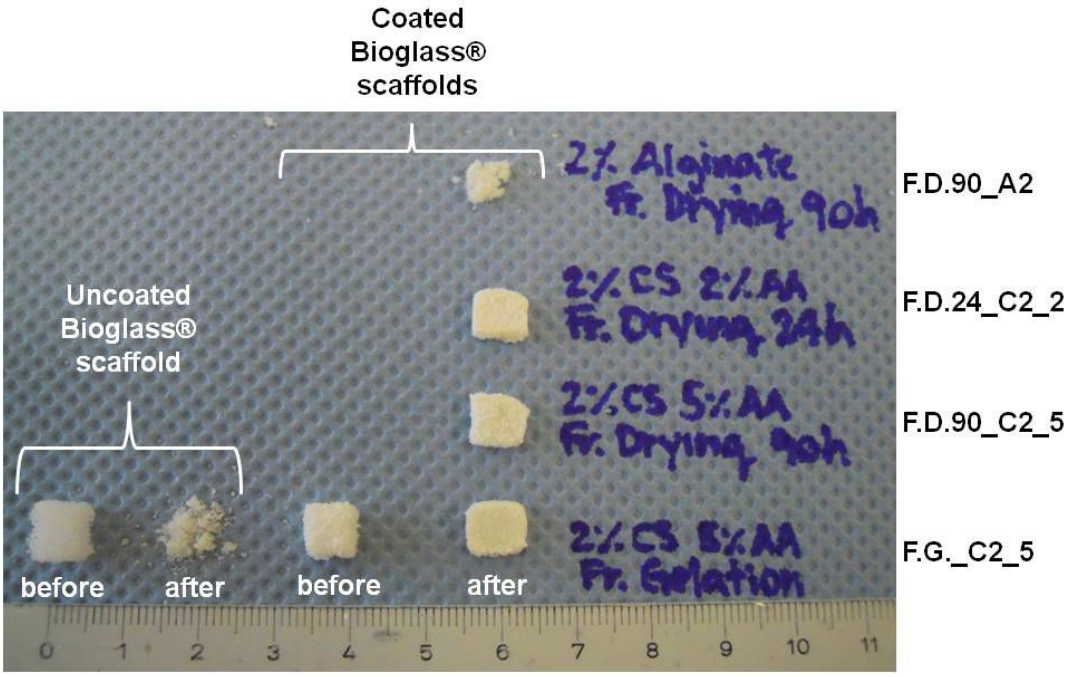

Figure 6.7 Digital camera image showing uncoated substrate before and after the compressive strength test (at left side), coated (F.G._C2_5) substrate before mechanical test, and all coated samples after the compressive strength test (at right side).

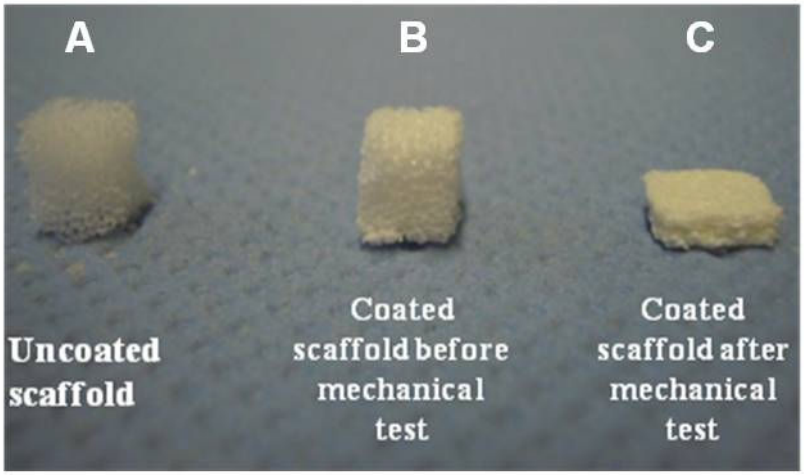

Figure 6.8 Digital camera image showing uncoated substrate before compressive strength test (A), coated (F.G._C2_5) substrate before (B) and after compressive strength test (C).

This result was in broad agreement with data reported in the literature [19-21], which highlights the positive effect of incorporating a flexible polymer coating on the fracture resistance of bioceramic scaffolds. The stress-strain curves obtained in compression, show in Figure 6.6, confirmed this behavior. The irregularities in that curves were due to the high scaffold porosity that affects sample behavior during compression loading. For comparison, the stress-strain curve corresponding to the uncoated scaffold is also reported in the same figure 6.6.

6.2.5.2 ATR/FT-IR analysis

ATR/FT-IR analysis was performed, as previously described in § 2.5.2, on coated scaffolds that presented the highest compressive strength (F.G._C2_5) in order to investigate possible inhibition in scaffold bioactivity due to the presence of the coating. In Figure 6.9, the spectrum of the coated scaffold after 7 days of immersion in SBF is reported. According to the literature [22], the peaks at 1060 cm^{-1}(νP-O) and at 560 and 600 cm^{-1}(δP-O) present in the spectrum indicate the formation of hydroxyapatite on the surface of the scaffold upon immersion in SBF (7 days), which confirms that the substrate bioactivity was not affected by the presence of the coating, at least by the qualitative evaluation of SBF immersed samples.

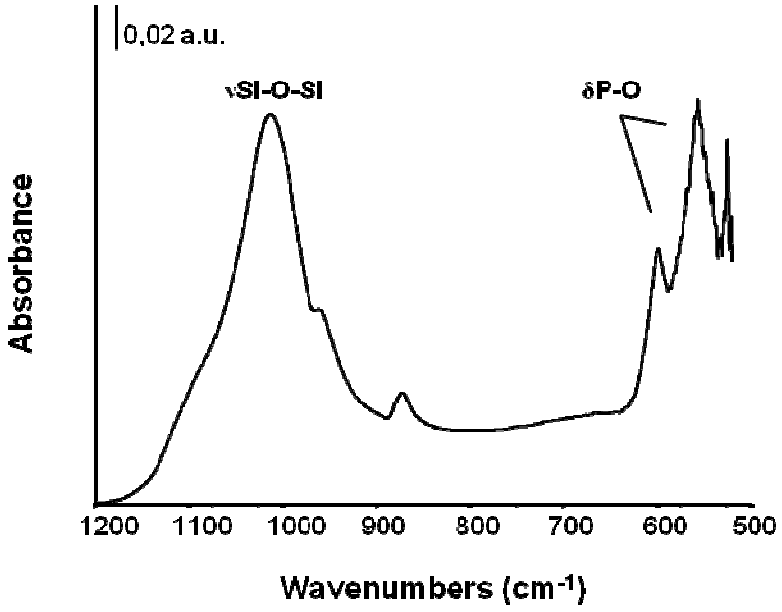

Figure 6.9 ATR/FT-IR spectrum of coated (F.G._C2_5) substrate after 7 days immersion in SBF, showing evidence of bioactivity (formation of hydroxyapatite on the surface).

6.3 Conclusions

In the present chapter, a simple method of integrating several scaffold fabrication techniques was developed to obtain a stratified composite structure, e.g. combining foam replica method, freeze drying and electrospinning. The best results were obtained using chitosan and freeze gelation to produce the intermediate layer, in terms of resistance to layer delamination, bioactivity and improvement in mechanical properties of the underlying bioactive glass scaffold.

The novelty of the stratified, layered system reported in the present work can be highlighted in terms of its versatility for application to several kinds of electrospun membranes that need to be combined with a rigid macroporous 3D structure. The electrospun membrane was used after its fabrication, as external coating, making the stratified composite fabrication method developed here independent from the electrospinning process itself. This kind of stratified structures could be suitable for several applications in the emerging field of interface tissue engineering [2], strictly related to the electrospun membrane functions, as for example, exploiting fiber topographical stimuli for cell signaling or using functionalized electrospun membranes as drug delivery systems or as filtering devices [23].

References

[1] Spalazzi JP, Doty SB, Moffat KL, Levine WN, Lu HH. Development of Controlled Matrix Heterogeneity on a Triphasic Scaffold for Orthopedic Interface Tissue Engineering. Tissue Engineering. 2006;12:3497-508.

[2] Lu H, Subramony S, Boushell M, Zhang X. Tissue Engineering Strategies for the Regeneration of Orthopedic Interfaces. Annals of Biomedical Engineering. 2010;38:2142-54.

[3] Seidi A, Ramalingam M, Elloumi-Hannachi I, Ostrovidov S, Khademhosseini A. Gradient biomaterials for soft-to-hard interface tissue engineering. Acta Biomaterialia. 2011;7:1441-51.

[4] Martin I, Miot S, Barbero A, Jakob M, Wendt D. Osteochondral tissue engineering. Journal of biomechanics. 2007;40:750-65.

[5] O'Shea TM, Miao X. Bilayered Scaffolds for Osteochondral Tissue Engineering. Tissue Engineering Part B: Reviews. 2008;14:447-64.

[6] Kon E, Delcogliano M, Filardo G, Fini M, Giavaresi G, Francioli S, et al. Orderly osteochondral regeneration in a sheep model using a novel nano-composite multilayered biomaterial. Journal of Orthopaedic Research. 2010;28:116-24.

[7] Harley BA, Lynn AK, Wissner-Gross Z, Bonfield W, Yannas IV, Gibson LJ. Design of a multiphase osteochondral scaffold III: Fabrication of layered scaffolds with continuous interfaces. Journal of Biomedical Materials Research Part A. 2010;92A:1078-93.

[8] Chen QZ, Thompson ID, Boccaccini AR. 45S5 Bioglass®-derived glass–ceramic scaffolds for bone tissue engineering. Biomaterials. 2006;27:2414-25.

[9] Teo W-E, Inai R, Ramakrishna S. Technological advances in electrospinning of nanofibers. Science and Technology of Advanced Materials. 2011;12:013002.

[10] Bhardwaj N, Kundu SC. Electrospinning: A fascinating fiber fabrication technique. Biotechnology Advances. 2010;28:325-47.

[11] Agarwal S, Wendorff JH, Greiner A. Progress in the Field of Electrospinning for Tissue Engineering Applications. Advanced Materials. 2009;21:3343-51.

[12] Agarwal S, Wendorff JH, Greiner A. Use of electrospinning technique for biomedical applications. Polymer. 2008;49:5603-21.

[13] Yunos DM, Ahmad Z, Boccaccini AR. Fabrication and characterization of electrospun poly-DL-lactide (PDLLA) fibrous coatings on 45S5 Bioglass® substrates for bone tissue engineering applications. Journal of Chemical Technology & Biotechnology. 2010;85:768-74.

[14] Yoon K, Kim K, Wang X, Fang D, Hsiao BS, Chu B. High flux ultrafiltration membranes based on electrospun nanofibrous PAN scaffolds and chitosan coating. Polymer. 2006;47:2434-41.

[15] Yunos DM, Ahmad Z, Salih V, Boccaccini AR. Stratified scaffolds for osteochondral tissue engineering applications: Electrospun PDLLA nanofibre coated Bioglass®-derived foams. Journal of Biomaterials Applications. 2011.

[16] Ho M-H, Kuo P-Y, Hsieh H-J, Hsien T-Y, Hou L-T, Lai J-Y, et al. Preparation of porous scaffolds by using freeze-extraction and freeze-gelation methods. Biomaterials. 2004;25:129-38.

[17] Hsieh C-Y, Tsai S-P, Ho M-H, Wang D-M, Liu C-E, Hsieh C-H, et al. Analysis of freeze-gelation and cross-linking processes for preparing porous chitosan scaffolds. Carbohydrate Polymers. 2007;67:124-32.

[18] Muzzarelli RAA. Chitins and chitosans for the repair of wounded skin, nerve, cartilage and bone. Carbohydrate Polymers. 2009;76:167-82.

[19] Yunos DM, Bretcanu O, Boccaccini A. Polymer-bioceramic composites for tissue engineering scaffolds. Journal of Materials Science. 2008;43:4433-42.

[20] Peroglio M, Gremillard L, Chevalier J, Chazeau L, Gauthier C, Hamaide T. Toughening of bio-ceramics scaffolds by polymer coating. Journal of the European Ceramic Society. 2007;27:2679-85.

[21] Fu Q, Saiz E, Rahaman MN, Tomsia AP. Bioactive glass scaffolds for bone tissue engineering: state of the art and future perspectives. Materials Science and Engineering: C. 2011;31:1245-56.

[22] Jones JR, Sepulveda P, Hench LL. Dose-dependent behavior of bioactive glass dissolution. Journal of Biomedical Materials Research. 2001;58:720-6.

[23] L. Liverani, J.A. Roether, P. Nooeaid, M. Trombetta, D.W. Schubert, A.R. Boccaccini. Simple fabrication technique for multilayered stratified composite scaffolds suitable for interface tissue engineering. Materials Science and Engineering: A. Submitted.

7. Chitosan-based foam scaffolds

Index

Abstract

In order to obtain foam scaffolds able to improve cell signaling and induction towards chondrogenesis and/or osteogenesis pathway, foam scaffolds composed by pure chitosan (CS) and chitosan with the addition of nanopowder of hydroxyapatite (HA) and bioactive glass (BG) particles were fabricated. Chitosan-based foam scaffolds were fabricated by using phase separation-based techniques. Foams fabrication protocol was progressively improved, in fact three different protocols were tested and evaluated. All the obtained samples were characterized in terms of morphology, chemical structure, mechanical properties and *in vitro* bioactivity. Positive results were obtained in terms of pore interconnectivity, foam swelling and porosity, and samples bioactivity.

7.1 Introduction

The major part of the bone extracellular matrix (ECM) contains calcium phosphates mineral phases which requires a mineralization step that is essential in the bone regeneration process. The existence of bone bioactive inorganic components within polymeric scaffold generally favors calcium phosphate mineralization followed by an osteogenic differentiation process. Therefore, several studies have focused on introducing a range of inorganic phases within the polymeric matrix with the ultimate aim of achieving both bone-specific bioactivity and improved polymeric scaffold mechanical properties [1, 2].

Chitosan is one of the most abundant polysaccharides; it is considered as one of the most attractive natural biopolymers for biomedical and biotechnological applications, also in particular in tissue engineering field, mainly due to its biocompatibility and biodegradability [3-5].

Polymeric porous scaffolds, similar to foam or sponge, could be obtained by using several methods, like saturation and release of CO_2 [6, 7], porogen leaching [8, 9] and phase separation techniques [10-12]. A well-established technique, widely used for scaffold fabrication, is the phase separation method, and in particular the thermally induced phase separation (TIPS) technique, that is based on the lowering of the polymeric solution temperature, in order to induce phase separation of the starting polymeric solution. The pore structure is generated by the voids introduced after the

removal of the frozen solvent in the polymeric solution. It is possible to regulate final scaffold porous structure, by varying several process parameters, like polymeric solution solvents, polymeric solution concentration, and freezing rate. Different techniques are used for solvent removal, preserving the neo-formed porous structure, avoiding pores collapse, as for example the freeze drying [13].

The focus of this chapter was the optimization of the protocol for the fabrication of chitosan-based foam scaffolds, in pure chitosan and chitosan with the addition of HA nanopowder or BG particles, by using phase separation-based techniques.

7.2 Results and Discussion

In this section the results obtained from the characterization of the chitosan-based foams fabricated with different protocols are presented. The paragraph is divided in subsections devoted to the explanation of different outcomes from several characterization analyses, organized in three subparagraphs dedicated to each fabrication protocol.

7.2.1 Protocol 1-based chitosan foam scaffolds

Foams fabricated with protocol 1 (previously described in §2.4.3), were characterized in terms of morphology, as follows.

7.2.1.1 Morphological analysis

SEM analysis was performed, according to § 2.5.1, on chitosan foam sample fabricated starting from solution A and B (according to the classification introduced in § 2.3, in which the solution A is 2% w/v chitosan in 2% v/v aq. solution of acetic acid and solution B is 2% w/v chitosan in 2% v/v aq. solution of lactic acid) and chitosan/HA sample starting from solution A. In the following figure sample SEM micrographs are reported.

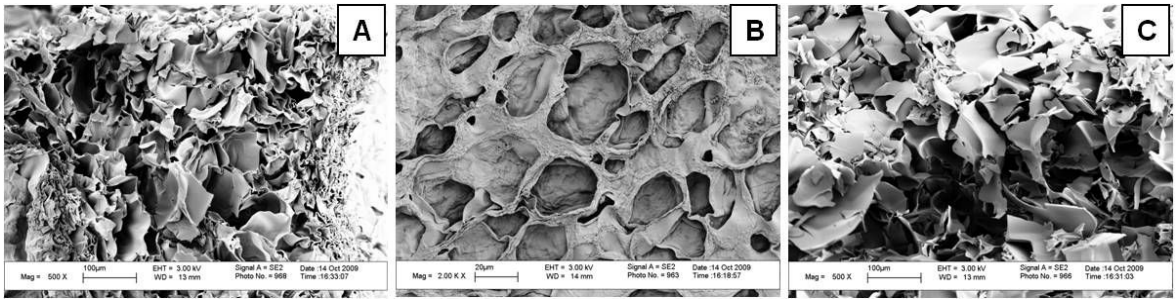

Figure 7.1 SEM micrographs of chitosan foam samples, starting from chitosan solution A (a), solution A with the addition of HA (b) and solution B (c).

Unsatisfactory results in terms of protocol complexity, time for sample preparation and final sample morphology, in particular pore size and interconnectivity were obtained. This protocol was modified as reported in § 2.4.3.

7.2.2 Protocol 2-based chitosan foam scaffolds

Foams fabricated with protocol 2 (previously described in §2.4.3), in pure chitosan (CS) and with the addition of hydroxyapatite (CSHA) nanopowder or bioactive glass (CSBG) particles, were characterized in terms of morphology, chemical structure, mechanical properties, foam swelling and porosity, pH alteration in aq. solution, and *in vitro* bioactivity, as follows.

7.2.2.1 Morphological analysis

Although light microscopy (LM) is an unsuitable technique to investigate the structure of 3D samples with an inhomogeneous superficial roughness, as previously noticed in § 6.2.2, this technique was used at first to evaluate the sample porous structure, as reported in figure 7.2.

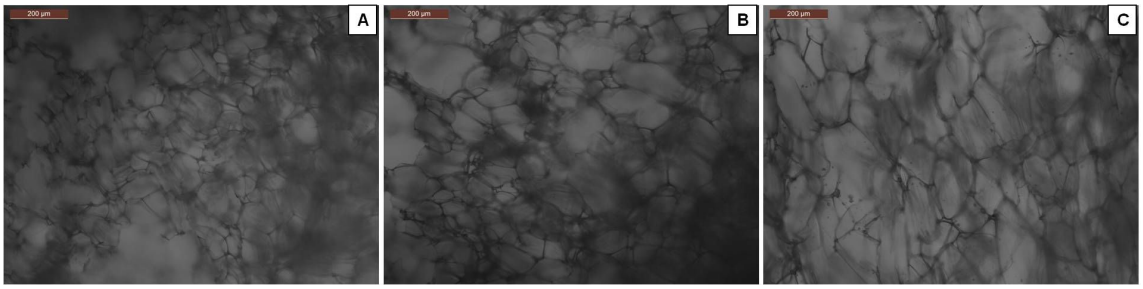

Figure 7.2 LM images of chitosan foam samples, in particular CS (a), CSHA (b), and CSBG (c).

All the samples (CS, CSHA and CSBG) presented a regular and homogenous porous structure. In particular in CSBG sample was also possible noticed the presence of BG particles (obtained by sol-gel process, accordingly to Rainer *et al.* [14]) inside the foam pore structure.

The same samples were then investigated by SEM analysis. SEM micrographs at different magnifications are reported in the following figures.

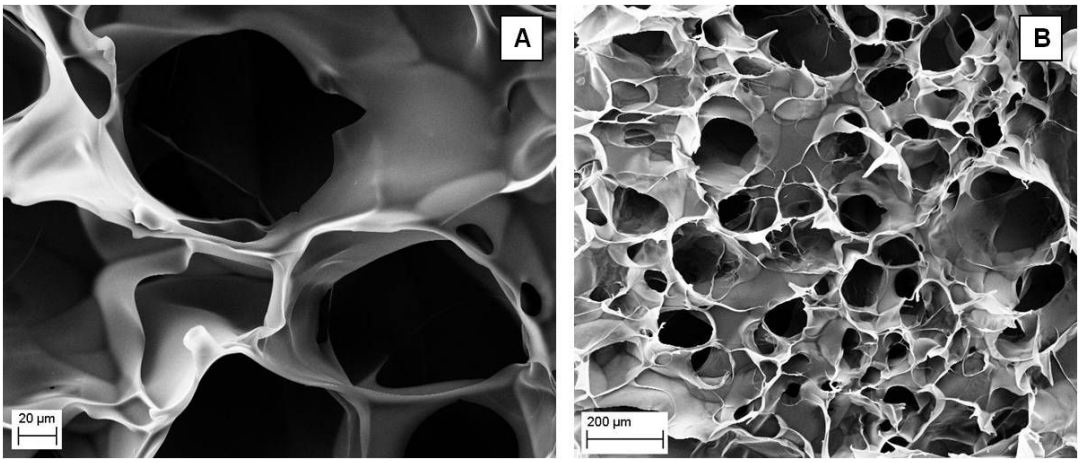

Figure 7.3 SEM micrographs of chitosan foam samples (CS) at different magnifications.

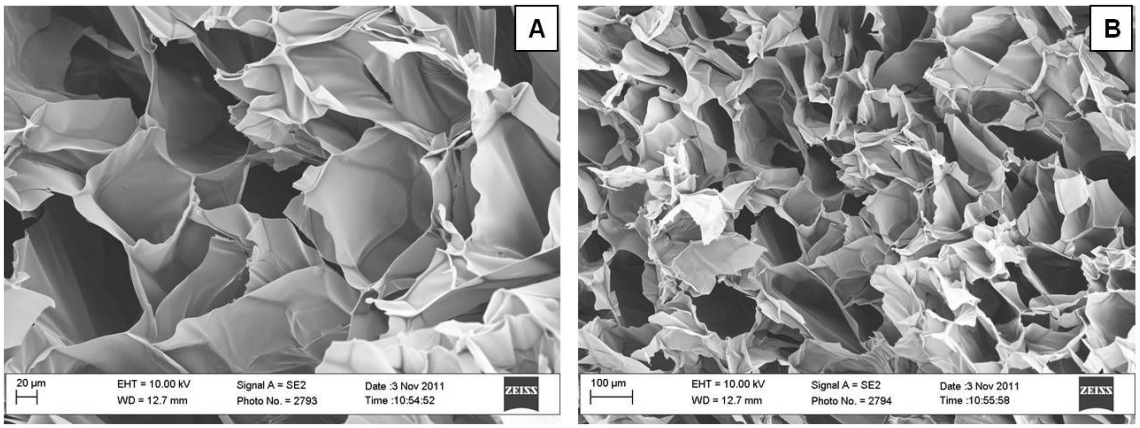

Figure 7.4 SEM micrographs of chitosan-based foam samples (CSHA) at different magnifications.

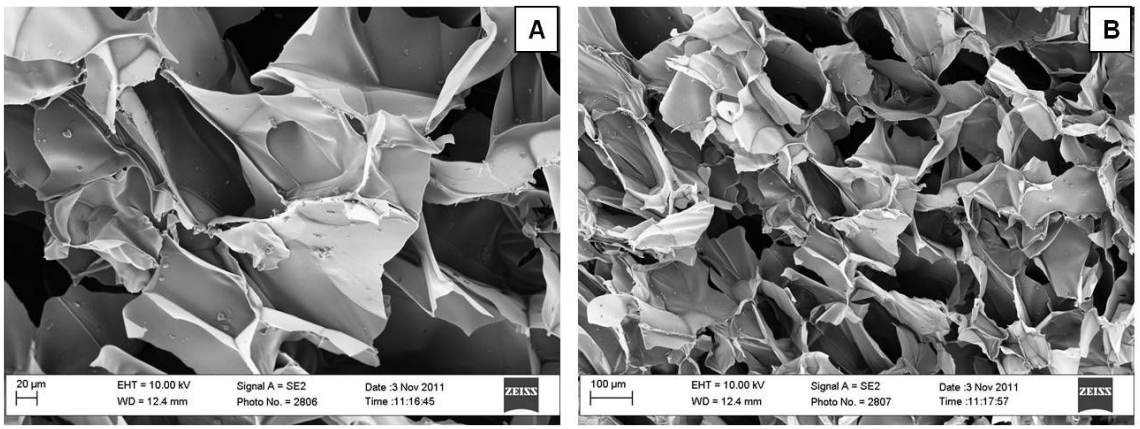

Figure 7.5 SEM micrographs of chitosan-based foam samples (CSBG) at different magnifications.

All the samples (CS, CSHA and CSBG) presented a regular and homogenous porous structure, as reported in figures 7.3, 7.4 and 7.5. In particular, in CSBG sample was also possible to notice the presence of BG particles inside the foam pore structure, while at reported magnifications it was not possible to appreciate the presence of the nanoparticles of HA, dispersed in sample pore structure. Samples average pore size was not affected by the presence of HA or BG particles.

7.2.2.2 ATR/FT-IR analysis

ATR/FT-IR analysis was performed, according to § 2.5.2, in order to evaluate the presence of HA and BG in chitosan foams, and eventual interactions chitosan-HA and chitosan-BG. The spectra of CS, CSHA and CSBG samples are reported in figure 7.6.

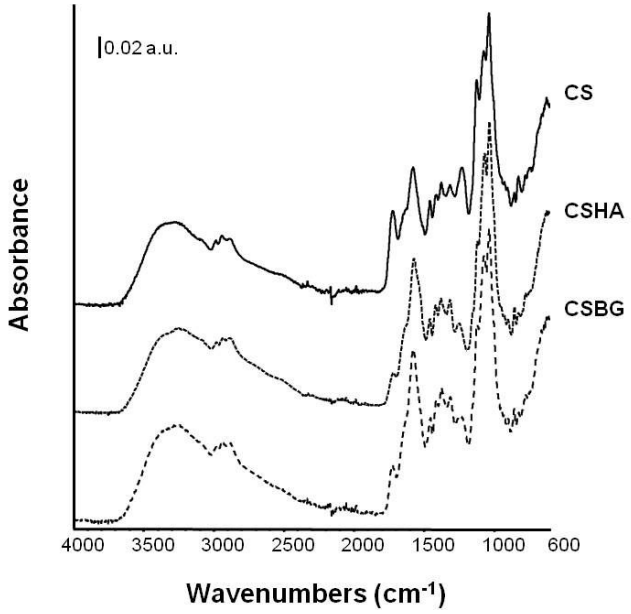

Figure 7.6 ATR-FT-IR spectra of CS, CSHA and CSBG foam scaffolds.

All the spectra CS, CSHA and CSBG were dominated by chitosan absorption. In order to deeply investigate chitosan-HA and chitosan-BG interactions, subtraction spectra are reported in figure 7.7. and 7.8.

In fact the spectra of CS and CSHA samples and the spectrum arisen from the subtraction of CS spectrum from the CSHA one is reported in the same figure (7.7). A component centered at 1150 cm^{-1} in the subtraction spectrum, due to the different stretching vibration of C-N, respect to pure CS sample, was observed. The presence of HA was revealed by the band centered at 1030 cm^{-1}, due to the vibration of the phosphate group.

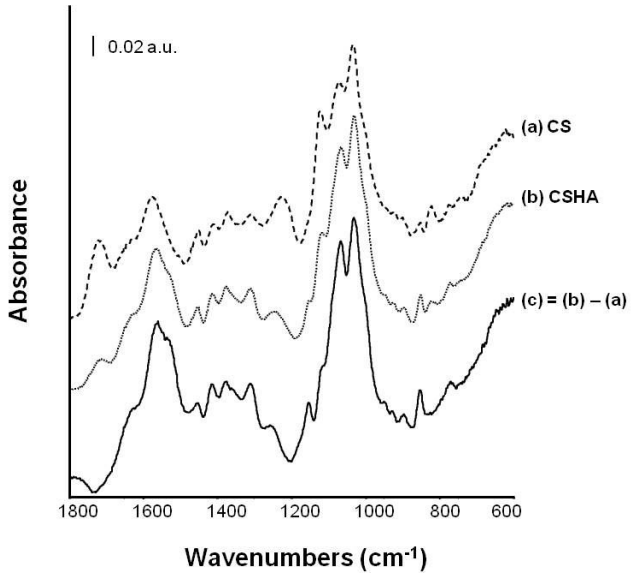

Figure 7.7 ATR/FT-IR spectra in the fingerprint region of CS (a), CSHA (b) samples, and the subtraction spectrum CSHA – CS (c).

Also the interaction chitosan-BG was evaluated and the presence of BG in CSBG sample was observed in the subtraction spectrum (CSBG – CS spectrum in figure 7.8). In particular, the peak at 1030 cm^{-1} was due to stretching vibration of Si-O-Si, according to [16] and the peak shift respect to the BG powder spectrum, as the presence of another peak at 1070 cm^{-1}, were due to chitosan- BG interaction.

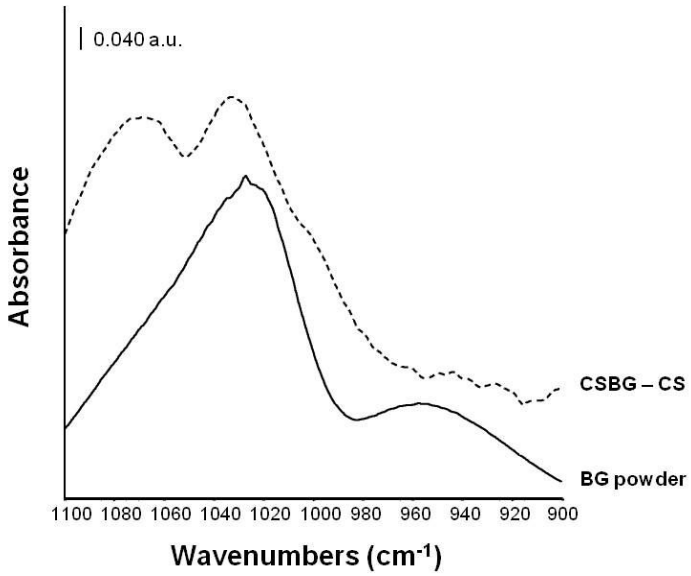

Figure 7.8 ATR/FT-IR spectra of BG powder and the subtraction spectrum of CSBG – CS.

7.2.2.3 Mechanical properties

All the samples were characterized from mechanical point of view, according to § 2.5.4. The mechanical properties values of CS, CSHA and CSBG samples are recorded in table 7.1.

	Young's Modulus [kPa]	Maximum stress (50% strain) [kPa]	Residual strain [mm/mm]
CS	201 ± 40	75 ± 18	0.39 ± 0.02
CSHA	1684 ± 754	107 ± 17	0.44 ± 0.01
CSBG	1226 ± 624	95 ± 14	0.43 ± 0.01

Table 7.1 Summary of mechanical properties values of samples CS, CSHA and CSBG (Young's modulus, maximum stress at 50% strain, and residual strain) measured during compressive test.

As observed from the data recorded in table 7.1, the addition of HA and BG improved the sample stiffness, even if a decrease in elastic behavior was noticed in CSHA and CSBG samples, as highlighted by a slight increase in the residual strain values.

7.2.2.4 Porosity measurement

Porosity measurement were performed by liquid displacement, accordingly to [15], as reported in §2.5.6. Briefly, hexane was used as displacement liquid and it was possible to calculate the scaffold total volume (V) and the scaffold porosity (ε), by the following equations.

Scaffold total volume: V = (V2 – V1) + (V1 – V3) = V2- V3, where: (V2 – V1) is the volume of the chitosan foam and (V1 – V3) is the volume of hexane within the scaffold. While the porosity of the scaffold (ε) was obtained by

$$\varepsilon = \frac{V1 - V3}{V2 - V3} \cdot 100$$

Porosity measurement was performed on pure chitosan (CS) and chitosan with hydroxyapatite (CSHA) and bioactive glass (CSBG) foams and the values are summarized in the following table:

	w0 [g]	V1 [mL]	V2 [mL]	V3 [mL]	Scaffold total volume V [mL]	Porosity ε [%]
CS	0.0115	5	5.5	4.6	0.9	**44**
CSHA	0.0137	5	5.8	4.8	1	**20**
CSBG	0.0105	5	5.8	4.7	1.1	**27**

Table 7.2 Summary of the values related to the porosity measurement. Relevant the values of scaffold total volume (V) and foam porosity (ε).

Results showed a decrease in porosity in the samples containing HA or BG. Both samples showed close values of porosity, as reported in table 7.2.

7.2.2.5 Swelling

Immersion of all samples (CS, CSHA and CSBG) in dH_2O was performed to evaluate the swelling in aqueous solution, as previously described in § 2.5.7. Swelling ratio was calculated by using the following equation, according to [16]:

Swelling ratio $= \frac{W_w - W_0}{W_0}$, where Ww is the sample wet weight after immersion in aq. solution, and W0 is the sample dry weight before immersion (t0).

Results reported in the following figure, showed a similar behavior of all analyzed samples, indicating that the addition of HA or BG did not affect the foam swelling.

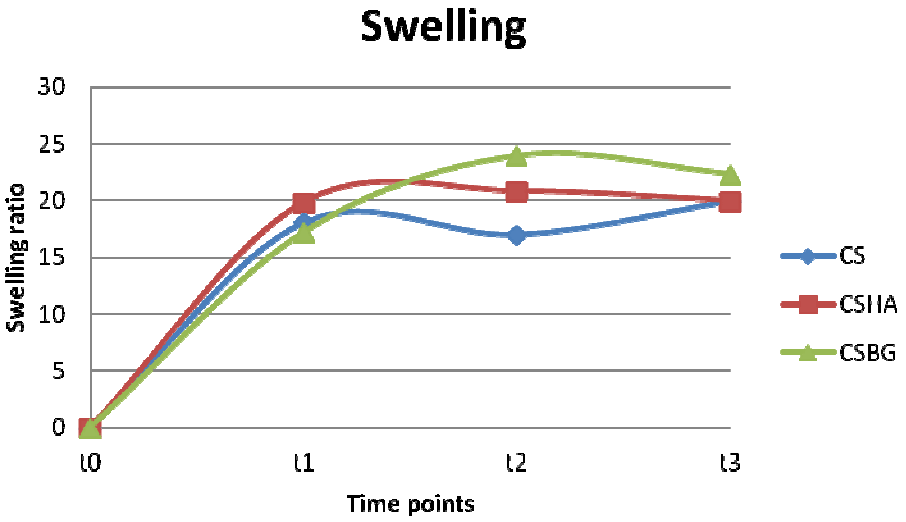

Figure 7.9 Samples CS, CSHA, and CSBG swelling ratio at each timepoints.

7.2.2.6 pH measurements

After samples immersion in cell basal medium (protocol reported in § 2.5.8), a color change was observed in the medium after the immersion of all the samples (CS, CSHA, and CSBG). For that reason, further investigations and tests on pH measurements were necessary and performed according to the protocol reported in § 2.5.8.

In the table below, there are reported the pH values of DI water after the immersion of all foams (CS, CSHA, and CSBG), at different timepoints (note that at t0 = 0 min the pH measured value is the pH value of DI water without any sample in it).

Timepoints	**t0**	**t1**	**t2**	**t3**	**t4**	**t5**	**t6**	**t7**	**t8**	**t9**	**t10**	**t11**
t[min]	**0**	**0.5**	**1**	**2**	**3**	**4**	**5**	**6**	**7**	**8**	**9**	**10**
CS	7.25	5.5	4.49	4.38	4.33	4.17	4.16	4.13	4.13	4.13	4.13	4.13
CSHA	7.27	6.72	6.20	4.54	4.38	4.30	4.25	4.21	4.21	4.21	4.21	4.21
CSBG	7.05	5.14	4.98	4.69	4.64	4.29	4.28	4.24	4.16	4.15	4.16	4.16

Table 7.3 Summary of the pH values of DI water after the immersion of all foams (CS, CSHA, and CSBG), at different timepoints.

The pH variation of DI water after samples immersion was plotted in figure 7.10, underlying the great decrease in pH value, that occurred immediately after sample immersion. Similar behavior was showed for all kind of chitosan-based samples.

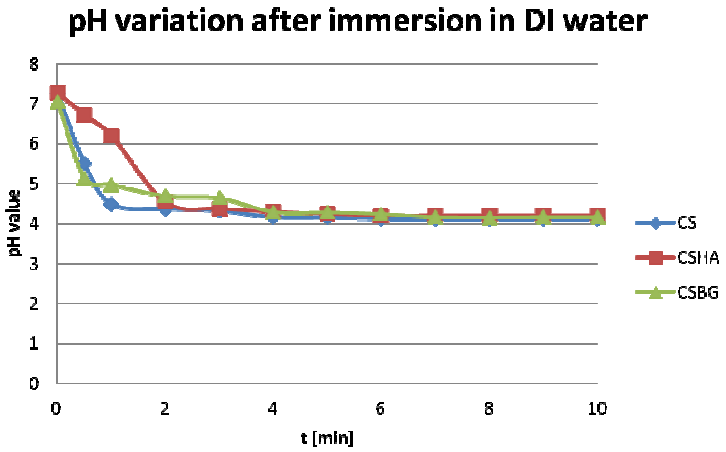

Figure 7.10 Plot of the trend of pH variation of DI water after samples immersion for all chitosan-based foams (CS, CSHA and CSBG).

In order to reduce the phenomenon of DI water acidification, that inhibits the possibility to use those foams for any kind of biological assessment, all the foam samples were neutralized by immersion in some basic solutions. The results of immersion in different solutions are reported below. Samples were immersed for 30 minutes in NaOH 0.25 M aq. solution, then all the samples were rinsed in DI water three times. In the table below, there are reported the pH values of DI water after the immersion of all foams (CS, CSHA, and CSBG) treated by immersion in NaOH 0.25 M aq. solution, at different timepoints.

NaOH 0.25 M	**t[min]**			
	0	**10**	**30**	**60**
CS	7.21	11.51	11.65	11.55
CSHA	7.21	11.56	11.55	11.09
CSBG	7.21	11.68	11.63	11.57

Table 7.4 Summary of the pH values of DI water after the immersion of all foams (CS, CSHA, and CSBG) treated by immersion in NaOH 0.25 M aq. solution, at different timepoints.

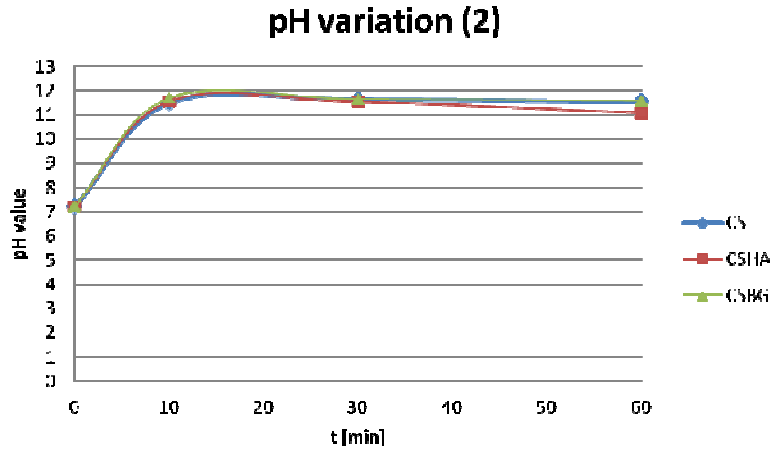

Figure 7.11 Plot of the trend of pH variation of DI water after samples immersion for all chitosan-based foams (CS, CSHA and CSBG), treated by immersion in NaOH 0.25 M aq. solution.

As observed in the measured pH values recorded in table 7.4 and in the plot reported in figure 7.11, sample neutralization induced an excessive increase in the pH value after samples immersion in DI water. For that reason a diluted NaOH aq. solution was tested for samples neutralization.

Samples were immersed for 30 minutes in NaOH 0.1 M aq. solution. Then, all the samples were rinsed in DI water three times. In the table below, there are reported the pH values of DI water after the immersion of all foams (CS, CSHA, and CSBG) treated by immersion in NaOH 0.1 M aq. solution, at different timepoints.

NaOH 0.1 M (30 min)	**t[min]**			
	0	**10**	**30**	**60**
CS	7.02	9.13	9.07	8.63
CSHA	7.02	9.20	9.03	8.95
CSBG	7.02	8.98	8.84	8.81

Table 7.5 Summary of the pH values of DI water after the immersion of all foams (CS, CSHA, and CSBG) treated by immersion in NaOH 0.1 M aq. solution (for 30 min), at different timepoints.

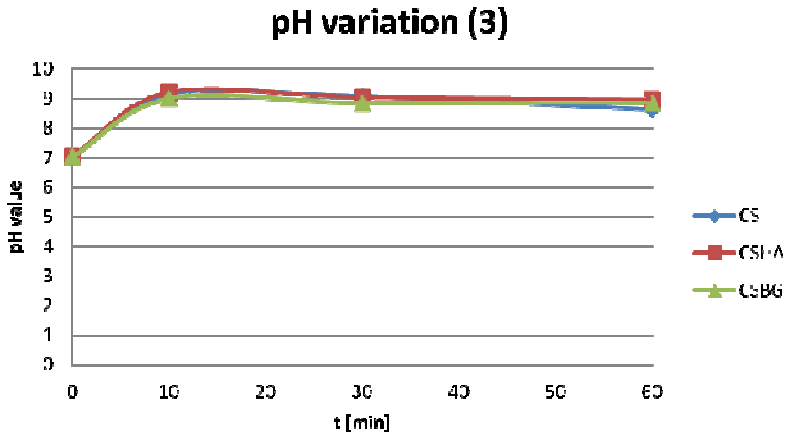

Figure 7.12 Plot of the trend of pH variation of DI water after samples immersion for all chitosan-based foams (CS, CSHA and CSBG), treated by immersion in NaOH 0.1 M aq. solution (for 30 min).

Also in this case, after the treatment in NaOH 0.1 M solution for 30 minutes, pH values showed an undesirable increase, as reported in table 7.5 and figure 7.12. For that reason, the time of samples immersion in the NaOH solution was reduced.

Samples were immersed for 10 minutes in NaOH 0.1 M aq. solution, then all the samples were rinsed in DI water three times. In the table below, there are reported the pH values of DI water after the immersion of all foams (CS, CSHA, and CSBG) treated by immersion in NaOH 0.1 M aq. solution, at different timepoints.

NaOH 0.1 M (10 min)	**t[min]**			
	0	**10**	**30**	**60**
CS	7.05	7.25	7.32	7.33
CSHA	7.05	7.18	7.21	7.19
CSBG	7.05	7.20	7.18	7.22

Table 7.6 Summary of the pH values of DI water after the immersion of all foams (CS, CSHA, and CSBG) treated by immersion in NaOH 0.1 M aq. solution (for 10 min), at different timepoints.

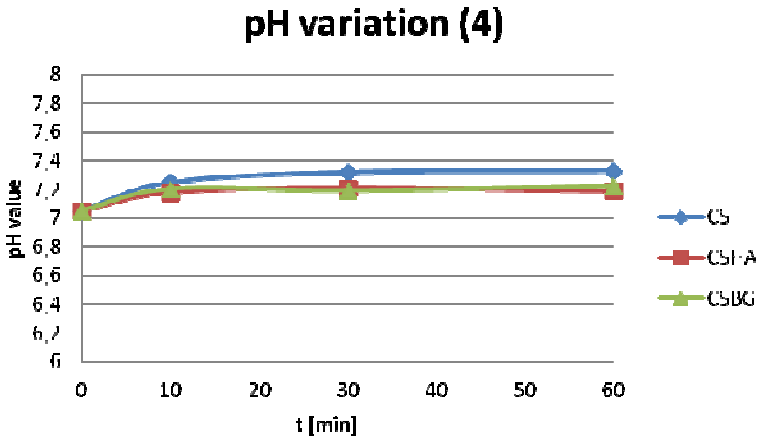

Figure 7.13 Plot of the trend of pH variation of DI water after samples immersion for all chitosan-based foams (CS, CSHA and CSBG), treated by immersion in NaOH 0.1 M aq. solution (for 10 min).

Satisfactory results were obtained for all the samples after the last neutralization treatment, as reported in table 7.6 and figure 7.13.

7.2.2.7 Bioactivity test (Simulated Body Fluid)

The bioactivity of the samples (CSHA and CSBG) was assessed by samples immersion in a simulated body fluid (SBF) solution, according to [17], as reported in § 2.5.9. Samples modifications were evaluated by SEM analysis and ATR/FT-IR spectroscopy. SEM micrographs are reported in the following figures (7.14 and 7.15).

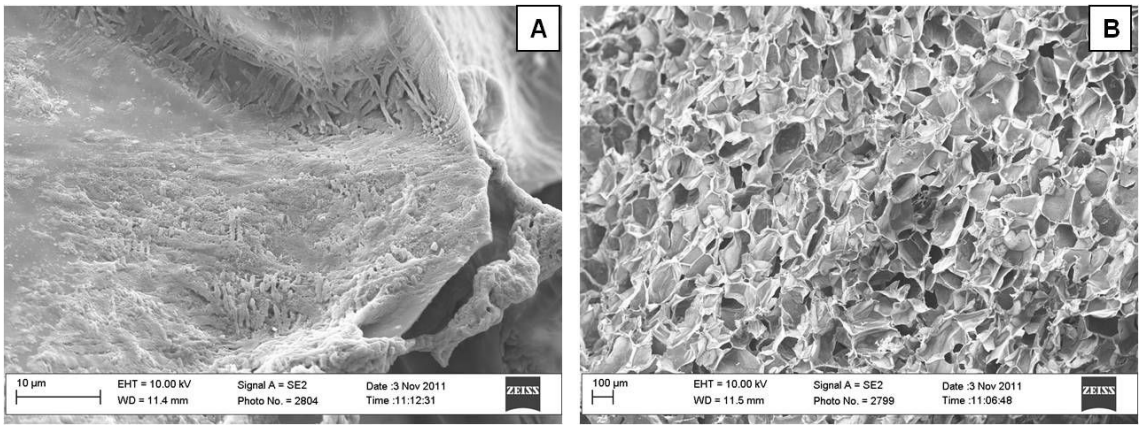

Figure 7.14 CSHA sample after 7 days of immersion in SBF solution at different magnifications.

Figure 7.14 showed that CSHA sample was covered by a deposited layer, after the immersion in SBF solution for 7 days. Sample characteristic porous structure was preserved after the immersion in SBF.

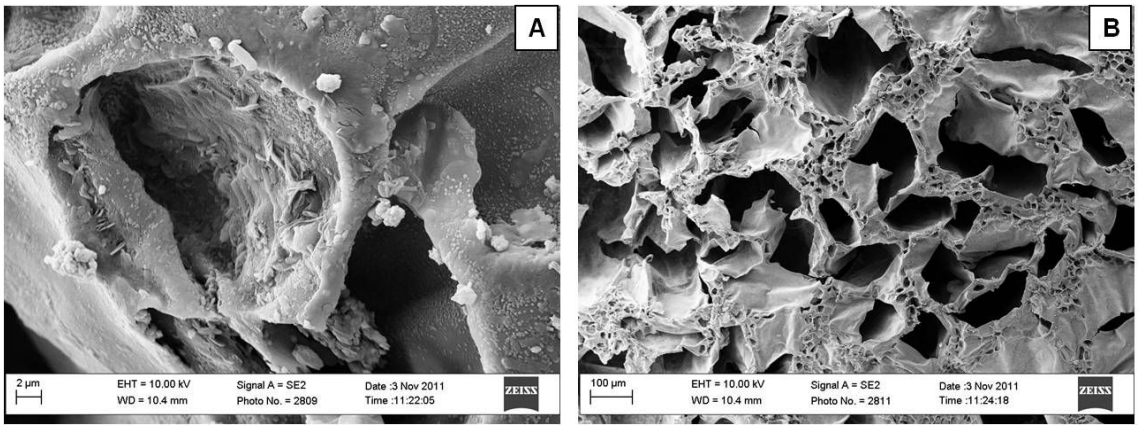

Figure 7.15 CSBG sample after 7 days of immersion in SBF solution at different magnifications.

Similarly to the CSHA sample, also CSBG sample showed the precipitation of some deposits on pore surface. Same porous structure was preserved, even if some modifications in surface morphology were observed.

ATR/FT-IR spectra of CSHA and CSBG samples after immersion in SBF are recorded. In order to evaluate the effects of samples immersion in SBF, the subtraction spectra between the sample immersed for 7 days (d7 sample) and the samples before immersion (d0 sample) are reported in figure 7.16 for both CSHA and CSBG samples.

In particular in those spectra, an increase in the band ascribable to the vibration of phosphate group, was observed in both subtraction spectra, indicating the samples bioactivity after immersion in SBF solution.

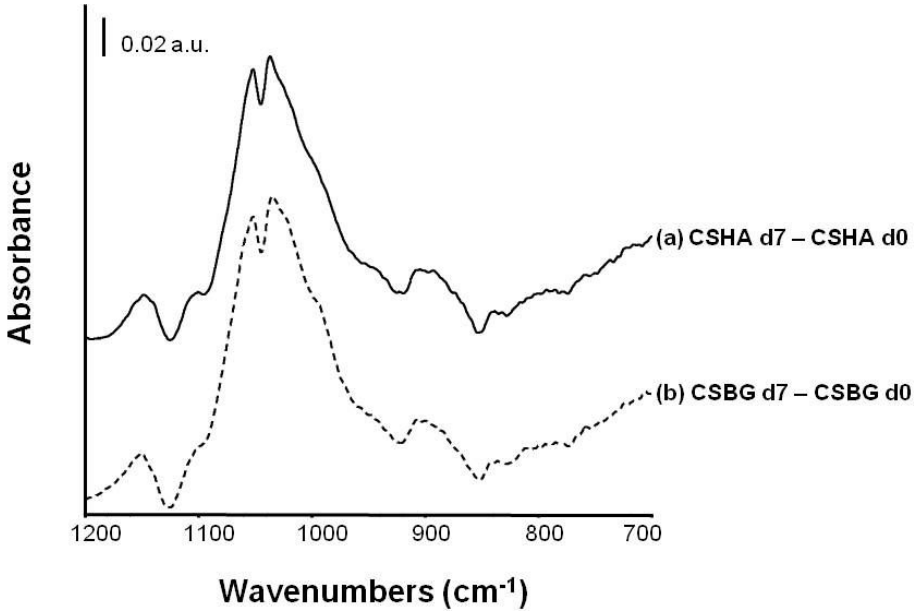

Figure 7.16 ATR-FTIR subtraction spectra between samples before and after 7 days of immersion in SBF solution: CSHA d7 – CSHA d0 (a), and CSBG d7 – CSBG d0 (b).

7.2.3 Protocol 3-based chitosan foam scaffolds

Protocol 2 was optimized and simplified, generating the protocol 3, previously reported in §2.4.3. Foams fabricated with protocol 3, in pure chitosan (CS) and with the addition of hydroxyapatite (CSHA) nanopowder, were characterized in terms of morphology, chemical structure, mechanical properties, foam swelling and porosity, pH alteration in aq. solution, and *in vitro* bioactivity, as follows.

7.2.3.1 Morphological analysis

The same samples (CS and CSHA) were investigated by SEM analysis (ref. § 2.5.1). SEM micrographs at different magnifications are reported in the following figures.

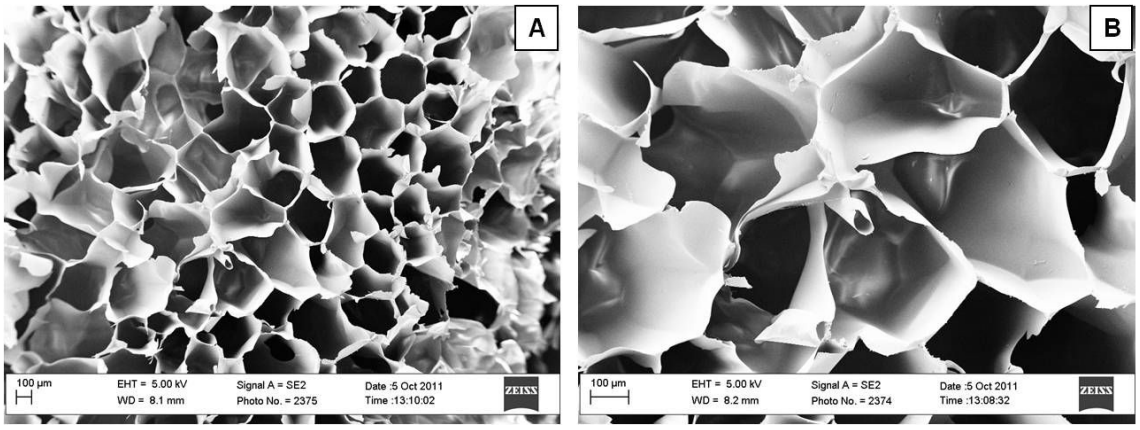

Figure 7.17 SEM micrographs of chitosan foam samples (CS) at different magnifications.

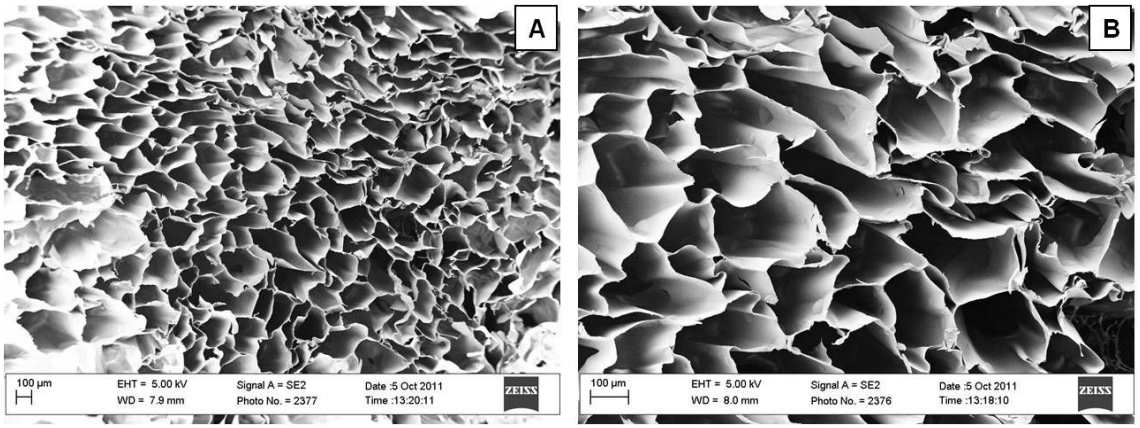

Figure 7.18 SEM micrographs of chitosan-based foam samples (CSHA) at different magnifications.

All the samples (CS, and CSHA) presented a regular and homogenous porous structure, as reported in figures 7.17, and 7.18. In particular, the average pore size of both samples was calculated by software image analysis (Image J, NIH, USA) and the values were 212 ± 64 µm and 179 ± 44 µm for CS and CSHA samples, respectively. Average pore size was not affected by the addition of HA nanopowder.

7.2.3.2 ATR/FT-IR analysis

ATR/FT-IR analysis was performed, according to § 2.5.2, in order to evaluate the presence of HA in chitosan foam, and eventual interactions chitosan-HA. The spectra of CS and CSHA samples in the fingerprint region are reported in figure 7.19. In order to

point out the differences introduced by the presence of HA, the spectrum arisen from the subtraction of CS spectrum from the CSHA one is reported in the same figure.

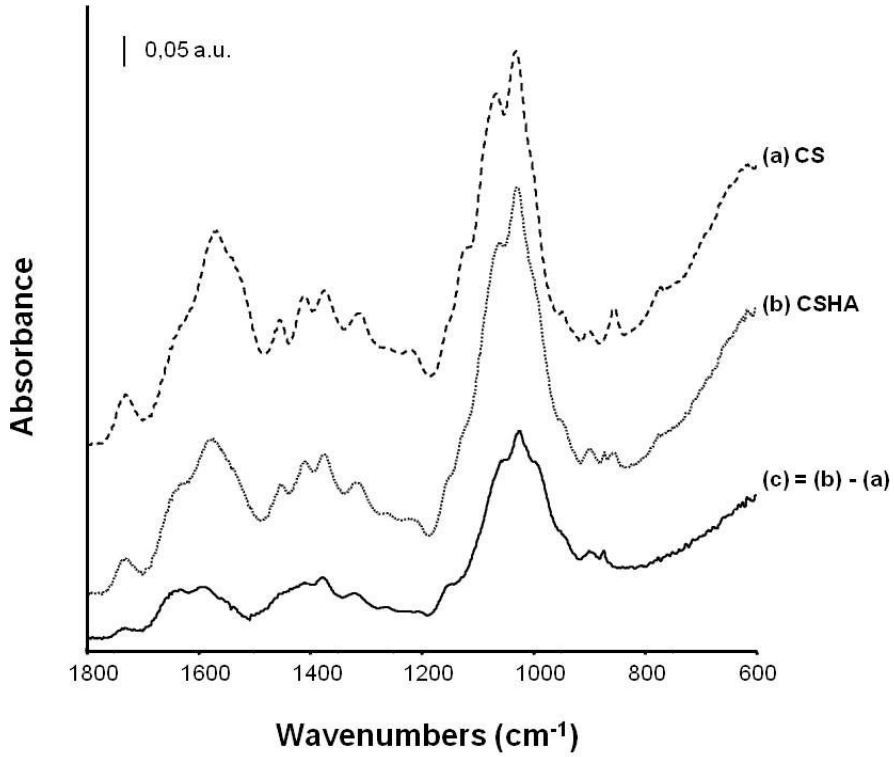

Figure 7.19 ATR/FT-IR spectra in the fingerprint region of CS (a), CSHA (b) samples, and the subtraction spectrum CSHA – CS (c).

All spectra were dominated by chitosan absorption. A component centered at 1150 cm^{-1} in the subtraction spectrum, due to the different stretching vibration of C-N, respect to pure CS sample, was observed. The presence of HA was revealed by the peak at 1025 cm^{-1} and its component at 990 cm^{-1}, due to the vibration of the phosphate group. These components were shifted (shift of about 30 cm^{-1}) respect to the spectrum of HA nanopowder (not showed here), because of the interaction between HA and chitosan, in fact phosphate group was involved in H binding with hydroxyl group and amino group of chitosan chain.

7.2.3.3 Mechanical properties

Sample mechanical properties were investigated by compressive test. The protocols of samples preparation and tests were previously described in §2.5.4. Samples stress-strain

curves are reported in figure 7.20. The mechanical properties values of CS, and CSHA samples are recorded in table 7.7.

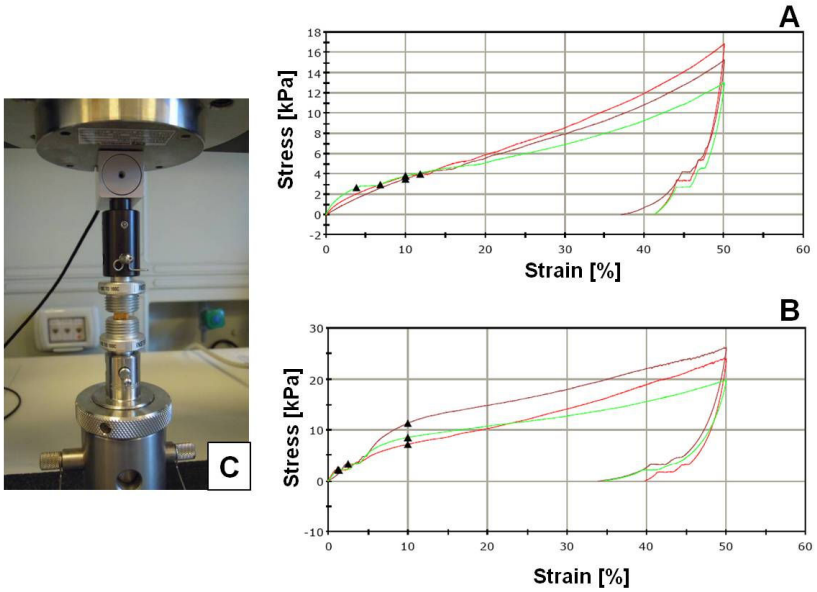

Figure 7.20 Stress-strain curves of CS (a), and CSHA (b) samples, and a digital camera image of the sample during the test.

	Young's Modulus [kPa]	Maximum stress (50% strain) [kPa]	Residual strain [mm/mm]
CS	57 ± 9	15 ± 2	0.40 ± 0.02
CSHA	122 ± 51	23 ± 3	0.36 ± 0.03

Table 7.7 Summary of mechanical properties values of the samples CS and CSHA (Young's modulus, maximum stress at 50% strain, and residual strain) measured during the compressive test.

As observed from the data recorded in table 7.7, the addition of HA improved the sample stiffness, (increase in Young's modulus value, and in maximum stress at 50% strain value), while the values of the residual strain was similar for both samples.

7.2.3.4 Porosity measurement

Porosity measurement was performed, as reported above in §7.2.2.4, on pure (CS) and chitosan with hydroxyapatite (CSHA) foams and the values are summarized in the following table:

	w0 [g]	V1 [mL]	V2 [mL]	V3 [mL]	Scaffold total volume V [mL]	Porosity ε [%]
CS	0.0169	5.5	6	5	1	**50**
CSHA	0.0194	5.5	6.2	5	1.2	**42**

Table 7.8 Summary of the values related to the porosity measurement. Relevant the values of scaffold total volume (V) and foam porosity (ε).

Results showed a slight decrease in the porosity of CSHA samples. While an increase in all porosity values was observed, respect to the porosity values obtained for the foams prepared by using the protocol 2 (compare table 7.2 with 7.8 values).

7.2.3.5 Swelling

Immersion of both samples (CS and CSHA) in dH_2O was performed to evaluate the swelling in aqueous solution, as previously described in §7.2.2.5.
Results reported in the following figure, showed differences in the samples behavior, in fact the swelling ratio value decrease in CSHA sample (30%) respect to CS (40%) one.

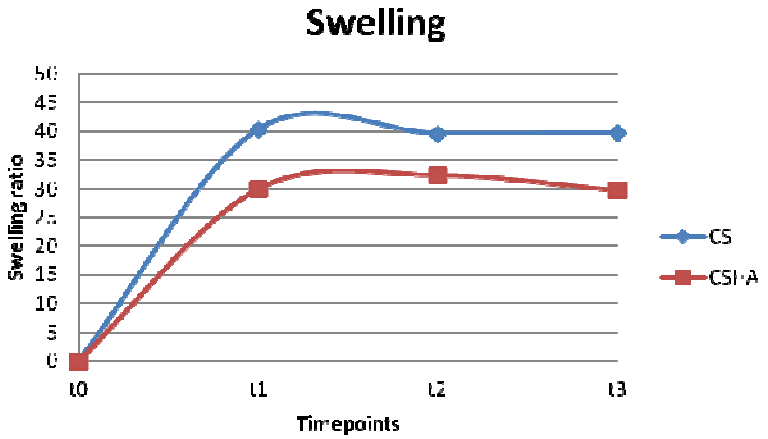

Figure 7.21 Samples CS and CSHA swelling ratio at each timepoints.

7.2.3.6 pH measurements

Positive results at the colorimetric test performed with cell basal medium (protocol reported in §2.5.8) were observed. In fact the medium did not change its characteristic color after samples (CS and CSHA) immersion. Further investigations and tests on pH measurements were not necessary.

7.2.3.7 Bioactivity test (Simulated Body Fluid)

The bioactivity of the sample CSHA was assessed by sample immersion in a simulated body fluid (SBF) solution, according to [17], as reported in § 2.5.9. Samples modifications were evaluated by SEM analysis (ref. to § 2.5.1), and SEM micrographs are reported in the following figure 7.22.

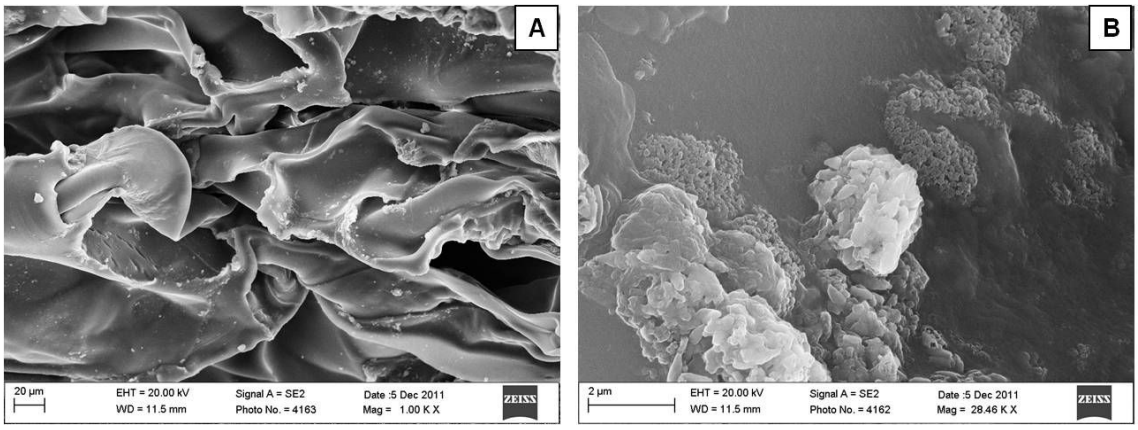

Figure 7.22 SEM micrographs of CSHA sample after 7 days of immersion in SBF solution at different magnifications.

Figure 7.22 showed that CSHA sample presented some precipitated deposits on pore surface, after the immersion in SBF solution for 7 days. Sample characteristic porous structure was preserved after the immersion in SBF.

7.2.3.8 Biocompatibility assay

Preliminary tests about cell viability of CS and CSHA samples were performed in triplicate for each sample and for each time point, according to the protocols previously reported in § 2.5.10.

Sample cytotoxicity evaluation (by using G6PD assay) showed that the cell viability was higher than 90% for both samples (CS and CSHA), as reported in figure 7.23.

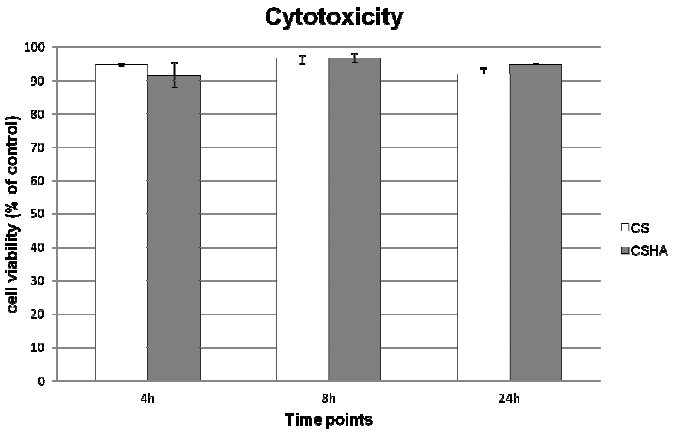

Figure 7.23 Cell viability of CS and CSHA samples, evaluated by G6PD assay.

Proliferation assay showed a progressive increase in the number of cells, for both samples (CS and CSHA), as showed in figure 7.24. Values reported in the graph were normalized respect to T0 values for both CS and CSHA samples.

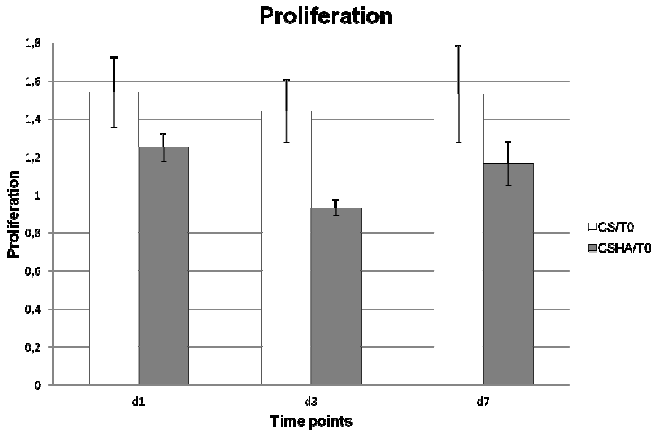

Figure 7.24 Cell proliferation of CS and CSHA samples, evaluated by MTT assay.

7.3 Conclusions

The present chapter reports about the preparation of foam scaffolds constituted by pure chitosan (CS) and chitosan with the addition of nanopowder of hydroxyapatite (HA) and bioactive glass (BG) particles. Chitosan-based foam scaffolds were prepared by using phase separation-based techniques. Foams fabrication protocol was progressively optimized and improved. In fact, three different protocols were tested and evaluated. All the obtained samples were characterized in terms of morphology, chemical structure, mechanical properties and *in vitro* bioactivity. Positive results were obtained in terms of pore interconnectivity, foam swelling and porosity, and samples bioactivity. Positive outcomes of *in vitro* biocompatibility assays, performed on optimized samples, suggest that these samples are suitable for tissue engineering applications.

References

[1] Olszta MJ, Cheng X, Jee SS, Kumar R, Kim Y-Y, Kaufman MJ, et al. Bone structure and formation: A new perspective. Materials Science and Engineering: R: Reports. 2007;58:77-116.

[2] Oliveira JM, Rodrigues MT, Silva SS, Malafaya PB, Gomes ME, Viegas CA, et al. Novel hydroxyapatite/chitosan bilayered scaffold for osteochondral tissue-engineering applications: Scaffold design and its performance when seeded with goat bone marrow stromal cells. Biomaterials. 2006;27:6123-37.

[3] Muzzarelli RAA. Chitins and chitosans for the repair of wounded skin, nerve, cartilage and bone. Carbohydrate Polymers. 2009;76:167-82.

[4] Di Martino A, Sittinger M, Risbud MV. Chitosan: A versatile biopolymer for orthopaedic tissue-engineering. Biomaterials. 2005;26:5983-90.

[5] Nettles DL, Elder SH, Gilbert JA. Potential Use of Chitosan as a Cell Scaffold Material for Cartilage Tissue Engineering. Tissue Engineering. 2002;8:1009-16.

[6] Mooney DJ, Baldwin DF, Suh NP, Vacanti JP, Langer R. Novel approach to fabricate porous sponges of poly(d,l-lactic-co-glycolic acid) without the use of organic solvents. Biomaterials. 1996;17:1417-22.

[7] Harris LD, Kim B-S, Mooney DJ. Open pore biodegradable matrices formed with gas foaming. Journal of Biomedical Materials Research. 1998;42:396-402.

[8] Chen G, Ushida T, Tateishi T. A biodegradable hybrid sponge nested with collagen microsponges. Journal of Biomedical Materials Research. 2000;51:273-9.

[9] Ma J, Wang H, He B, Chen J. A preliminary in vitro study on the fabrication and tissue engineering applications of a novel chitosan bilayer material as a scaffold of human neofetal dermal fibroblasts. Biomaterials. 2001;22:331-6.

[10] Liu X, Jin X, Ma PX. Nanofibrous hollow microspheres self-assembled from star-shaped polymers as injectable cell carriers for knee repair. Nat Mater. 2011;10:398-406.

[11] Schugens C, Maquet V, Grandfils C, Jerome R, Teyssie P. Biodegradable and macroporous polylactide implants for cell transplantation: 1. Preparation of macroporous polylactide supports by solid-liquid phase separation. Polymer. 1996;37:1027-38.

[12] Gu ZY, Xue PH, Li WJ. Preparation of the porous chitosan -membrane by cryogenic induced phase separation. Polymers for Advanced Technologies. 2001;12:665-9.

[13] Ho M-H, Kuo P-Y, Hsieh H-J, Hsien T-Y, Hou L-T, Lai J-Y, et al. Preparation of porous scaffolds by using freeze-extraction and freeze-gelation methods. Biomaterials. 2004;25:129-38.

[14] Rainer A, Giannitelli SM, Abbruzzese F, Traversa E, Licoccia S, Trombetta M. Fabrication of bioactive glass–ceramic foams mimicking human bone portions for regenerative medicine. Acta Biomaterialia. 2008;4:362-9.

[15] Tığlı R, Gümüşderelioğlu M. Evaluation of alginate-chitosan semi IPNs as cartilage scaffolds. Journal of Materials Science: Materials in Medicine. 2009;20:699-709.

[16] Peter M, Binulal NS, Soumya S, Nair SV, Furuike T, Tamura H, et al. Nanocomposite scaffolds of bioactive glass ceramic nanoparticles disseminated chitosan matrix for tissue engineering applications. Carbohydrate Polymers. 2010;79:284-9.

[17] Kokubo T, Takadama H. How useful is SBF in predicting in vivo bone bioactivity? Biomaterials. 2006;27:2907-15.

8. Conclusions

The present PhD thesis is focused on tissue engineering, in particular to the fabrication of chitosan-based scaffolds potentially useful for the regeneration of osteochondral tissue.

The chitosan versatility allows the fabrication of scaffold for tissue engineering by using several fabrication techniques, as the electrospinning and the phase separation ones.

For what concerns the electrospun scaffold fabrication, an optimization of pure chitosan electrospinning process, without the addition of copolymer, was pursued, and homogeneous defect-free nanofibrous electrospun meshes of pure chitosan were obtained. Moreover, the investigation and the optimization of the crosslinking processes, needed to enhance chitosan electrospun samples resistance to physiological environment, were performed. In particular, two different crosslinking methods (labeled two-steps and one-step method, referring to the integration of the electrospinning and crosslinking processes), were evaluated. Two chitosan crosslinkers were compared: (i) glutharaldehyde, used for both methods, and (ii) genipin, used only for the one-step method. All the obtained chitosan electrospun crosslinked samples were characterized in terms of morphology, chemical structure and mechanical properties. Both the investigated methods allowed performing successful crosslinking of the obtained electrospun chitosan nanofibers. Samples obtained by one-step process were characterized by a decrease in average fiber diameters. Glutaraldehyde-based crosslinking techniques affected sample mechanical properties, instead of the genipin-based crosslinking method (ref chapter 3).

Keeping in mind the final scaffolds function and the tissue target of regeneration, a biomimetic approach aiming to the fabrication of scaffolds with structure and composition similar to natural bone, was pursued by the introduction of inorganic phase (hydroxyapatite (HA) nanopowder or bioactive glass (BG) particles) within the polymeric fibers. The addition of HA or BG was evaluated separately because it required accurate investigations and analysis of obtained samples. The addition of HA was evaluated in terms of modifications in the chitosan solution spinnability and in the electrospinning parameters. All the obtained chitosan/HA electrospun uncrosslinked and crosslinked (by using two-steps method) samples were characterized in terms of

morphology, chemical structure, mechanical properties and bioactivity. In particular, a deep investigation was performed to confirm that the introduction of HA in chitosan solution (acid environment) and the processes of electrospinning and crosslinking did not modify HA structure. Positive results were obtained in terms of yield of electrospinning process, fabrication of homogeneous nanofibrous sample morphology, preservation of HA structure in the obtained samples, and samples bioactivity. In HA-containing samples, a decrease in fiber average diameter, and an increase in sample mechanical properties, were observed (ref. chapter 4).

For what concerns the use of BG particles dispersed in chitosan solution before the electrospinning process, the fabrication of a biomimetic composite required an optimization of the electrospinning process. The obtained chitosan/BG electrospun uncrosslinked and crosslinked (by using two-steps method) samples were characterized in terms of morphology, chemical structure, mechanical properties and bioactivity. Composite scaffolds showed homogeneous fibrous structure, with a decrease in fiber average diameter, respect to pure chitosan meshes. Moreover, the addition of the ceramic phase increased *in vitro* bioactivity of pure chitosan. Encouraging results were obtained from preliminary biocompatibility studies performed on these composite samples (ref. chapter 5).

A possible application of the obtained chitosan-based electrospun membranes was presented in this PhD work, as the external coating in a stratified multilayer composite scaffold for osteochondral tissue engineering. This stratified composite constructs were obtained by the integration of three different techniques widely used for scaffold fabrication: the foam replica method, the freeze drying and freeze gelation, and the electrospinning. 45S5 Bioglass® was used for the fabrication of the rigid bioactive substrate intended to be in contact with bone tissue; chitosan, alginate, and gelatin solutions were used for building the interface between the Bioglass®-based scaffold and the soft cartilage side of the construct, constituted by chitosan-based electrospun membrane. In this design, the intermediate layer has multiple functions providing adherence between the other scaffold components, preventing delamination and acting as soft coating for the rigid Bioglass® substrate. Morphological analysis, bioactivity tests in simulated body fluid (SBF), as well as mechanical and wettability tests were performed on all samples to assess the optimal stratified scaffold combination. The best results were obtained using chitosan and freeze gelation to produce the intermediate

layer, in terms of resistance to layer delamination, bioactivity and improvement in mechanical properties of the underlying bioactive glass scaffold.

The novelty of this stratified, layered system can be highlighted in terms of its versatility for application to several kinds of electrospun membranes that need to be combined with a rigid macroporous 3D structure. The electrospun membrane was used after its fabrication, as external coating, making the stratified composite fabrication method developed here independent from the electrospinning process itself. This kind of stratified structures could be suitable for several applications in the emerging field of interface tissue engineering, strictly related to the electrospun membrane functions, as for example, exploiting fiber topographical stimuli for cell signaling or using functionalized electrospun membranes as drug delivery systems or as filtering devices (ref. chapter 6).

The other kind of scaffold produced in the present work was obtained by using phase separation technique for the fabrication of chitosan foam scaffolds. Also in this case, a biomimetic approach was pursed and HA and BG particles were dispersed inside chitosan porous structure. These scaffolds were obtained after progressive fabrication protocol improvement and optimization, and they were characterized in terms of morphology, chemical structure, mechanical properties and *in vitro* bioactivity. Positive results were obtained in terms of pore interconnectivity, foam swelling and porosity, and samples bioactivity. Finally, positive outcomes of *in vitro* biocompatibility assays, performed on optimized samples, suggest that they are suitable for further tissue engineering applications (ref. chapter 7).

In conclusion, the use of chitosan for scaffold fabrication, having different morphology, properties and functions was presented. The obtained positive results confirm chitosan polymer versatility and suitability for the applications in this specific field of tissue engineering.

Acknowledgments

In this section I would like to thank all the people that gave me their contributions (intentional or unintentional) to reach this important objective.

First of all, I am deeply grateful to my PhD supervisor, Prof. Marcella Trombetta, even if I know that these few words cannot express properly my gratitude towards her. With her enthusiasm, her expertise, her wise advices, she introduced me in the fantastic world of the Research since I was a young Bachelor student and she helped me to grow from professional and personal point of view during these years.

I would like to express my sincere gratitude to Dr. Alberto Rainer, for his enthusiasm, his precious advices and his helpful presence during my PhD research activities. In particular thanks a lot for his contribution (professional and personal) in helping me to become a researcher.

I would like to show my gratitude to Dr. Franca Abbruzzese and Dr. Pamela Mozetic for their contributions in my PhD research activities and, in particular, for their friendship.

I could not forget to thank my PhD student colleagues (but also labmates and special friends) Ms. Sara Maria Giannitelli and Mr. Matteo Centola. We shared a lot of time during these years, becoming more than colleagues, appreciating the amazing results of successful team work. Finally, thanks to all the students that I had the honor to support, as the co-advisor of their Bachelor or Master thesis research activities.

I am sincerely grateful to Prof. Aldo R. Boccaccini, Head of Institute of Biomaterials, Department of Material Science and Engineering, at Friedrich Alexander Universität Erlangen-Nuremberg, for gave me the great opportunity to spend my PhD visiting period (summer 2011) at his Institute, and to collaborate with his Staff on an interesting research project. In particular, I would like to thank the people I had the honor to collaborate with: Dr. Judith A. Roether, Ms. Patcharakamon Nooeaid and Dr. Ranjana Rai, and all the other people belonging to the Staff of the Institute of Biomaterials, Department of Material Science and Engineering, at Friedrich Alexander Universität Erlangen-Nuremberg, for their kind welcome and professional expertise.

It is a pleasure to thank those who made this thesis possible, my dear family and in particular Alessandra, for their constant support and silent presence every day of my

life, for believing in my capabilities since I was a child and for sharing with me pain and joy.

Last but not least in my heart, I am grateful to all my friends (I am sorry, but I cannot list here all of their names) for supporting and bearing me, in particular during my PhD study.